EXPRESSION AND CHARACTERIZATION OF THE NOVEL HUMAN EPOXIDE HYDROLASES EH3 AND EH4

DISSERTATION

zur
Erlangung der naturwissenschaftlichen Doktorwürde
(Dr. sc. nat.)
vorgelegt der
Mathematisch-naturwissenschaftlichen Fakultät
der
Universität Zürich
von

Martina Marion Elisabeth Decker

aus
Deutschland

Promotionskomitee

Prof. Dr. Michael Arand
Prof. Dr. Jean-Marc Fritschy
Prof. Dr. Thierry Hennet

Zürich, 2010

ACKNOWLEDGEMENTS

First, I would like to thank Michael Arand for supervising me and giving me the opportunity to do my PhD in his group. Many thanks for sending me to San Diego and Baltimore (the best steak ever) and of course for the intensive proofreading and his help during writing this thesis.

I would also like to thank “Miss Annette” Cronin for simply everything. For helping me with any problems in the lab and outside the lab, for answering all my questions on LC-MS/MS and protein purification and for wonderful barbecues with wonderful potato salad. It was great going to Las Vegas and Baltimore with you! I am really going to miss you.

Also a big thank you to Magdalena Adamska, for introducing me into the secrets of molecular biology and for granting me asylum in the very beginning of my PhD. Also for being there and backing me up whenever I had the feeling that something was wrong.

Many thanks go to all the people of the Toxi group, those who are still there and those who are already gone. In particular to Severine for all the nice and relaxing “coffee and cigarettes” and for going to Kondi, which always helps to keep in shape. Thanks a lot to Kathrin - Katruschka for keeping an eye on insect cells and for constantly providing me with fresh and lively cells! Also thanks a lot to my “Masters of Desasters” - Janine and Francesca. Thank you for the nice time, the help and support in the lab, for cheering me up and for going to Sauna.

I would also like to thank my office buddy Marc, for all the delicious mensa meals we had, for making me laugh and for being there even when everyone else already has finished work.

Also “merci vielmals” to Jean-Mary Fritschy, who always responded to emails immediately and helped me with all the difficult questions about “Zirkulationskreise”, “Gutachten” and other important paperwork.

Thanks a million also to all the people outside the institute, who made it possible for me to accomplish my PhD. Especially to Oli and Wibi, for giving me advise and for always having an ear, for having drinks and fun, for playing handball together with me and for being such friends.

I also want to thank my parents who always cared and always supported me. Thanks for welcoming me at home whenever I was homesick and felt like going back to the roots. Thanks for patiently coping with my bad moods. Thanks for always believing in me and for being proud of me.

Last but not least I would like to thank two very important people in my life, Katharina and Philipp. I would probably have never been able to finish this PhD without them. Thank you very much for believing in me, supporting me, loving me, listen to me, being there for me whenever I desperately needed someone. I know I could have always called you. This is impayable.

TABLE OF CONTENTS

1 SUMMARY / ZUSAMMENFASSUNG

Epoxide hydrolases are enzymes that catalyze the hydrolysis of epoxides to their corresponding diol by the addition of a water molecule. The most prominent and best investigated human epoxide hydrolases are microsomal epoxide hydrolase (mEH) and soluble epoxide hydrolase (sEH). The role of these enzymes for the human organism is at least of dual function. Historically, these enzymes were regarded as responsible for the detoxification of potential harmful epoxides. However, intensive research over the last decade has proven that they also act on endogenous lipid derived epoxides, an important class of signaling molecules. They thereby contribute to the regulation of physiological processes. Both enzymes belong to the α/β hydrolase fold super family and share characteristic sequence motives that are conserved among all α/β hydrolase fold epoxide hydrolases. By using these highly conserved sequence motives as query for Blast searches of the human genome, putative novel epoxide hydrolases can be discovered. Recently, our group identified two novel epoxide hydrolase genes – *EPHX3* (EH3) and *EPHX4* (EH4). This raises the following questions that are addressed in the present thesis:

a) Is EH4 an enzymatically active epoxide hydrolase?

b) What is the substrate spectrum of EH3 and what can we learn from this?

As a first step to characterize EH4, different prokaryotic and eukaryotic expression systems were established in order to investigate EH4 enzymatic activity towards various epoxide substrates and to generate an EH4 specific antibody. Rabbit immune sera obtained after immunization, with either truncated protein that was recombinantly expressed in *E. coli* or synthetic EH4 peptides, failed to specifically detect EH4. As an alternative method, LC-MS/MS based peptide analysis was established, which allowed detection of EH4 in insect cell lysates. To investigate the enzymatic activity, recombinant EH4 expressed in *E. coli* and insect cells was incubated with different radiolabeled and unlabeled epoxides and the presence of the respective enzymatic products was analyzed by autoradiography and LC-MS/MS. There was no significant reproducible difference in the amount of diol in EH4 lysates detectable as compared to the control. *In vivo* expression analysis in mouse revealed presence of EH4 mRNA in the brain, which is in agreement with the data available on expression databases. Experiments to determine the subcellular localization of EH4 suggest that EH4 is membrane associated, which confirmed the prediction that the N-terminal amino acids of EH4 display a membrane anchor.

In order to analyze the relevance of EH3 for the human organism, the substrate spectrum was assessed and the kinetic parameters of selected substrates were determined. The activity towards lipid derived epoxides was investigated in cell lysates of EH3 expressing Sf9 cells and analyzed by LC-MS/MS. EH3 was found to be capable of hydrolyzing a variety of different arachidonic acid and linoleic acid derived epoxides with proven biologic activity. Among the tested epoxides, epoxyeicosatrienoic acids (EETs) and leukotoxin were identified as the best substrates for EH3. The catalytic efficiency of EH3 towards these substrates is comparable to that of mEH and sEH. EETs have important biological effects on blood pressure, inflammation, pain perception and insulin secretion, whereas the linoleic acid derived leukotoxin is involved in the development of a severe

pulmonary injury, called adult respiratory distress syndrome (ARDS). Due to its important role in turnover of EETs, sEH became a pharmaceutical target. A series of specific sEH inhibitors (sEHi) was developed for the treatment of hypertension, inflammatory diseases, pain and diabetes. A set of established sEHi was tested towards their effects on EH3 enzymatic activity. Inhibition experiments showed, that EH3 was inhibited by a subclass of this urea derived compounds at a concentration that is usually employed for *in vivo* inhibition of sEH.

In a comprehensive series of experiments, enzymatic activity of EH4 towards the tested epoxides could not be proven. Possible reasons are (i) inactive expression of the protein as a result of incorrect folding or (ii) the tested epoxides are no substrates for EH4. Further research is required to unveil the physiological substrate of this novel enzyme and its role for the human organism. Based on the results obtained in this work, the role of EH3 can be ascribed to physiological regulation by turnover of endogenous epoxides. The enzyme is capable of converting different fatty acid derived signaling molecules, which recently gained interest and are now intensively investigated. The fact that fatty acid like inhibitors affect enzymatic activity of EH3, whereas structurally different established sEHi do not, further indicates that EH3 preferentially acts on lipid derived epoxides and thus is relevant for regulation of physiological processes in the human body. Inhibition of sEH by selective sEHi can exploit the beneficial effects of EETs and is a promising target for the treatment of hypertension, pain and diabetes. Most certainly it must be taken into account that some inhibitors are not sEH specific but rather equally affect EH3, and thus have an additional target with different expression pattern. This leads to a modified biological activity as compared to sEH-selective compounds. Importantly, the hydrolysis product of leukotoxin has been reported to be a potent mediator of ARDS, a lung injury that can result in multiple organ failure. The kinetic data on leukotoxin turnover by EH3 and the fact that EH3 is expressed in the lung, strongly suggest a role of this enzyme in ARDS. The generation of an EH3 knock out mouse would be a good approach to study the expression and regulation of EH3 and to unveil the physiological role of EH3. Detailed analysis of the substrate spectrum will give more insight into the role of EH3 as physiological regulator and thereby might enable understanding of different diseases and hence the development of novel therapeutics.

ZUSAMMENFASSUNG

Epoxidhydrolasen (EH) sind Enzyme, welche die Hydrolyse von Epoxiden zu ihren entsprechenden Diolen katalysieren. Die beiden bekanntesten Epoxidhydrolasen, die cytosolische EH (sEH) und die mikrosomale EH (mEH), sind für den menschlichen Organismus in zweierlei Hinsicht von Bedeutung. Zum einen sind Epoxidhydrolasen historisch gesehen detoxifizierende Enzyme, die als für die Entgiftung potentiell schädlicher Epoxide verantwortlich galten. Innerhalb der letzten Jahrzehnte wurde jedoch gezeigt, dass beide Enzyme auch in der Lage sind endogene, biologisch aktive Epoxide umzusetzen und damit auch in die Regulation physiologischer Prozesse eingreifen. Epoxidhydrolasen sind Mitglieder der sogenannten „α/β-hydrolase fold"- Familie und weisen die für Enzyme dieser Familie charakteristischen Sequenzmotive auf. Diese Motive können herangezogen werden, um in humanen Genomdatenbanken nach neuen Mitgliedern der α/β - hydrolase fold EH´s zu suchen. Zwei neue EH-Gene, *EPHX3* (EH3) und *EPHX4* (EH4), wurden vor kurzem in unserer Gruppe identifiziert. Daraus resultierend stellen sich die beiden folgenden Fragen, welche in dieser Arbeit beantwortet werden sollen:

a) Besitzt EH4 eine Epoxidhydrolase - Aktivität?

b) Welches Substratspektrum besitzt EH3 und was können wir daraus lernen?

Für die Charakterisierung der EH4 wurden verschiedene prokaryotische und eukaryotische Expressionssysteme entwickelt und etabliert, um einerseits einen Antikörper gegen EH4 herzustellen und andererseits die enzymatische Aktivität des neuen Enzyms untersuchen zu können. Immunseren von Kaninchen zeigten nach Immunisierung mit entweder einem verkürzten Protein oder synthetischen Peptiden, keine spezifische Immunreaktivität gegenüber EH4. Als Alternative wurde eine LC-MS/MS basierte Methode entwickelt, die einen genauen Proteinnachweis von EH4 aus Zellysat ermöglicht. Für die Analyse der enzymatischen Aktivität von EH4 wurde das rekombinante EH4-Protein zuerst mit verschiedenen radioaktiv markierten und unmarkierten Substraten inkubiert, um im Anschluss daran die Anwesenheit des entsprechenden Produktes (Diol) mittels Autoradiographie und LC-MS/MS zu analysieren. Im Vergleich zu Kontroll-Lysaten war in EH4 - Lysaten kein signifikanter Unterschied in der entsprechenden Diol-Menge nachzuweisen. Eine Analyse des *in vivo* Expressionsmusters von EH4 in verschiedenen Organen der Maus, ergab eine deutliche Expression von EH4 im Gehirn. Dies steht mit den vorliegenden Daten der Expressionsdatenbanken im Einklang. Experimente zur Untersuchung der sub-zellulären Lokalisation von EH4 lassen vermuten, dass EH4 ein Membran-assoziiertes Protein ist. Dies bestätigt die Voraussage einer *in silico* Untersuchung die besagt, dass EH4 wahrscheinlich ein membrangebundenes Enzym darstellt, da die N-terminalen Aminosäuren Charakteristika eines Membranankers aufweisen.

Um beurteilen zu können, welche Rolle EH3 für den menschlichen Organismus spielt, wurde das Substratspektrum untersucht und die kinetischen Parameter einiger wichtiger Substrate bestimmt. Wie Untersuchungen zur enzymatischen Aktivität von EH3 in rekombinanten Insektenzellen zeigten, ist EH3 in der Lage verschiedene Epoxide der Arachidon- und Linolsäure umzusetzen. Von diesen biologisch aktiven Signalmolekülen werden Epoxyeicosatriensäuren (EETs) und Leukotoxin am besten umgesetzt. Die katalytischen Parameter der Umsetzung von physiologisch relevanten EET-Regioisomeren sowie von Leukotoxin wurden ermittelt, und mit denen von mEH und sEH verglichen.

Das Ergebnis zeigt, dass die katalytische Effizienz von EH3 mit derjenigen von mEH und sEH vergleichbar ist. EETs sind Signalmoleküle und haben einen wichtigen Einfluss auf Blutdruck, Entzündung, Schmerzwahrnehmung und Diabetes. Leukotoxin hingegen spielt eine Rolle bei der Entstehung von ARDS (acute respiratory distress syndrome), einem schwerwiegenden Lungenversagen, das als eine Folge von direktem oder indirektem Lungenschaden auftritt. Aufgrund der wichtigen Rolle der sEH im Umsatz von biologisch aktiven endogenen Epoxiden, im Besonderen im Umsatz von EETs, wurde eine Reihe von sEH- Inhibitoren (sEHi) entwickelt, die zur Behandlung von Bluthochdruck, Entzündung, Schmerz und Diabetes eingesetzt werden sollen. Einige dieser verschiedenen Verbindungen wurden auf ihre inhibitorische Wirkung gegenüber EH3 getestet. Die Untersuchungen ergaben, dass das Enzym von einer bestimmten Gruppe dieser Inhibitoren gehemmt wird, und zwar in einem Konzentrationsbereich der auch *in vivo* in eingesetzt wird.

Eine enzymatische Aktivität von EH4 gegenüber den getesteten Substraten war in einer umfassenden Reihe von Experimenten nicht nachzuweisen. Mögliche Erklärungen dafür sind i) das Protein ist falsch gefaltet und von daher inaktiv exprimiert oder ii) die getesteten Epoxide sind keine Substrate für EH4. In jedem Fall sind weitere Untersuchungen nötig, um die physiologischen Substrate von EH4 zu identifizieren und die Rolle des Enzyms für den humanen Organismus zu enthüllen. Die Ergebnisse zur Untersuchung des Substratspektrums sowie des Inhibitorprofils von EH3 weisen darauf hin, dass EH3 durch den Umsatz von endogenen biologisch aktiven Epoxiden eine wichtige Rolle in der physiologischen Regulation spielt. Das Enzym ist in der Lage eine Reihe verschiedener biologisch aktiver Epoxide umzusetzen, welche in letzter Zeit zunehmend an Interesse gewinnen und aktuell intensiv erforscht werden. Zudem ist die Tatsache, dass nur Inhibitoren mit struktureller Ähnlichkeit zu Fettsäuren die enzymatische Aktivität von EH3 beeinflussen, ein weiterer Hinweis auf das Substratspektrum und die Funktion von EH3 für die Regulation physiologischer Prozesse im menschlichen Organismus. Die Inhibierung der sEH durch spezielle sEH- Inhibitoren (sEHi) stellt eine Möglichkeit dar, die positiven Wirkungen der EETs zu nutzen und als therapeutischen Ansatz für die Behandlung von Bluthochdruck, Entzündung, Schmerz und Diabetes einzusetzen. Wie die Ergebnisse der Arbeit zeigen muss jedoch berücksichtigt werden, dass mit großer Wahrscheinlichkeit einige sEH-Inhibitoren unspezifisch sind und ebenfalls eine Wirkung auf EH3 haben. Ein zusätzliches Target, dass verglichen mit sEH ein anderes Expressionsmuster und Substratspektrum aufweist, kann zu veränderter biologischer Aktivität und unerwünschten Nebenwirkungen der sEHi führen. Die Tatsache dass Leukotoxin-Diol mit der Entstehung von ARDS (Schocklunge) in Verbindung gebracht wird, zusammen mit den kinetischen Daten des Leukotoxin-Umsatzes und der Expression von EH3 in der Lunge, legen einen Rolle der EH3 in der Entstehung dieses progressiven Lungenversagens nahe. Die Entwicklung und Herstellung einer EH3 knock-out Maus wäre von grossem Nutzen um die physiologische Rolle von EH3 genauer aufzuklären. Darüber hinaus kann eine genauere Analyse des Substratspektrums, sowie nähere Untersuchungen der Expression und Regulation von EH3, zum besseren Verständnis von EH3 als physiologischen Regulator beitragen. Dies hilft die Ursachen verschiedener Krankheiten besser zu verstehen und ist von Bedeuting für die Entwicklung neuer Medikamente.

2 INTRODUCTION

2.1 Epoxide hydrolases

Epoxide hydrolases (EHs, EC 3.3.2.3) are enzymes that catalyze the hydrolysis of exogenous and endogenous epoxides to their corresponding diols by addition of water (figure 2-1).

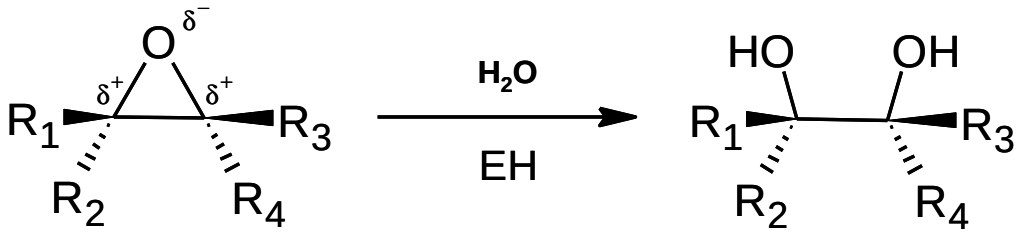

Figure 2-1: *Enzymatic reaction catalyzed by epoxide hydrolases. Addition of a water molecule results in the formation of the corresponding vicinal diol.*

EHs are ubiquitously found in nature and are present in various organisms including microorganisms, plants, insects and mammals. In bacteria, EHs are important for catabolic pathways that enable microorganisms to use specific carbon sources as food. One example is the epoxide hydrolase from *Rhodococcus erythropolis*, which catalyzes the hydrolysis of limonene-1,2-epoxide to limonene-1,2-diol (van der Werf, Overkamp et al. 1998) and enables the bacteria to thrive on limonene as carbon source. Like in bacteria, insect EHs are also involved in the catabolism of different compounds. Many chemicals produced by plants for defense against arthropodes are detoxified by insect EHs (Mullin 1988). In addition, by degradation of signaling molecules such as juvenile hormones (JH), epoxide hydrolases are involved in the physiological regulation of these hormones (reviewed in (Newman, Morisseau et al. 2005).

Bacterial and insect EHs are key players in degradation of specific carbons, whereas EHs in plants play a role in anabolic processes like cutin biosynthesis, which is the formation of the waxy cuticle that covers the aerial parts of plants and hence serves as barrier for pathogens (Heredia 2003). EHs are found in several higher plants investigated so far (e.g. soybean, tobacco and potato) and are moreover important for synthesis of antifungal chemicals that function in pathogen defense (Guo, Durner et al. 1998) and stress response (Kiyosue, Beetham et al. 1994).

Regarding mammalian EHs, five enzymes have been described so far: soluble epoxide hydrolase (sEH), microsomal EH (mEH), cholesterol EH (ChEH), hepoxilin hydrolase and leukotriene A4 (LTA4) hydrolase (reviewed in (Decker, Arand et al. 2009). Among vertebrates, mEH and sEH are the ones best investigated and much is known about their structure, function and physiological relevance. Their role in detoxification of exogenous epoxides has been intensely investigated. More recently research started focusing on their role in physiological regulation by hydrolysis of endogenous, biologically active epoxides (see chapter 2.2.2). Both mEH and sEH show structural characteristics that classify them as members of the α/β hydrolase fold superfamily and suggest parentage from a common ancestor protein (2.1.1). In contrast, LTA4 hydrolase and most likely ChEH do not belong to the α/β hydrolase fold superfamily.

To date, there is no gene sequence of ChEH known and no data on the characterization of the purified enzyme available, although its activity towards cholesterol-5α-6α-epoxide was already described by Aringer et al. in 1974 (Aringer and Eneroth 1974). LTA4 hydrolase is an enzyme relevant for immune response. It hydrolyzes the arachidonic acid derived Leukotriene A4 to biologically active Leukotriene B4 (McGee and Fitzpatrick 1985), that plays a role in adhesion and activation of leukocytes, chemo attraction of neutrophils and in ROS generation (reactive oxygen species). The tertiary structure and the catalytic mechanism of LTA4 hydrolase is different from that of mEH and sEH, giving the enzyme a unique position among EHs. In contrast to the vicinal diols generated by members of the α/β-hydrolase fold EHs, LTA4 hydrolase introduces hydroxyl groups located eight carbon atoms apart from each other (Arand, Cronin et al. 2003). Mammalian LTA4 hydrolase is, like FosX epoxide hydrolase from *Mesorhizobium loti*, a Zn2+ and Mn2+ dependent metalloenzyme (Haeggstrom, Kull et al. 2002; Fillgrove, Pakhomova et al. 2003; Rigsby, Fillgrove et al. 2005).
The hydrolase activity of hepoxilin epoxide hydrolase against the arachidonic acid derived hepoxilin A3 was first demonstrated by Pace-Asciak and colleagues (Pace-Asciak and Lee 1989) who isolated and purified the enzyme from rat liver cytosol. However there is reason to believe that the observed activity is actually attributable to sEH (oral communication of unpublished data by Dr. Annette Cronin).

2.1.1 The α/β hydrolase fold family

Most epoxide hydrolases of known sequence are members of the so called α/β hydrolase fold superfamily. The α/β hydrolase fold is a very common tertiary fold found in many different proteins of which all diverged from a common ancestor. Although these proteins differ in amino acid sequence and substrate spectra, all share the same structure and arrangement of the catalytic residues which compose the conserved catalytic triad. Examples of α/β hydrolase enzymes besides EHs are lipases, esterases (e.g. acetycholine esterase), proteases and dehalogenases. The α/β hydrolase fold, first identified by Ollis et al. in 1992 (Ollis, Cheah et al. 1992), is a subclass of α/β proteins that is composed of central β-sheets which are mostly arranged in parallel and surrounded by α-helices on both sides. mEH and sEH were classified as α/β fold hydrolases due to their structural similarity (Arand, Grant et al. 1994; Lacourciere and Armstrong 1994) to haloalkane dehalogenase (Janssen, Pries et al. 1989). The typical features of the α/β hydrolase fold domain are illustrated in figure 2-2, which depicts the 3D structure of the EH from *Agrobacterium radiobacter*. It was the first published X-ray structure of an epoxide hydrolase (Nardini, Ridder et al. 1999) that showed sequence similarity with mammalian EHs, in particular with sEH. The 3D structure of the EH of *A. radiobacter* revealed the following conserved structural elements of α/β hydrolase fold EHs (schematic illustration figure 2-3): the central core, that consists of eight central β-sheets that are surrounded by α-helices, is covered by a variable lid domain inserted between strand 6 and 7. Thereby it provides the epoxide binding pocket at the interaction site. The catalytic residues are highly conserved among α/β hydrolase fold EHs: the catalytic nucleophile (aspartate) is located after strand β5, the acidic residue (aspartate or glutamate) is positioned after β7 and the highly conserved water activating histidine residue is situated after the last β strand which takes part in building the charge relay system together with the acidic residue.

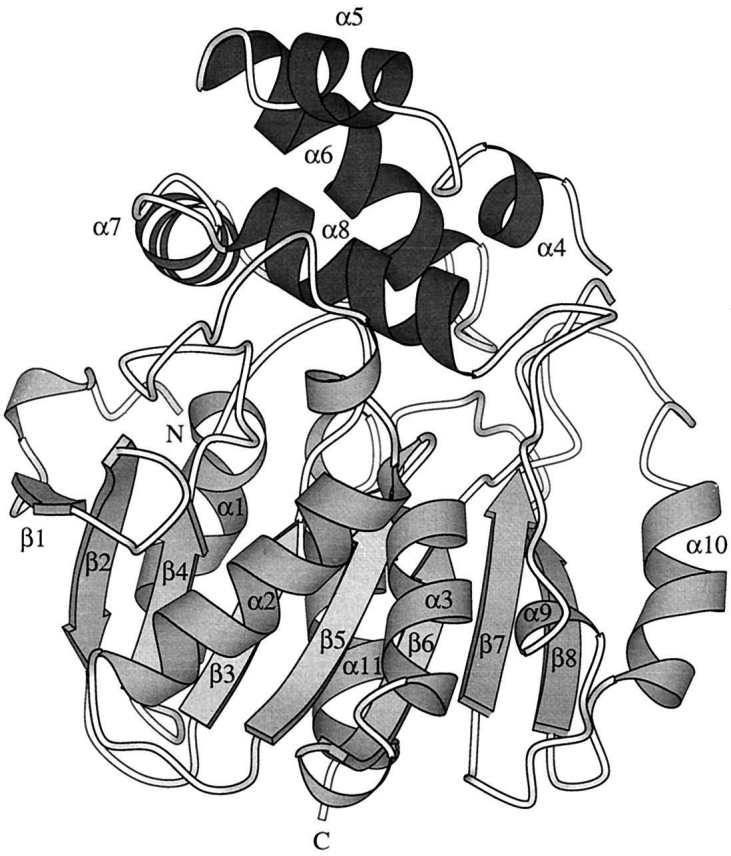

Figure 2-2: *Schematic view of the secondary structure elements of the epoxide hydrolase from Agrobacterium radiobacter. α-helices, β-strands, and coils are represented by helical ribbons, arrows, and ropes, respectively. The α-helices of the cap domain are shown in dark gray. (Krig, Jin et al. 2007)*

The αC helix (figure 2-3) plays a key role in positioning of the nucleophilic residue and thus is well conserved among α/β hydrolase fold proteins. The aspartate is located in a sharp turn, the so called “nucleophilic elbow”, where it can be easily approached by the substrate and the hydrolytic water molecule (Nardini and Dijkstra 1999). The nucleophilic elbow is identified by the sequence motif Sm-X-Nu-X-Sm-Sm (Sm: small residue, X: any residue, Nu: nucleophile) (Arand, Grant et al. 1994). Other conserved sequence motives are the oxyanion hole, located between β3 and αC (figure 2-3), and the G-X-Sm-X-S/T motif, located between the oxyanion hole and the catalytic nucleophile. While the latter is of unknown function, the oxyanion hole (H-G-X-P) stabilizes the negatively charged transition state that appears during hydrolysis. Residue X of the H-G-X-P motif, usually an aromatic amino acid, acts together with the residue directly following the catalytic nucleophile (van Loo, Kingma et al. 2006) to form this stabilizing unit. Two tyrosine residues, which discriminate EHs from other family members, are located in the lid domain and position the epoxide within the active site. Apart from the highly conserved sequence motifs described above, the amino acid sequence varies highly among the EH family. Nevertheless, these motifs can be used to identify putative EHs and distinguish them from related α/β-hydrolase fold enzymes like esterases and dehalogenases (see 2.4).

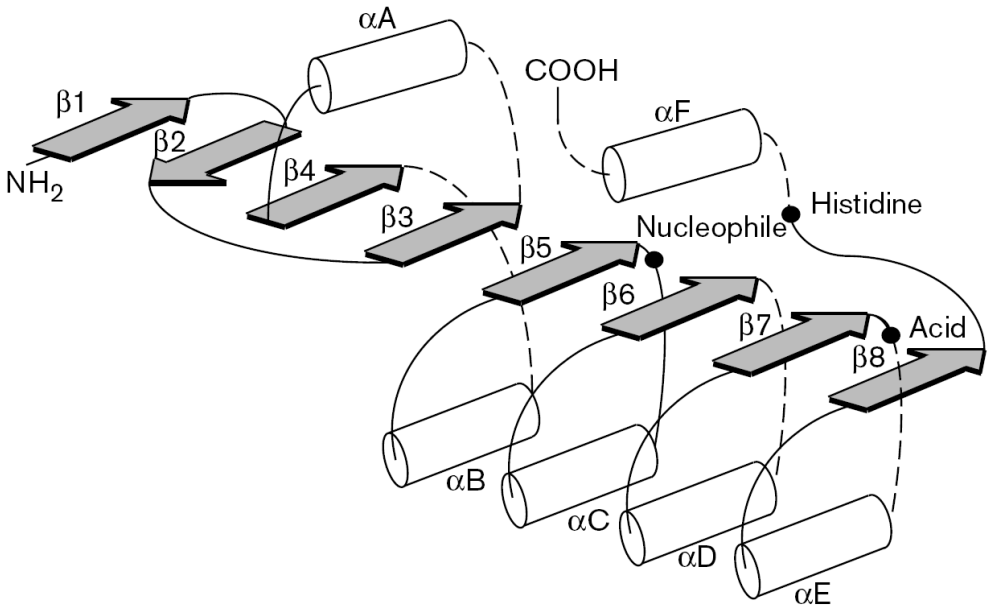

Figure 2-3: *Secondary structure of the α/β- hydrolase fold domain. α- helices and β-barrels are shown as white cylinders and gray arrows, respectively. The catalytic triad is indicated by black dots. (picture taken from (Nardini and Dijkstra 1999)*

2.1.2 Mechanism of epoxide hydrolysis

The sequence similarity of mEH and sEH, to bacterial haloalkane dehalogenase (HAD) led to the assumption that the catalytic mechanism of these two EHs is similar to that of the bacterial enzyme (Arand, Grant et al. 1994). The catalytic mechanism of HAD was unveiled by Verschueren et al. and is characterized by a two step process that involves the formation of a covalent alkyl ester intermediate (Verschueren, Seljee et al. 1993). The work of Lacourciere and Armstrong could demonstrate the formation of an ester intermediate for mEH by showing that during single turnover experiments the oxygen of $H_2{}^{18}O$ is incorporated in the protein and not in the corresponding diol (Lacourciere and Armstrong 1993), and thus provided evidence for the suggested two step mechanism. Several other studies to enlighten the mechanism of epoxide hydrolysis supported the initial hypothesis and helped to elucidate the mechanism in detail (figure 2-4) (Arand, Wagner et al. 1996; Muller, Arand et al. 1997; Laughlin, Tzeng et al. 1998; Argiriadi, Morisseau et al. 1999; Armstrong and Cassidy 2000; Arand, Cronin et al. 2003).

First, the substrate enters the binding pocket and binds to the active site. The active site is composed of the catalytic triad Asp – His – Asp/Glu (figure 2-4). At the same time the hydroxyl groups of two tyrosine residues position and polarize the epoxide by forming hydrogen bonds with the epoxide oxygen. In the first step, one of the two carbon atoms (usually the more accessible and most reactive one) in the epoxide is attacked by the catalytic nucleophile (carboxylic acid of Asp) which leads to formation of an ester intermediate. In the second step, the covalent ester – intermediate is hydrolyzed by an activated water molecule to release the diol product and the regenerated enzyme. The water molecule is activated by proton abstraction through the histidine residue leading to a positive charge in the aromatic amino acid. The negatively charged tetrahedral intermediate is compensated by the

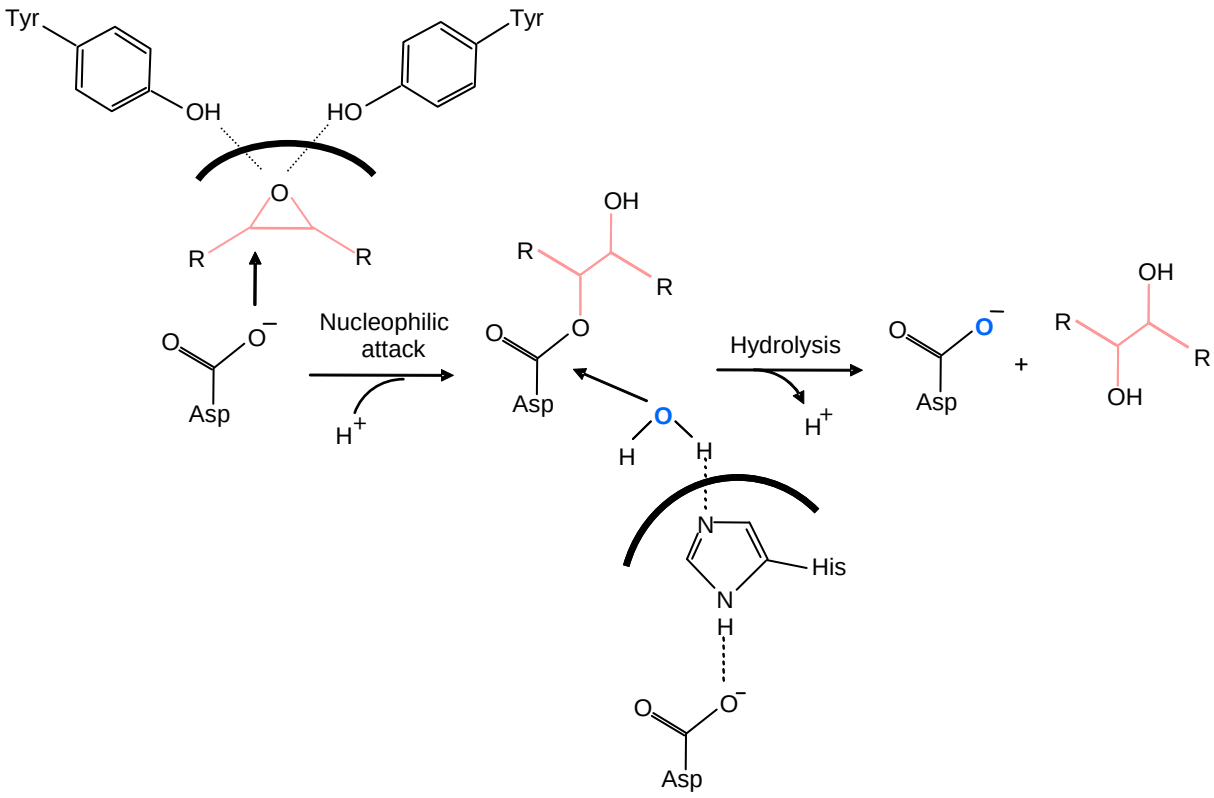

***Figure 2-4**: Catalytic mechanism of epoxide hydrolysis. The ring opening and formation of the covalent ester intermediate is assisted by two tyrosine residues, which position the epoxide in the active site. The ester intermediate is then hydrolyzed by an activated water molecule to subsequently release the diol and the original enzyme.*

backbone amides of the “oxyanion hole” (see 2.1.1) and the acidic aspartate (glutamate residue in case of mEH; Verschueren, Seljee et al. 1993).

All α/β hydrolase fold EHs share this mechanism, which is deduced from the mechanism of bacterial haloalkane dehydrogenase (HAD). Before the similarity of these enzymes to HAD was discovered, it was generally assumed that the hydrolysis by EHs follows a single step mechanism, like the one used by bacterial limonene epoxide hydrolase (LEH) from *Rhodococcus erythropolis* (Arand, Hallberg et al. 2003). This mechanism displays a faster epoxide hydrolysis but is associated with a narrow substrate spectrum due to the spatial fixation of the catalytic nucleophile. Regarding α/β-hydrolase fold enzymes, the catalytic nucleophile is located in a flexible turn (“nucleophilic elbow”) and thus can adapt to various spatially different epoxides which has some implications in the detoxification of genotoxic epoxides by EHs.

2.2 Function and human relevance of sEH and mEH

Whereas the functions of EHs in plants and bacteria can be ascribed to host defense, cutin biosynthesis and growth, the role of mammalian EHs is at least of dual function. Firstly, EHs play a key role in detoxification of a variety of genotoxic epoxides. Secondly, it has recently become evident that they are involved in the regulation of certain epoxides that act as physiological signaling molecules (figure 2-5).

2.2.1 Epoxide hydrolysis - role in detoxification

Epoxide hydrolases have first been identified as detoxifying enzymes (Oesch 1973), because many epoxides have genotoxic and cytotoxic properties: the high ring tension and the positive charge of the carbon atom lead to electrophilic reactivity of these compounds, enabling them to react with nucleophilic sites in proteins and nucleic acids. Modification of DNA bases at exocyclic amino groups or nitrogen atoms of purin bases leads to misincorporation during DNA replication which can result in permanent mutation. Since mutations in protooncogenes or tumor suppressor genes are critical in terms of induction of tumor formation, many epoxides are generally regarded as carcinogens. Genotoxic epoxides arise during phase I metabolism in the human liver where CYP 450 mediated monooxygenation of double bonds in aromatic ring systems and alkenes of xenobiotic compounds bioactivate initial harmless substances to genotoxic epoxides. Hence the deactivation and metabolic control by epoxide hydrolysis to produce the less reactive and more water soluble diol is an important mechanism for defense against carcinogenesis (Arand, Hallberg et al. 2003).

The microsomal EH is generally regarded as responsible for the detoxification of most genotoxic epoxides due to its broad substrate specifity, high expression level in the liver and in other metabolizing organs, and its inducibility by foreign compounds like phenobarbitone and N-acetylaminofluorene (Astrom, Maner et al. 1987; Hassett, Turnblom et al. 1989). Good substrates for mEH are lipophilic *cis* – configurated epoxides such as styrene oxide, *cis* – stilbene oxide, benzo[a]pyrene oxide, carbamazepine-10,11-oxide as well as the endogenous signaling molecule 11(12) epoxyeicosatrienoic acid (11(12) EET; (Decker, Arand et al. 2009). The turnover and metabolism of styrene, the precursor of the widely used plastic polystyrene, is an example for the role of mEH in detoxification. The DNA reactive styrene 7, 8-oxide (STO) is the major metabolite formed by CYP epoxygenases in the liver (Sumner and Fennell 1994) and is regarded as a potential carcinogen. In the liver, STO is rapidly hydrolyzed by mEH to the less toxic phenyl glycol and thus terminates the genotoxic potential. A study among plastic workers showed that specific STO biomarkers (DNA and albumin adducts, sister chromatid exchange) correlate with STO exposure rather than styrene exposure (Rappaport, Yeowell-O'Connell et al. 1996). This means that endogenous STO arising from exposure to exogenous styrene is sufficiently detoxified in the liver whereas already low exposure to STO shows genotoxic effects, because the compound is not detoxified until it reaches the liver. Work from Herrero et al. showed that V79 cells that express mEH are protected against the genotoxic effects of STO, whereas the control cells exhibit DNA-strand breaks as a result of STO treatment (Herrero, Arand et al. 1997).

However, some genotoxic substrates cannot be hydrolyzed and detoxified by mEH. The soluble EH somewhat complements the substrate spectrum of mEH in that it can convert slim *trans* 1, 2-disubstituted or trisubstituted epoxides such as *trans*-stilbene or *trans*-ethylstyrene oxide which both are not hydrolyzed by mEH (Arand, Cronin et al. 2003). In recent years it became evident that the enzyme preferentially acts on lipid epoxides and that its major function is the control of endogenous, fatty acid derived signaling molecules and thus takes part in physiological regulation.

2.2.2 Epoxide hydrolysis - role in physiology

Apart from their function in detoxification, EHs also play a role in physiological regulation by hydrolysis of endogenous epoxides that serve as signaling molecules. Although sEH was first thought to be involved in xenobiotic metabolism like mEH, due to the high expression in liver and kidney and its complementing substrate spectrum, it is nowadays regarded as the primary enzyme in the turnover of several endogenous epoxides, in particular in the hydrolysis of epoxyeicosatrienoic acids (EETs) to their corresponding dihydroxyeicosatrienoic acids (DHETs; see figure 2-5).

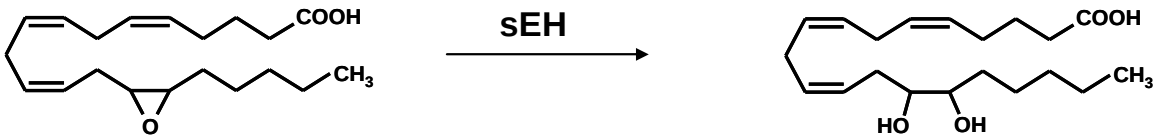

Figure 2-5: *Hydrolysis of 14(15) EET to the corresponding 14(15) DHET by soluble epoxide hydrolase.*

Endogenous epoxides like EETs do have little genotoxic potential due to their low chemical reactivity, but they have various biological effects including vasodilation, inflammation, cell proliferation, angiogenesis and analgesia, depending on cell and tissue type as well as regioisomer. EETs are synthesized from arachidonic acid (AA) by a variety of CYP 450 enzymes, mainly CYPs of the 2C and 2J subfamilies. According to the different double bonds, four EET regioisomers are produced: 5(6)-EET, 8(9)-EET, 11(12)-EET and 14(15)-EET, each in two different configurations (R and S enantiomers). The hydrolysis of EETs by sEH, with the order of preference 14(15)-EET > 11(12)-EET > 8(9)-EET > 5(6)-EET, is regarded as the deactivation step of biological activity. Vasodilation is the most extensively studied EET function. One important observation was that EETs function as endothelium derived hyperpolarization factors (EDHFs), which leads to vasodilation in small resistance vessels and coronary arteries, independent of nitric oxide or prostacycline (Fisslthaler, Popp et al. 1999). Several *in vivo* studies with sEH inhibitors and $sEH^{-/-}$ mice indicated that EETs do have an effect on blood pressure regulation (Imig, Zhao et al. 2002; Fang 2006; Li, Carroll et al. 2008) and inflammation. Anti-inflammatory effects of EETs were shown by Smith et al., where tobacco-smoke induced inflammation in rats was attenuated after sEH inhibition (Smith, Pinkerton et al. 2005).

Moreover there is evidence that EETs also regulate or influence cell proliferation, cell migration and angiogenesis (Sun, Sui et al. 2002; Potente, Fisslthaler et al. 2003; Michaelis, Fisslthaler et al. 2005). The overall mechanism of autocrine and paracrine EET activity is still not clear and under debate. It is supposed that they either bind to putative membrane receptors (GPCRs) on the cell surface, to activate intracellular signaling pathways, or directly act on ion channels (K_{ATP}, TRPV4, L-type Ca^{2+}), fatty acid binding proteins and/or transcription factors like PPARγ; (Widstrom, Norris et al. 2001; Liu, Zhang et al. 2005). The different cellular effects of EETs on cellular functions have recently been reviewed (Spector and Norris 2007). The role of sEH in EET turnover is generally accepted as the main function of this epoxide hydrolase and therefore reduces the implication of this enzyme as classical detoxification enzyme. This is supported by the fact that the recently discovered phosphatase activity of the N - terminal sEH domain (Cronin, Mowbray et al. 2003) plays a role in turnover of endogenous lipid phosphates.

In addition to EETs, there are other arachidonic and linoleic acid derived lipid mediators, which are involved in different physiological processes, and have been shown to be hydrolyzed by sEH. One of the first reports of turnover of physiological epoxide was the turnover of leukotoxin (Moghaddam, Motoba et al. 1996). Leukotoxin (9(10) EpOME) is synthesized in leukocytes from linoleate (Ozawa, Sugiyama et al. 1989) and is associated with acute respiratory distress syndrome (ARDS). ARDS is a reaction of the lung to various injuries and is characterized by inflammation of lung parenchyma that leads to impaired gas exchange, release of inflammatory mediators and hypoxemia. Leukotoxin was originally found in plasma of patients suffering from ARDS after severe burns (Ozawa, Sugiyama et al. 1989; Hayakawa, Kosaka et al. 1990; Kosaka, Suzuki et al. 1994). It was shown that leukotoxin and its derivate isoleukotoxin (12(13) EpOME) are synthesized by cytochrome P450 2C9 epoxygenation (Draper and Hammock 2000) from linoleic acid. Investigations *in vitro* (Moghaddam, Grant et al. 1997; Moran, Weise et al. 1997) and *in vivo* (Zheng, Plopper et al. 2001) showed that not the epoxide of linoleic acid but the epoxide hydrolase product leukotoxin-diol (9(10) DiHOME) is actually the more cytotoxic reagent. Swiss Webster mice dosed with 300mg/kg leukotoxin diol died from ARDS-like respiratory distress, whereas leukotoxin treated mice survived at the same dose. A 100% mortality was only observed after higher dosage of leukotoxin (600mg/kg) which indicates, that the leukotoxin diol is more toxic *in vivo*. In line with this is the observation that after treatment with 4-phenylchalcone oxide, an inhibitor of sEH, the mortality of leukotoxin treated mice decreased. In contrast, there was no protective effect on mortality of mice that received the dihydroxy derivate (Zheng, Plopper et al. 2001). Though the biological effects of leukotoxin-diol are known, the mechanism of leukotoxin-diol toxicity is not fully elucidated. There are indications that point towards mitochondrial disfunction (Sisemore, Zheng et al. 2001) and eNOS/iNOS stimulation (Nakanishi, Ishizaki et al. 2000).

Although the role of sEH in turnover and bioactivation of leukotoxin has been elucidated several years ago, the impact of sEH hydrolysis and regulation of other epoxy lipids still is less investigated and only recently started to evolve and gain interest.

The ethanol amide of arachidonic acid – anandamide – is an endocannabinoid that activates the G_i protein coupled cannabinoid receptors CB1 and CB2 (Pacher, Batkai et al. 2006). The work of Snider showed that anandamide, similar to arachidonic acid, can be epoxygenated by the CYP450 monooxygenase CYP2D6 (Snider, Sikora et al. 2008) and that one of the arising epoxides, 5(6)- EET-EA, also is a CB2 receptor agonist (Snider, Nast et al. 2009). The study demonstrated that 5(6)-EET-EA binds to CB1 and CB2 receptors expressed in CHO cells, albeit affinity to CB2 is orders of magnitudes higher than to CB1. In addition to that, they could demonstrate that incubation of 5(6)-EET-EA in mouse brain homogenates led to a decrease of the respective epoxide and to an increase in the formation of 5(6)-dihydroxyeicosatrienoic acid ethanol amide (5(6)-DHET-EA) over time. This effect was AUDA (12-(3-adamantan-1-yl-ureido) dodecanoic acid) sensitive and hydrolysis was dose - dependently inhibited by the inhibitor, suggesting that 5(6) EET-EA is hydrolyzed by sEH in the brain.

Besides epoxidation of arachidonic acid, linoleic acid and anandamide, epoxidation of polyunsaturated long chain fatty acids (PUFA) like eicosapentaenoic acid (EPA) and docosahexaenoic acid (DHA) has been demonstrated. The polyunsaturated ω-3 fatty acid EPA is a substrate for human CYP1A1 (Schwarz, Kisselev et al. 2004). One major epoxy metabolite, 17(18) EETeE (epoxyeicosatetraenoic acid), induces relaxing effects on human pulmonary artery and airway smooth muscles (bronchi) in a

concentration dependent manner (Morin, Sirois et al. 2009). The effect can be reversed by addition of inhibitors targeting BK-type calcium activated potassium ion channels. This study confirms the finding of Lauterbach et al. (Lauterbach, Barbosa-Sicard et al. 2002), who showed a BK potassium channel - dependent, 14fold increase of K^+ current with 17(R),18(S) EETeE compared to a 6fold increase by equimolar concentration of 11(12) EET in rat cerebral vascular smooth muscle cells (VSMC).

Currently there is no data on specific CYP450 epoxygenation of DHA available. However, hepatic and renal microsomes react with DHA to produce the respective epoxy metabolites (VanRollins, Baker et al. 1984). Chemically synthesized DHA epoxides (e.g. 19(20) epoxydocosapentaenoic acid; 19(20) EDPE) inhibit platelet aggregation and have vasodilative effects on porcine arterioles (VanRollins 1995; Ye, Zhang et al. 2002) which points towards possible physiological relevance of these compounds.

Both fatty acids, DHA and EPA, are components of fish oil and some of the cardio protective and antihypertensive effects described for fish oil diet might be attributed to epoxy derivatives of these molecules and their effects on platelet aggregation and vasodilation.

Hepoxilins (Hepoxilin A3 (HxA3) and B3 (HxB3)) are hydroxyl-epoxy metabolites of arachidonic acid and are formed by the 12-lipoxygenase (12*S*-LOX) pathway (Nigam, Zafiriou et al. 2007) from arachidonic acid. Their intrinsic biologic activity relates to inflammation, insulin secretion and intracellular Ca^{2+} release as well as Ca^{2+} transport. HxA3 plays an important role in the regulation of neutrophil migration in inflammatory processes (Mrsny, Gewirtz et al. 2004) and is thought to have proinflammatory effects in the skin (Anton, Puig et al. 1998). Together with the fact that mutations in the lipoxygenase pathway are associated with ichthyiosis, this indicates that hepoxilins may play a role in epidermal differentiation and skin barrier function. Hydrolysis and degradation of hepoxilins to their corresponding trioxilins has been reported to be catalyzed by hepoxilin epoxide hydrolase, first described two decades ago (Pace-Asciak and Lee 1989). Nevertheless, there is evidence that sEH is the actual enzyme relevant for hepoxilin hydrolysis, since kinetic studies on hepoxilin turnover by sEH point towards higher turnover and catalytic efficacy compared to the published data from Pace-Asciak (unpublished work from Dr. Annette Cronin).

2.3 sEH as pharmacological target - development of sEHi

Due to the important role of sEH in EET regulation, the enzyme became a potential target for treatment of hypertension, inflammatory diseases, pain, diabetes and stroke. The challenge was to develop potent sEH inhibitors (sEHi) that were active *in vivo* and which could be used to investigate the physiological roles of EETs as well as to clarify the role of sEH in the metabolism of these biologically active epoxides. In addition to that, sEHi are developed to yield drugs that can be used as therapeutic in humans and exploit the beneficial effects of EETs as described above.

Chalcone oxides (Mullin and Hammock 1982) and phenylglycidols (Dietze, Kuwano et al. 1991) were the first selective sEH inhibitors. These epoxide containing compounds act as alternative substrates that are slowly converted by the epoxide hydrolase and thus only transiently inhibit the enzyme (Morisseau, Du et al. 1998). Those compounds were not useful for *in vivo* application due to the reversibility of inhibition and to the fact that these compounds are unstable and inactivated rapidly by

glutathione and glutathione transferases (Mullin and Hammock 1982). Morriseau and his colleagues discovered substituted ureas and carbamates as more stable and very potent inhibitors of sEH (Morisseau, Goodrow et al. 1999). They permanently inhibit sEH activity with nanomolar Ki by imitating features of the covalent intermediate transition state. The more effective urea pharmacophore interacts with the active site by hydrogen bonds and salt bridges. This was demonstrated by x-ray crystallography studies on mouse sEH complexed with disubstituted urea derived inhibitors (Argiriadi, Morisseau et al. 2000).

Altogether, these urea based inhibitors were more useful for *in vitro* experiments to investigate the endogenous role of sEH, but still less applicable for *in vivo* studies due to the limited water solubility. Yet, the *in vivo* effect was demonstrated by studies in animal hypertension models with DCU (N,N-dicyclohexylurea) (Yu, Xu et al. 2000) and CDU (1-cyclohexyl-3-dodecyl-urea) (Imig, Zhao et al. 2002), where single and chronic administration of sEHi led to lowered blood pressure. To enhance water solubility, functional polar groups were integrated into the alkyl side chain of 1,3-disubstitued ureas, which resulted in compounds that were weak mimics of EETs but maintained their potency (Morisseau, Goodrow et al. 2002; Kim, Heirtzler et al. 2005). One of these inhibitors, 12-(3-adamantan-1-yl-ureido) dodecanoic acid (AUDA), showed improved physicochemical properties and inhibited sEH in both cultured cells and animals (Dorrance, Rupp et al. 2005; Jung, Brandes et al. 2005; Sellers, Sun et al. 2005; Li, Carroll et al. 2008). Although AUDA can be administered orally and is a potent inhibitor, ongoing developments targeted to further increase the bioavailability of this sEHi by incorporation of secondary pharmacophores, resulted in the production of *t*-AUCB (Hwang, Tsai et al. 2007). This compound has high bioavailability and potency. Beside the effort to improve sEHi for experimental use, the development of compounds for application and therapeutic use in humans has progressed. Currently a sEHi is tested in Phase II clinical trial for the treatment of hypertension and diabetes (Arete Therapeutics Inc 2009).

2.4 Identification of novel epoxide hydrolases

The fact that mEH and sEH do have human relevance in terms of detoxification and physiological regulation, and even became a pharmaceutical target, raises the question if there are other hitherto unknown epoxide hydrolases with similar properties. Such enzymes would open up novel regulatory pathways and therapeutic targets or could reveal protective mechanisms towards xenobiotic carcinogens. Since the sequence motives of α/β-hydrolase fold enzymes are highly conserved, they can be used to identify putative novel epoxide hydrolases. Previous sequence comparisons (Arand, Grant et al. 1994) showed that the amino acid sequence RVIAPDLRGYGDSDKP can be used as bait in database searches for novel epoxide hydrolase candidates.

The search motif is sufficient in length and degree of conservation and contains the G-X-Sm-X-S/T sequence motif (RVIAPDLR**GYGDS**DKP) as described in chapter 2.1.1. By searching the genome based human protein database with this 16 amino acid query (http://www.ncbi.nlm.nih.gov/genome/seq/BlastGen/ BlastGen.cgi?taxid=9606), three novel putative EHs were identified in our group: EH3 (ABHD9), EH4 (ABDH7) and peg1/MEST (figure 2-7). Sequence alignment of EH3 and EH4 with other mammalian EHs showed that they are related to sEH,

and similarity was seen after alignment with two recently identified epoxide hydrolases of C. elegans (Harris, Aronov et al. 2008). Figure 2-7 shows the overall relationship of the novel candidate enzymes EH3 and EH4 with other known epoxide hydrolases. Further it depicts that EH3 and EH4 represent a new subfamily of mammalian EHs due to their 45% sequence identity. Direct sequence analysis and comparison with sEH shows that EH3 and EH4 share all characteristic sequence motifs of α/β-hydrolase fold EHs that are necessary for epoxide hydrolase function (figure 2-8).

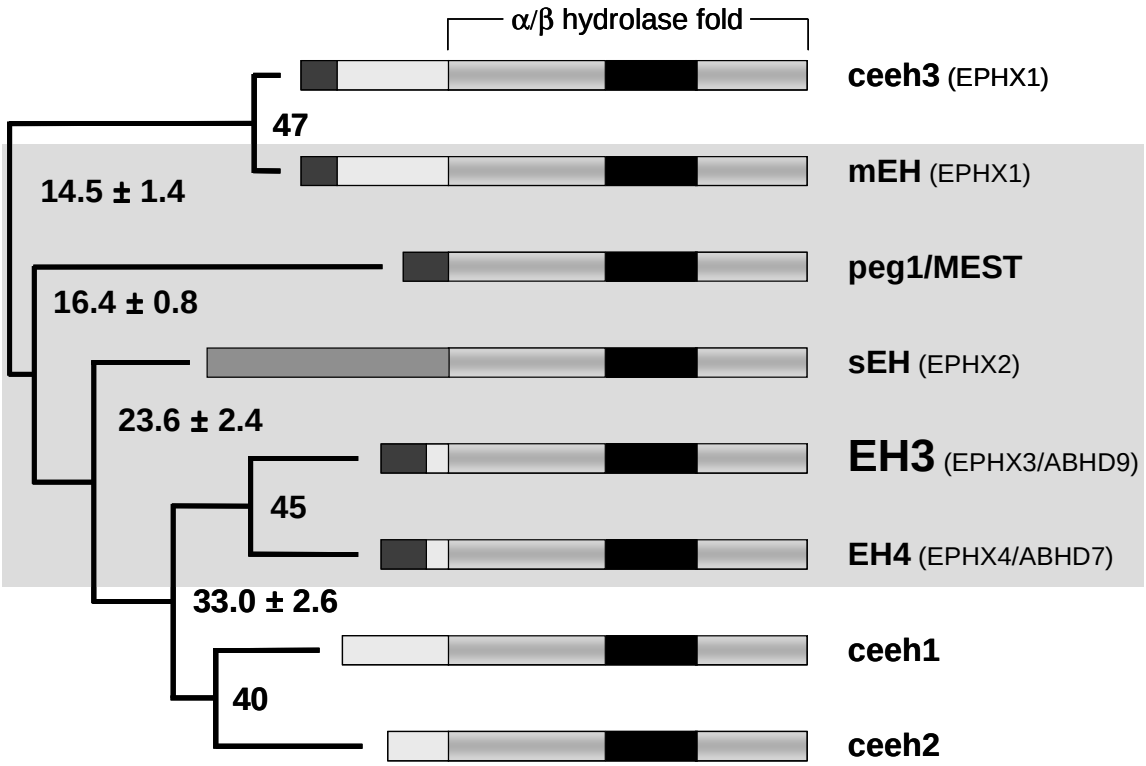

Figure 2-6: *Relationship tree of known and putative mammalian epoxide hydrolases and epoxide hydrolases of C. elegans (ceeh). EH3 and EH4 represent a novel subfamily of mammalian epoxide hydrolases (mammalian EHs are highlighted in grey).*

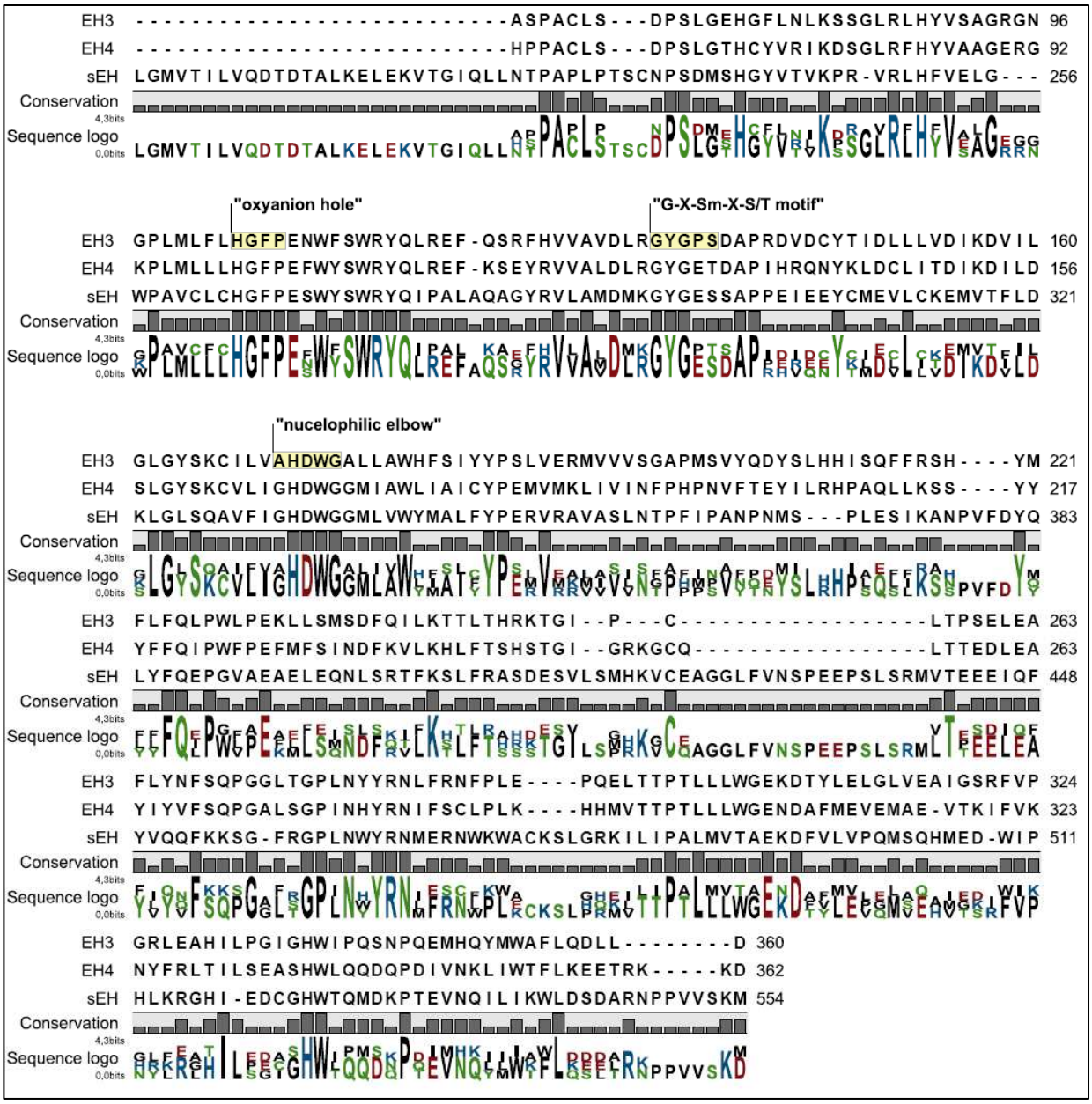

Figure 2-7: *Sequence alignment of candidate enzymes EH3 and EH4 with human soluble epoxide hydrolase. The characteristic and highly conserved sequence motives for α/β-hydrolase fold EHs are indicated.*

3 AIM OF THE STUDY

The aim of this work was to biochemically and functionally characterize the putative new human epoxide hydrolases EH3 (ABHD7) and EH4 (ABHD7), in order to gather insight into their potential toxicological and/or physiological relevance for the human organism. Since there is no data on EH4 activity available to date, the main objective is to investigate whether EH4 is an enzymatically active epoxide hydrolase. The characterization of EH4 comprises two approaches:

a) the recombinant expression of enzymatically active EH4 protein in order to investigate the enzymatic activity towards different epoxides,

b) the generation of a detection tool that would allow the detection of EH4 in recombinant lysates and different tissues.

Previous work in our group demonstrated that EH3 has epoxide hydrolase activity. Epoxide hydrolases fulfill two different functions for the human organism. Depending on the substrate spectrum, they either play a role in the detoxification of genotoxic epoxides, or in the turnover of endogenous signaling molecules. This raises the question if EH3 is a detoxifying enzyme or a physiological regulator. To answer this question, the respective substrate spectrum of EH3 should be analyzed. The characteristics of the substrate spectrum could give information on the preferred substrates of EH3 and therefore on the relevance of the novel epoxide hydrolase for the human organism.

4 MATERIALS AND METHODS

4.1 Chemicals and enzymes

All chemicals were obtained from Roth (Roth AG, Arlesheim, Switzerland) and Sigma (Sigma-Aldrich, Basel, Switzerland) if not indicated otherwise. Restriction endonucleases were derived from NEB (New England BioLabs). Fatty acid derived epoxy substrates were purchased at CaymanChemicals, EETs and DHETs were kindly provided by Dr. John Falck (University of Texas). Taq Polymerase and Pfu Polymerase were kindly provided by Dr. Annette Cronin (University of Zurich, Switzerland).

4.2 Vectors and plasmids

The IRAK plasmid containing the EH4 cDNA (clone library NIH_MCG_121 ;(Gerhard, Wagner et al. 2004)) was derived from imaGens (Berlin, Germany). The expression plasmids pRSET b, c and pFastBac™ were obtained from Invitrogen (Invitrogen™, Switzerland) and pIRESneo was purchased from Clonetech (Clonetech, Europe). The vector named pGEFGSTN was constructed by Dr. Annette Cronin via subcloning of the GST gene from the pGEX vector system (Amersham) into pGEF II (Arand, Hemmer et al. 1999) by using BspHI and NcoI restriction sites present in the applied primers (GST-Sf *5`- cat gtc atg acc cct ata cta ggt tat tgg aaa-3`* and GST-Sr *5`- cat gcc atg gcg ctt cca cgc gga acc aga tcc ga-3`*). Insertion of a His-cassette into pGEF II by the use of the following cassette primers resulted in the vector labeled pGEF-HisC (kindly provided by Dr. Annette Cronin): His pFastBac for *5'-g cat cac cat cac cat cac ta-3'* and His pFastBac rev *3'-acgtc gta gtg gta gtg gta gtg attcga-5'* . Expression vector pGEFHisCnEH2 and EH3 baculovirus originated from previous work of Dr. Magdalena Adamska.

4.3 Basic molecular biology methods

This chapter briefly describes the standard methods used for cloning and generating the respective expression constructs used in this work.

4.3.1 PCR

A specific nucleotide sequence (up to ~10kb) is generally amplified by using PCR technique. Amplification of DNA was typically carried out in a volume of 50µl PCR mix containing 250µM dNTPs (Fermentas), PCR buffer (10x PCR buffer: 200 mM Tris HCl,100 mM $(NH_4)_2$ SO_4, 100 mM KCl, 20 mM $MgSO_4$, 1% Triton X-100, 1mg/ml BSA, Tris pH 8.8), 25 pmol sense- and antisense-primer, 1µl Taq or Pfu Polymerase and 50-100 ng template (for cloning purposes) on a thermal cycler (TGradient, Biometra®).

4.3.2 TOPO cloning

Zero Blunt® TOPO® PCR Cloning Kit for Sequencing (Invitrogen) is used for direct insertion of blunt end PCR products into a plasmid vector (pCR4Blunt-TOPO®).The resulting plasmid can be analyzed by sequencing and/or control digestion to confirm the sequence of the cDNA of interest. The reaction was set up according to the manufacturer's protocol. In brief: 2 - 2.5 µl purified PCR product was added to the TOPO® cloning reaction mix. The reaction was incubated 3h at RT before transforming (see 4.3.3.) the TOPO-construct into electrocompetent *E. coli* (Top10). The transformed *E. coli* cells were plated on either ampicillin (100 µg/ml) or kanamycin (50 µg/ml) selective agar plates and incubated over night at 37℃.

4.3.3 Transformation and plasmid amplification

To amplify a particular plasmid or construct, the DNA was transformed into electrocompetent Top10 (genotype: F- mcrA Δ(mrr-hsdRMS-mcrBC) Φ80lacZΔM15 ΔlacX74 recA1 araD139 Δ(araleu) 7697 galU galK rpsL (StrR) endA1 nupG). Typically 1-3 µl of the respective plasmid or ligation mix was added to 40 µl electrocompetent cells and incubated on ice for 5 min, before the cells were electroporated at 1.35 kV and 25 µF (BioRad Gene Pulser® Cuvette, 0.1cm electrode; BioRad Gene Pulser™). Subsequently 500 µl LB medium (1% tryptone, 0.5% yeast extract, 1% NaCl) was added and cells were incubated (37 ℃, 220 rpm) for 45 min to allow the expression of the respective antibiotic resistance gene(s). 100 µl of the suspension was plated on selective agar plates (3% agar (Applichem, Germany) in LB medium) and incubated ON at 37℃ in an incubator (HERAEUS). 1-50 ml LB medium (100 µg/ml ampicillin) was inoculated with selected colonies the following day and cultured ON (37℃, 220 rpm) for amplification of the plasmid .

4.3.4 Plasmid isolation

In terms of further processing and analyzing the plasmid and its sequence, the plasmid was isolated using the HiSpeed® Plasmid Midi Kit (50-150 ml overnight *E. coli* culture) or QIAPREP® Spin Miniprep Kit (1-5 ml overnight *E. coli* culture) (QIAGEN, Switzerland). Bacterial cells were harvested, centrifuged (4.000 rpm, 15 min) and plasmid was isolated according to the suppliers manual. For stable transfection into mammalian cells and insect cells, the plasmid /DNA elution was performed under sterile conditions.

4.3.5 Analyzing plasmid

Plasmid was analyzed for correct insert first by appropriate control digestion and subsequent agarose gel electrophoresis. The plasmid was incubated with restriction endonucleases and the recommended NEB buffer for 1h at the appropriate temperature and then analyzed by 1 - 2% agarose gel electrophoresis. To further confirm the nucleotide sequence of the inserted cDNA, the plasmid was sent for sequencing (Microsynth AG, Balgach, Switzerland).

4.3.6 Cloning of cDNA into target vector

To clone the cDNA of interest into the respective expression vector, the cDNA containing plasmid (TOPO vector or any other plasmid) and the target vector were digested with the respective restriction enzymes (1h, 37℃, recommended NEBbuffer). The targ et vector was subsequently dephosphorylated for 30 min at 37℃ by alkaline phosphatase to preve nt self ligation of the vector. DNA was separated electrophoretically and isolated using QIAquick Gel Extraction Kit (QIAGEN, Switzerland). The linearized dephosphorylated vector and the respective cDNA fragment was ligated to construct the expression vector (Ligase mix (10µl) contains: 2µl 5x Ligase buffer (Invitrogen), 1µl T4 Ligase (Invitrogen), 20-50ng vector, 30-100 ng insert).

4.4 mRNA isolation

For in vitro and in vivo expression analysis by reverse transcriptase PCR (RT-PCR) total mRNA was isolated from cultured cells or animal tissues using the Qiagen RNeasy Mini Kit (QIAGEN, Switzerland). Cells and animal tissue were first frozen in liquid nitrogen and then mechanically disrupted using mortar and pestle. All steps were carried out under RNase free conditions on ice until addition of RLT buffer. The subsequent isolation and purification procedure was conducted according to the provided manual.

4.5 cDNA synthesis

The First Strand cDNA Synthesis Kit (Fermentas) was used for the synthesis of first strand cDNA from mRNA templates. cDNA was generated using random hexamer primers (supplied by the kit) according to the manufacturers manual. The resulting cDNA was directly analyzed by PCR for presence of the target transcript using sequence specific primers (PCR conditions and primer sequences see appendix). Amplificates were sent for sequencing (Microsynth, Balgach, Switzerland) to confirm expression of the respective gene.

4.6 Recombinant protein expression

4.6.1 Recombinant expression in E. coli

For recombinant expression in *E. coli*, the respective expression plasmids were transformed (see 4.3.3) into arabinose inducible *E. coli* BL21AI (Genotype: F- ompT hsdSB (rB- mB-) gal dcm araB::T7RNAP-tetA). The strain contains the T7 RNAP gene (RNA polymerase) inserted behind the araBAD promoter that allows the regulation of expression by arabinose in the medium. Expression was induced with arabinose at different concentrations (20 µM - 100 µM) and protein was expressed at various temperatures (18℃ - 37℃, 220 rpm) for a given time period (4 - 12 h). *E. coli* cells were then harvested and centrifuged (15 min, 4.000 rpm, Megafuge 1.0R), resuspended in the designated buffer and disrupted by using a French® Pressure Cell Press (SIM Aminco, Spectronic Instruments;

(Vanderheiden, Fairchild et al. 1970)). Soluble and insoluble protein fractions were analyzed by SDS Page and western blot as described in chapter 4.7.

4.6.2 Recombinant expression in mammalian cells

For recombinant protein expression in mammalian cells, stable transfectants of Cos-7 (african green monkey kidney) (Gluzman 1981) and V79 (chinese hamster lung fibroblasts) (Ford and Yerganian 1958) cells were established and analyzed.

4.6.2.1 Cultivation of mammalian cells

Cos-7 and V79 cells were cultivated in DMEM medium (Gibco) supplemented with 10% FCS and 2mM Glutamine at 37 ℃ with 5% CO_2 (Forma Scientific). Cells were grown until they reached confluency and split 1:5 to 1:10 every 2-3 days by using 0.25% Trypsin/EDTA (Gibco).

4.6.2.2 Stable transfection

For stable transfection Cos-7 cells were seeded in 6 well/plate at 1.5 x 10^5 and V79 cells at 2.5 x 10^5 cells/well and cultured ON to reach 50-60% confluency. To introduce DNA into the cells the jetPEI™ DNA transfection reagent (POLYPLUS-TRANSFECTION, Illkirch Cedex, France) was used according to the manufacturers instruction. In brief: 2- 4 µg of DNA and 5 µl jetPEI™ transfection reagent were diluted in 150 mM NaCl (sterile) to a final volume of 100 µl. To form the DNA/jetPEI™ complex, the jetPEI solution was added to the DNA solution and the mix was then incubated for 15-30 min at RT prior to addition of the mix into the medium. The control well was treated with the NaCl / jetPEI™ mix, to test for cytotoxicity of the transfection reagent and/or the recombinantly expressed protein. Stable transfected cell lines were obtained by G418 selection (500 µg/ml) during 1 month of cell culturing as follows: transfected cells were seeded in 10 cm dishes and cultivated in selective medium until single clones were visible. Clones were then isolated, transferred into a 12-well plate and cultivated. Cells were analyzed for expression of recombinant protein by RT-PCR.

4.6.3 Recombinant expression in insect cells

For recombinant protein expression in insect cells the baculovirus expression vector system (BEVS, Invitrogen) was used. To express heterologous proteins, insect cells are infected with a recombinant baculovirus. The gene that encodes for the matrix protein polyhedrin of the wild-type baculovirus is replaced with the recombinant gene and hence controlled by a baculovirus specific promoter. After infection of the host cells, these cells express the recombinant protein at the very late state of infection (4-5 days post infection) and the protein is generally processed, modified and targeted to the respective cellular location.

4.6.3.1 Generation of Bacmid

For the production of the recombinant baculovirus, a baculovirus shuttle vector (Bacmid) containing the gene of interest was generated by using the Bac-to-Bac® Baculovirus Expression System (Invitrogen). This system is based on site specific transposition of an expression cassette that is located on a donor plasmid, into the baculovirus genome (present as large bacmid in specifically engineered E. coli cells). The transposition into the bacmid proceeds in modified E. coli cells (DH10Bac™) by taking advantage of the bacterial Tn7 transposon (Luckow, Lee et al. 1993). First, the gene of interest is cloned into the pFastBac™ donor plasmid to generate a recombinant donor plasmid (figure 4-1). The expression cassette of the donor plasmid is flanked by the two transposase binding sites Tn7R and Tn7L respectively and controlled by the Autographa californica multiple nuclear polyhedrosis virus (AcMPNV) polyhedrin (PH) promoter (pPolh). The recombinant donor plasmid is then transformed into chemically competent DH10Bac™ E. coli cells to form the recombinant baculovirus (figure 4-3). DH10Bac™ cells contain a baculovirus shuttle vector (Bacmid) that replicates in E. coli like a large plasmid and yields infectious virus particles when introduced into insect cells. Besides the recombinant bacmid that contains a mini attTn7 target site, DH10Bac™ cells include a helper plasmid which provides Tn7 transposase (figure 4-2). The transposase encoded on the helper plasmid binds to the transposase binding sites Tn7R and Tn7L on the donor plasmid and leads to transposition of the expression cassette into the mini attTn7 target site within the bacmid. Since all three plasmids display different antibiotic resistance genes and insertion into the mini attTn7 site disrupts LacZα reading frame, positive recombinant bacmids can be indentified by using selective conditions and blue/white screening (Ullmann, Jacob et al. 1967). Positive bacterial clones are inoculated into LB medium (kanamycin 50 µg/ml, gentamycin 7 µg/ml, tetracycline 10 µg/ml) and cultured ON (37°C, 220 rpm). The Bacmid was isolated as described in 4.3.4. (For subsequent transfection of the bacmid into insect cells, elution of the bacmid DNA from the DH10Bac™ cells needs to be performed under sterile conditions).

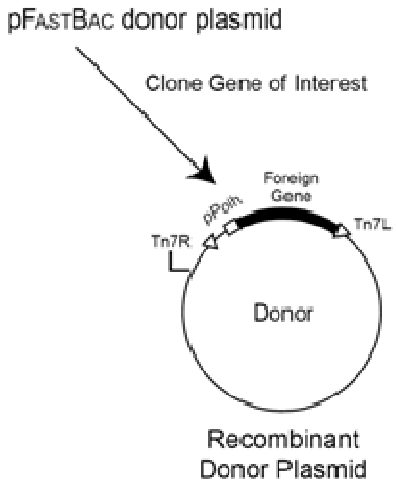

Figure 4-1: *Generating a recombinant donor plasmid*

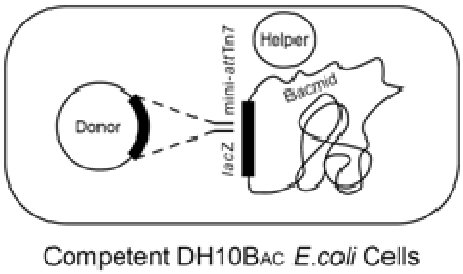

Figure 4-2: *Transposition of expression cassette into Bacmid in DH10Bac™*

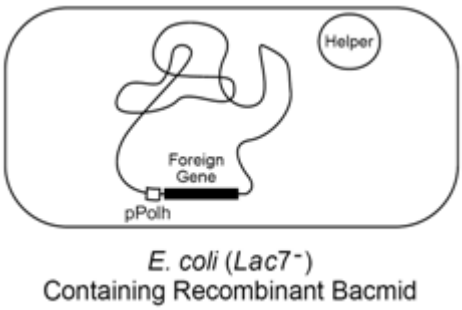

Figure 4-3: *Recombinant Bacmid containing the foreign gene*

4.6.3.2 Transfection of insect (Sf9) cells

The Sf9 cell line used in this study derives from clonal isolation of the *Spodoptera frugiperda* cell line IPLB-Sf21-AET, which was originally isolated from ovarian tissue of the fall armyworm (Vaughn, Goodwin et al. 1977). For introducing the recombinant bacmid DNA into the cells, the jetPEI™ DNA transfection reagent (POLYPLUS-TRANSFECTION, Illkirch Cedex, France) was used as described in 4.6.2.2. For transfection of Sf9 cells, 4x105 cells/well were seeded in a 6-well plate and cultured ON in TMN-FH Insect Medium (BD Bioscience, Belgium) to form a monolayer culture. After transfection with the bacmid DNA, the plate was incubated at 28℃ (He raeus) for 3-4 days until signs of infection (compared to control plate) were visible. The Virus was harvested by collecting the medium and used as virus stock (labeled P0). Then immediately 200 µl lysis buffer (10 mM Tris, pH 7.5; 130 mM NaCl; 1% Triton™-X-100; 10 mM NaF, 10 mM NaPi, 10 mM NaPPi) was added to the well, cells were scraped and transferred to a 1.5 ml tube (Eppendorf). The sample was incubated on ice for 45 min and then homogenized by passing the lysate 3 times through a 27G syringe. Subsequent analysis for recombinant protein expression by western blot was performed as described in 4.7.3.

4.6.3.3 Routine cultivation and expression of recombinant protein

Sf9 cells were generally sub cultured as monolayer in a 75 cm^2 flask (28℃, TMN-FH Insect Medium) and split 1:20 when they reached 80 - 100% confluency. For recombinant expression of proteins, Sf9 cells were cultured in suspension (RT, 100 rpm). Insect cells can adapt from monolayer to suspension culture conditions because the cells are not anchorage dependent per se. Typically 25-100 ml SF-3 BaculoExpress ICM medium (Amimed®, Switzerland) was inoculated with cells to reach a density of 0.5 - 1x10^6 cells/ml and cells were infected when they reach a density of 2x10^6 cells/ml. Virus titer was determined by EPDA (End-point dilution assay) and Plaque assay as described in the Baculovirus Expression Vector System Manual (Pharmingen 1999). Cells were infected with a MOI (multiplicity of infection) between 1 and 5 and incubated (RT, 100 rpm) for 4 -6 days. Cells were harvested, washed with assay buffer (10mM Tris, 1mM EDTA, 100mM NaCl, 6% Glycerol, pH7.4) and disrupted by French® pressure cell press. Aliquots were frozen in liquid nitrogen and stored at -80℃ for up to 6 months.

4.7 Protein analysis and characterization

4.7.1 SDS-PAGE

Separation of proteins was done by either Tris-Glycine (Laemmli 1970) or Tris-Tricine SDS- PAGE (Schagger and von Jagow 1987) according to the molecular size of the target protein. Tricine SDS-PAGE is the preferred method for separating molecules smaller than 30kDa.

Proteins are concentrated in the stacking gel (pH 6.8) and separated due to molecular weight in the running gel (pH 8.8). The composition of the running and stacking gels are shown below (tables 4-1 and 4-2). Samples were mixed with laemmli buffer (15% SDS, 10% Glycerol, β-Mercaptoethanol 1:10 (added before use)) and incubated at RT for 10 min or at 60℃ for 5 min since EH3 turned out to be

heat sensitive during the present work. Tris-Glycine electrophoresis was performed in polyacrylamide running buffer (1x PAA buffer: 25 mM TrisBase, pH 8.3, 250 mM Glycine, 0.1% SDS). The Tris Tricine buffer system consists of two different buffers: anode buffer (0.2M Tris, pH 8.9) and cathode buffer (0.1M Tris, 0.1M Tricine, 0.1%SDS, pH 8.25) which were added separately to the lower electrode (anode buffer) and upper electrode (cathode buffer) respectively.

Tris Glycine SDS-Page

	stacking gel (5%)	**running gel (12.5%)**
	[ml]	**[ml]**
Rotiphorese® Gel 30	5.6	29.12
0.5M Tris, pH 6.8	0.875	-
1.5M Tris pH 8.8	-	17.5
H2O bidest	28	21.7
10% SDS	0.35	0.7
10% APS	0.35	0.7
TEMED	0.035	0.07

Table 4-1: *Composition of PAA gels for Tris-Glycine SDS-PAGE. Volumes given in the table are adequate for preparation of 7 gels (8x9cm).*

Tris Tricine SDS PAGE

	stacking gel (6%)	**running gel (16%)**
	[ml]	**[ml]**
Rotiphorese® Gel 30	7.2	33.6
Gel buffer (3M Tris, 0.3% SDS)	4.5	21
Glycerol (99.5%)	-	8.19
H2O	24.3	0.21
10% APS	0.3	0.214
TEMED	0.03	0.021

Table 4-2*: Composition of PAA gels for Tris-Tricine SDS-PAGE. Volumes given in the table are adequate for preparation of 7 gels using (8x9cm).*

4.7.2 Coomassie staining

To visualize the separated proteins in polyacrylamide gels, the respective gels were stained with Coomassie (6µM Brilliant Blue R, 6µM Brilliant Blue G, 45% methanol, 10% acidic acid) for 20 minutes. Unspecific non-protein bound coomassie was destained by incubation in destaining solution (10% acetic acid, 15% 2-propanol) for at least 2 hours.

4.7.3 Western blot analysis

To detect specific proteins in tissue homogenates of cell lysates, western blot analysis was performed. Proteins were blotted onto a PVDF membrane (Immobilion-P, Millipore, USA) using semi dry blotting technique. The PVDF membranes for blotting were first activated in methanol and subsequently equilibrated in blotting buffer (10% PAA buffer, 20% methanol) prior to use. The PVDF membrane and the PAA gel was placed between two layers of filter membranes (3 filter membranes each, equilibrated in blotting buffer). After blotting for 2h at 0.17 mA /cm2 the membrane was blocked in 5% non fat dried milk in TBST (10 mM Tris, 150 mM NaCl, 0.5% Tween 20, pH 8.0) for 1h at room temperature on an orbital shaker. Incubation with the first antibody (at a dilution of 1:1000 for both α-His and α-EH3) was carried out in 5% non fat dried milk in TBST or *E. coli* lysate (6 mg/ml total protein) for 3h at room temperature or ON at 4℃. Membranes were rinsed thr ee times for 5 min in TBST prior to incubation with the second antibody. After the incubation with the second AP conjugated antibody (anti rabbit IgG, whole molecule, F(ab`)2 fragment, Sigma, 1:10.000) for 1h at room temperature (orbital shaker), the membrane was washed twice for 5 min in TBST before equilibrating with AP-buffer (100 mM NaCl, 100 mM Tris, 5 mM MgCl, pH 9.5) for 5 min. For analysis of protein expression in human tissues a total protein western blot of human tissues was purchased from AMS Biotechnology (AMS Biotechnology, Europe, Lugano) and analyzed as described above. Protein was visualized using BCIP and NBT as colorigenic substrate.

4.7.4 Protein purification

4.7.4.1 GST affinity chromatography

For batch purification of GST-tagged proteins the Glutathione sepharose 4B (Amersham) was used. A 50% GSH sepharose slurry in binding buffer (PBS: 140 mM NaCl, 2.7 mM KCl, 10 mM, Na2HPO4, 1.8 mM KH2PO4, pH 7.4) was prepared as described in the manufacturers manual. The protein solution corresponding to approx. 10 mg GST fusion protein was incubated with GSH sepharose for 1 hour at 4℃ (60rpm). The suspension was then centrifuged (5 min, 500g) to sediment the sepharose and the supernatant (unbound proteins) was discarded. The sepharose pellet was then washed three times with binding buffer (10 times the bed volume) before incubation with elution buffer (10 mM GSH, 50 mM Tris, pH 8.0) for 10 minutes at RT and 60 rpm. To collect the eluted proteins the suspension was centrifuged (5 min, 500 g) and the supernatant was collected. The elution was repeated twice. The different fractions were analyzed by SDS-Page.

4.7.4.2 Affinity chromatography of His-tagged proteins

Histidine is an amino acid that interacts with immobilized Ni2+ ions by forming coordination bonds between the electrons of the imidazole ring and the metal ion. Proteins or peptides that contain a sequence of histidine residues are retained on a Ni2+ affinity matrix and may be eluted by adding free imidazole. Sf9 cells (1.8x108 in 35 ml PBS; MOI 5, dpi 8) recombinantly expressing His-tagged protein were resuspended in start buffer (500mM NaCl, 20% glycerol, 20mM sodium phosphate, pH 7.5) and

disrupted by French® pressure cell press. Cell lysates were centrifuged (45 min, 14.000 rpm) and the sterile filtered supernatant was injected on the column. Samples were separated on a HiTrap Chelating HP column (1 ml, Amersham Biosciences) using a Biologic DuoFlow system from BioRad. The mobile phase consisted of (A) 500mM NaCl, 20% glycerol, 20mM sodium phosphate, pH 7.5 and (B) 500mM imidazole, 500mM NaCl, 20% glycerol, 20mM sodium phosphate, pH 7.5 at a flow rate of 1ml/min. Starting conditions (97% A, 3% B) were maintained for 5 minutes before injection of 40 ml sample for 40 min, followed by isocratic flow (97% A, 3% B) for 7minutes to load the total sample volume on the column. A 2-step linear gradient was applied as follows: from 3% to 20% B within 8 minutes followed by increasing buffer B from 20% to 100% within 8 minutes. An isocratic flow of 100% B was held for 2 minutes before conditions were reset to starting conditions (97% A, 3% B within 2 minutes) and maintained for 5 minutes.

His-tagged proteins expressed in *E. coli* were resuspended in ib buffer (6M Urea, 100mM Tris, NaN3, pH 8.5) to resolve inclusion bodies prior to purification.

4.7.5 Peptide Analysis by LC-MS/MS

LC-MS/MS is commonly used in proteomics to identify proteins from complex mixtures (e.g. blood samples, cell lysate) or to investigate specific posttranslational modifications of a target protein. Protein samples are first digested enzymatically before separation and analysis by liquid chromatography and mass spectrometry. The resulting MS data are used to identify proteins from primary sequence databases using the Mascot search engine.

In this work LC-MS/MS analysis was used to confirm the presence of proteins in whole Sf9 cell lysates.

4.7.5.1 Sample preparation from Sf9 culture (methanol extraction)

Sf9 cells were cultured in monolayer (6-well plate) and infected with a recombinant baculovirus for expression of foreign protein. 4 days after infection cells were harvested by scraping and sonified (Sonorex, Bandelin) before centrifugation at 14.000 rpm for 10 minutes (Centrifuge 5417R, eppendorf). The isolation of membrane proteins and sample preparation for LC-MS/MS analysis was performed according to the protocol of Blonder and colleagues (Blonder, Chan et al. 2006). Solubilisation buffer (60% methanol, 100mM NH_4HCO_3, pH 7.8) was added to the pellet to reach a final concentration of approximately 1µg/µl membrane proteins (based on the assumption that 7% of total pellet cell mass refer to total protein content of which approximately 10% are membrane proteins. The density of the pellet is estimated to 1g/ml). The pellet was solubilized by 10 cycles of sonification for 1 minute and vortexed for 2 minutes prior to protein denaturation for 1min at 90°C. After denaturation of the proteins the sample was immediately incubated on ice until further processing. Proteins were digested by adding trypsin directly into the solubilising buffer (with a trypsin/protein ratio of 1/50). Samples were incubated at 37°C for 5h bef ore the digest was centrifuged for 3 min at 14.000 rpm. The collected supernatant was lyophilized under a stream of nitrogen, resolved in 100 µl 10% acetonitrile in 0.1% formic acid and analyzed by LC-MS/MS.

4.7.5.2 Sample preparation from coomassie gel (in gel digestion)

Proteins of Sf9 lysates were separated on a 12.5 % SDS gel and stained with coomassie blue for visualization. The protein of interest was excised from the gel and cut in 1 mm3 pieces. To destain and shrink the gel pieces, samples were incubated twice with 50% acetonitrile in 20 mM NH4CO3 buffer for 30 min at 37°C, before gel pieces were dried under vacuum and proteins were digested with 5 ng/ml trypsin in 100 µl digestion buffer (10 mM NH4CO3, 10% acetonitrile, 0.01% Triton X-100, pH 8.0) ON at 37°C. After sonification for 5 min the supernatant was collected, dried under a stream of nitrogen and the peptides were resolved in 2% acetonitrile in 0.1% formic acid. Before LC-MS/MS analysis, the sample was filtered through 0.45 µm regenerated cellulose filter (infochroma AG, Zug, Switzerland).

4.7.5.3 LC-MS/MS measurement

The resulting peptides were separated on a Agilent 1100 liquid chromatography system using a Agilent ZORBAX 300SB-C18 narrow bore reversed phase column (2.1 µm x 150 mm, pore size 5 µm) connected to the corresponding ZORBAX 300 SB guard column. The mobile phase includes (A) 0.1% formic acid and (B) acetonitrile containing 0.1% formic acid, using a flow rate of 170 µl/min and an injection volume of 5 µl. Starting conditions of 2% buffer B were maintained for 5 min, followed by a linear gradient from 2% to 100% B within 50 min. An isocratic flow of 100% buffer B was applied for 5 min, and finally the column was re-equilibrated for 10 min with 2% buffer B. The HPLC system was coupled to a 4000 QTrap hybrid quadrupole linear ion trap mass spectrometer (Applied Biosystems) equipped with a TurboV source and ESI interface. For the selective identification of EH4 peptides, the QTrap system was configured to detect specific transitions in a MIDAS workflow using MRM in the positive mode with the following source-specific parameters: IS = 5000 V, TEM = 450 °C, curtain gas = 25 (CUR), nebulizer gas = 40 (GS1), heater gas = 50 (GS2) and collision gas = 10 (CAD). For detection of EH4 peptides, a list of MRM transitions was generated either by manual calculation or by the Applied Biosystems MIDAS software (see appendix for details). Transitions were included for tryptic peptides (maximum of one missed cleavage) for single- to triple-charged species for the Q1 mass range 400–2000 m/z using calculated collision energies and a dwell time of 14 ms for each MRM transition to ensure analysis during the peak elution time. In the triple-quadrupole scan function, the precursor ions were selected by the first quadrupole set with a unit mass window. Using an information-dependent acquisition (IDA) workflow, the mass spectrometer was switched to an enhanced product ion scan mode, when an individual MRM signal exceeded 200 counts. All MRM transitions were measured sequentially with the cycle time of 3.22 s looped throughout the length of the HPLC separation. Enhanced product ion scanning was carried out using parameters detailed in the appendix (8.6.4). Fragment spectra were matched against a protein sequence database (National Center for Biotechnology Information) using the Mascot search engine (Matrix Science Ltd.). All Mascot searches were performed species specific, with trypsin plus one missed cleavage, a peptide tolerance of 1.2 Da, and an MS/MS tolerance of 0.5 Da, allowing error-tolerant searches. In addition, data were examined manually using the features of the Analyst 1.4.2 software package.

4.7.6 Determination of subcellular localization

For an investigation of the cellular localization of proteins, cell lysates can be analyzed by differential centrifugation to separate subcellular compartments.

Whole Sf9 cell lysate (400µl) was centrifuged for 15 min at 800g to separate the nucleic fraction (N) from the cytosolic fraction (CytoI). The 800g pellet was homogenized in 400 µl 0.1 M phosphate buffer (pH 7.4) and centrifuged for 15 min at 8000g to pellet nuclei (N-8000g) (incubate on ice). The 800g supernatant (CytoI) was further processed to separate mitochondria from microsomal proteins. Mitochondria were pelleted after centrifugation for 15 min at 6.000g (6000g (Cyto)). The pellet was resolved and homogenized in 400 µl 0.1 M phosphate buffer to form mitochondrial fraction and stored on ice. Microsomal proteins were separated from pure cytosol by centrifugation at 100.000g (100.000g (CytoI)) for 1h (Beckmann Optima™TLX Ultracentrifuge; TLA 100.3, 100K RPM, S.N. 2809) and pellet was resolved and homogenized in 400µl phosphate buffer. The fractions were analyzed by western blot.

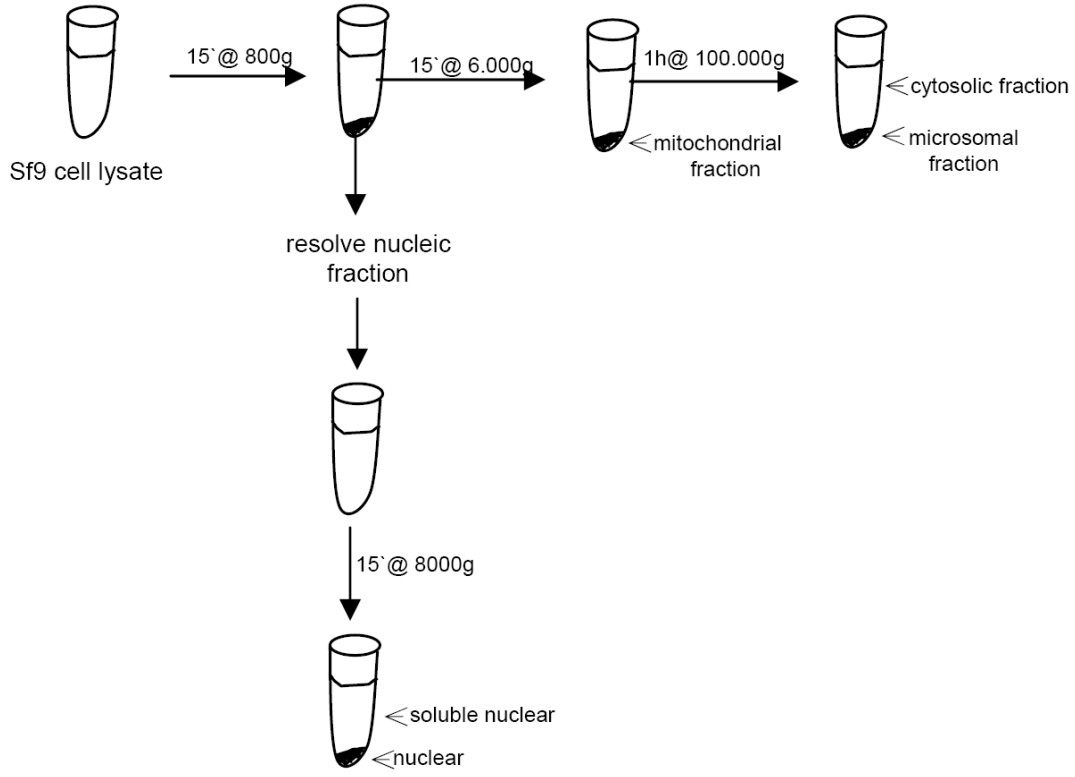

Figure 4-4: *Complete overview on the different centrifugation steps for subcellular centrifugation.*

4.7.7 Quantification of EH3

For calculation of the kinetic constants of EH3, the enzyme was immuno quantified in insect cell lysates. First, recombinant EH3 obtained as inclusion bodies in *E. coli* was washed in Tris-buffered saline (Tris-HCl, 20 mM, NaCl, 100 mM, pH 8.0). Inclusion bodies were recovered by centrifugation and dissolved in high SDS sample buffer (sodium dodecyl sulfate, 5 %, glycerol, 8 %, 2-mercaptoethanol, 3.3 %) to yield a final concentration in of 0.6 µg/µl. Ten microliters of 1:1 serial

dilutions of the dissolved EH3 protein were analyzed by SDS-PAGE and coomassie staining. The density of the protein bands was compared to samples with known, increasing concentrations (0.25 – 2 µg per lane) of a bovine serum albumin. Gels were photographed with the digital camera of a gel documentation system (GeneFlash®, Syngene, Cambridge, UK) and band intensities were quantified with the public domain software package ImageJ (NIH, USA), using the routines of the Analyze/Gels sub menu. ImageJ is an image processing and analyzing program that was used to quantify on the basis of grey level after signal density calibration. Pictures (.tiff) from coomassie gels and western blots were imported and the respective lanes that included the band of interest were marked, and density was measured. The resulting plot showed the density profile. The respective area under the curve was analyzed and used for calibration of density signals and hence quantification of proteins. The obtained calibration curve for EH3 signals from western blot was fitted with non linear regression by using the GraphPad PRISM® software.

4.8 Enzymatic activity assays

4.8.1 CDNB assay

The CDNB (1-chloro-2,4-dinitrobenzene) assay is used to detect the enzymatic activity of GST fusion proteins. The conjugation of CDNB with glutathione (GSH) by GST forms a product that can be measured at 340 nm. Bacterial lysates (corresponding to 5 µg total protein) disrupted by a French® pressure cell press were incubated at 37°C with 1mM GSH and 100µM CDNB diluted in reaction buffer (0.1M potassium buffer, pH 6.5) in a total volume of 200µl in a 96 well plate. Absorbance at 340nm was measured continuously using a SpectraMax GeminiXS plate reader (Molecular Devices) and SoftMax software for analysis.

4.8.2 Activity assay using radio labeled substrates

The radio labeled substrates [1-14C] styrene 7,8-oxid or [1-14C] 9,10 epoxystearic acid were used for analysis of epoxide hydrolase activity (Arand, Cronin et al. 2005). The activity of recombinantly expressed protein was assayed in the presence of 100 µM [1-14C] styrene 7,8-oxid (Arand, Cronin et al. 2003) or 1 µM [1-14C] 9,10 epoxystearic acid (Muller, Arand et al. 1997). 20 µl of bacterial lysates (16 µg/µl total protein in 0.1M phosphate buffer, pH 7.4) or 4.5 – 6x104 cells in 0.1M phosphate buffer (pH 7.4) were added to the buffer/substrate mix to reach a final volume of 200 µl and 100 µl respectively. After incubation at 37°C for 10 minutes, organic solvent was added and samples were vortexed and processed as follows: styrene oxide turnover was terminated by adding one volume (200µl) chloroform and the samples were centrifuged for 5 min at 14.000 rpm to extract the reaction product into the aqueous phase. 100µl of the upper phase was added to 2 ml Rotiszint® ecoplus (Roth, Germany) and radioactivity was measured using a liquid scintillation counter (Liquid scintillation analyzer TRI-CARB 2000 CA, Packard, Germany). ESA (9,10 epoxystearic acid) turnover was terminated by adding 2 volumes ethyl acetate. The suspension was centrifuged for 5 minutes at 14.000 rpm and 50 µl of the organic phase were spotted on a silica-gel 60 F254 plate. The thin layer

chromatogram was developed in n-hexane/diethyl ether/formic acid (30:70:2) buffer and exposed to a Storage Phosphor Screen and scanned in the Packard CycloneTM Storage Phosphor Scanner.

4.8.3 Activity assay using LC-MS/MS

LC-MS/MS analysis was used to test for a specific epoxide hydrolase activity towards different lipid derived epoxides (with proven or assumed physiological activity) and to determine kinetic parameters. Enzymatic activity of EHs was assayed by determining the formation of the corresponding dihydrodiol products.

4.8.3.1 Substrate screening I (EpOMEs, Hepoxilins, 19(20) EDPE, 17(18) EETeE)

To test for a specific activity towards19(20) EDPE, 17(18) EETeE, 9(10) EpOME, 12(13) EpOME, HxA3 and HxB3, 20µl EH3 or control lysate (infected with Rv3790; corresponding to 14ng enzyme) was incubated with the respective substrate for 15 – 30 min at 37℃ at a final concentration of 3 µM (EpoMEs, 19(20) EDPE, 17(18) EETeE) and 6µM (hepoxilins, Hxs) in assay buffer (10mM Tris, 1mM EDTA, 100mM NaCl, 6% Glycerol, pH7.4). Activity towards 19(20) EDPE and 17(18) EETeE was assayed by adding substrate to 20µl EH3 lysate (0.3 ng/µl) to reach a final concentration of 3 µM. For selective inhibition of EH3 turnover, samples were preincubated on ice with 1µM AUDA for 5 minutes before substrate was added. Enzymatic reaction was stopped by adding AcN (acetonitrile) to a total volume of 100 µl. Samples were centrifuged (10 min, 14.000 rpm) and analyzed by LC-MS/MS.

4.8.3.2 Substrate screening II (2-14(15)-EG / 2-14(15) EET ethanol amide)

To assess hydrolase activity towards 2-14(15)-EET ethanol amide (14(15)-EET-EA) and 2-(14(15)-epoxyeicosatrienoyl) glycerol (2-14(15)-EG) the formation of the corresponding diols 2-(14(15)-dihydroxyeicosatrienoyl) glycerol (2-DHG) or 2-(14(15)-dihydroxyeicosatrienoyl) ethanol amide (2-DHEA) was determined. 200µl aliquots of control infected or EH3 expressing Sf9 cell lysates were centrifuged (45 min, 50.000rpm) and the pellet was homogenized in 60µl assay buffer (10mM Tris, 1mM EDTA, 100mM NaCl, 6% Glycerol, pH7.4). 30 µl homogenate or hsEH (5 ng/µl) was incubated for 30min at 37℃ with 6.8 µM 14(15)-EET-EA and 5.8 µM 2-14(15)-EG respectively. Reaction was quenched by addition of 1 volume ethyl acetate to reach a final volume of 60 µl. After vortexing and centrifugation 30 µl of the upper phase was transferred to a fresh tube and solvent was evaporated under a stream of nitrogen, before resolving in 60 µl methanol and subsequent analysis by LC-MS/MS.

4.8.3.3 Determination of kinetic parameters and inhibitor studies

Substrate was added to 20µl EH3 (0.3 ng/µl), EH4 or mock expressing Sf9 cell lysates to the final concentration of 1-33 µM (leukotoxin) and 1-50 µM (EET regioisomers) in assay buffer (10mM Tris, 1mM EDTA, 100mM NaCl, 6% Glycerol, pH7.4) to determine kinetic parameters. Cell lysates were incubated at 37° for 5 min (leukotoxin) and 10 min (EET regioisomers) respectively. For inhibitor

assays of EH3 (0.3 ng/µl), Sf9 lysates and purified human sEH (0.5 ng/µl) were preincubated with various EH inhibitors (1 µM) or AUDA (1 nM - 1 µM) for 5 min on ice, prior to addition of 8(9) EET to a final concentration of 5 µM (inhibitors were kindly provided by Dr. Christophe Morriseau, University of Davis, California). Enzymatic reaction was stopped by adding acetonitrile to a final volume of 100 µl. The sample was centrifuged (5 min, 14.000g) and transferred to a MS vial and submitted to LC-MS/MS analysis. To calculate the catalytic constants the data were analyzed by kinetic modeling based on the equation *V = E * CS/ (CS+Km)* (where V is turnover in % of Vmax, E total amount of enzyme, CS is substrate concentration and Km refers to michaelis menten constant) assuming that V is in proportion to the amount of enzyme substrate complex formed and that substrate is present in excess.

4.9 LC-MS/MS analysis

4.9.1 I: EpOMEs, EETs, Hepoxilins, 19(20) EDPE, 17(18) EETeE

The sample separation was performed on an Agilent eclipse XDB-C18 reverse phase column (4.6 x 150 mm, 5 µm pore size) with a corresponding opti-gard pre-column using an Agilent 1100 liquid chromatography system. The mobile phase consisted of (A) 0.1% formic acid and (B) acetonitrile containing 0.1% formic acid at a flow rate of 400 µl/min (injection volume was 20 µl). HPLC conditions were identical for all substrates (EET regioisomers, leukotoxin, isoleukotoxin), except for Hepoxilin A3 and B3. Starting conditions of 70% buffer B were maintained for 2 min, followed by a linear gradient from 70% to 100% B within 8 min and 6 min (HxA3, HxB3), respectively. An isocratic flow of 100% B was held for 4.5 min (2.5 min HxA3/HxB3) and finally the column was re-equilibrated for 2 min with 70% B. At these conditions the compounds resolve at the following retention times as shown in the table below:

analyte	**transition [amu]**	**retention time [min]**
9,10 EpOME	295.2 → 171.1	14.1
12,13 EpOME	295.2 → 195.1	13.5
9,10 DiHOME	313.2 → 201.1	7.3
12,13 DiHOME	313.2 → 183.1	6.6
14,15 EET	319.2 → 301.1	12.8
14,15 DHET	337.2 → 206.9	6.8
11,12 EET	319.2 → 167.1	13.18
11,12 DHET	337.2 → 166.8	6.86
8,9 EET	319.2 → 301.1	14.2
8,9 DHET	337.2 → 126.8	8.8
HxA3	335.2 → 273.3	7.47
TrxA3	353.3 →126.9	4.18

HxB3	335.3 →316.9	8.06
TrxB3	353.3 → 195.1	4.73
19,20 EDPE	343.3 → 299.2	12.1
19,20 DiHDPE	361.3 → 272.9	6.17
17, 18 EETeE	317.2 → 299.0	10.7
17, 18 DiHETeE	335.2 → 246.9	5.46

Table 4-3: *Respective retention times and transitions of the analytes used in LC-MS/MS assay.*

The HPLC system was coupled to a 4000 QTRAP hybrid quadrupole linear ion trap mass spectrometer (Applied Biosystems) equipped with a TurboV source and electrospray (ESI) interface. Analytes were recorded using multiple reaction monitoring (MRM) in negative mode (-MRM) using the following source specific parameters: IS -4500V, TEM 450℃, curtain gas (CUR = 30), nebulizer gas (GS1 = 50), heater gas (GS2 = 70) and collision gas (CAD = 10). The compound specific parameters for the different substrates are represented in table 4-4.

analyte	**transition**	**CE**	**DP**
9,10 EpOME	295.2 → 171.1	-17	-55
12,13 EpOME	295.2 → 195.1	-17	-55
9,10 DiHOME	313.2 → 201.1	-23	-60
12,13 DiHOME	313.2 → 183.1	-23	-60
14,15 EET	319.2 → 301.1	-16	-70
14,15 DHET	337.2 → 206.9	-26	-70
11,12 EET	319.2 → 167.1	-18	-65
11,12 DHET	337.2 → 166.8	-26	-70
8,9 EET	319.2 → 301.1	-16	-70
8,9 DHET	337.2 → 126.8	-28	-70
HxA3	335.2 → 273.3	-20	-80
TrxA3	353.3 →126.9	-36	-55
HxB3	335.3 →316.9	-16	-55
TrxB3	353.3 → 195.1	-16	-55
19,20 EDPE	343.3 → 299.2	-16	-70
19,20 DiHDPE	361.3 → 272.9	-24	-90
17, 18 EETeE	317.2 → 299.0	-16	-85
17, 18 DiHETeE	335.2 → 246.9	-24	-95

Table 4-4: *Specific parameters for different compounds analyzed in LC-MS/MS. EP (entrance potential) value is -10 for all analytes. DP: declustering potential, CE: collision energy.*

All parameters were determined by direct infusion of standard solutions (100-300 ng/ml) in acetonitrile at a flow rate of 10 µl/min using the quantitative optimization function of the Analyst software 1.4.2. Samples were quantified by determining the peak AUC with the quantitation function of the Analyst software using the transitions as specified above. The background noise was assessed by analyzing blank samples and standard curves were generated using blank samples spiked with a series of control lipids ranging from 10-1000 ng/ml. For EpOMEs and DiHOMEs the limit of detection (LOD) was 1ng and 20 pg, and the limit of quantification (LOQ) was 3 ng and 200 pg (corresponding to a signal-to-noise ratio of 3 and 10).

4.9.2 II: 2-14(15)-EG (2-EG) / 2-14(15) EET Ethanolamide (2-EET-EA)

Neutral arachidonic acid derivatives were analyzed using silver cation coordination tandem mass spectrometry. This method uses the ability of silver cations to bind to the backbone of unsaturated fatty acids to form a charged complex $[M + AG]^+$. The complexes are easily analyzed by electrospray ionization in the positive mode. Silver ion coordination results in the detection of two characteristic $[M + AG]^+$ complex ions due to the natural isotopic distribution of silver ^{107}Ag (52%) and ^{109}Ag (48%) (Kingsley and Marnett 2003).

The sample separation was performed on an Agilent eclipse XDB-C18 reverse phase column (3.2 x 100 mm, 5 µm pore size) with a corresponding opti-gard pre-column using an Agilent 1100 liquid chromatography system. The mobile phase consisted of (A) 70 µM AgNO3 in H2O (B) 70 µM AgNO3 in methanol at a flow rate of 400 µl/min using an injection volume of 20 µl. Starting conditions of 50% buffer B were maintained for 1 min, followed by a linear gradient from 50% to 100% B within 3 min. An isocratic flow of 100% B was maintained for 5 min before the column was re-equilibrated for 2 min with 50% B. At these conditions the compounds resolve at the following retention times as shown in table 4-5. The HPLC system was coupled to a 4000 QTRAP hybrid quadrupole linear ion trap mass spectrometer (Applied Biosystems) equipped with a TurboV source and electrospray (ESI) interface. Analytes were recorded using multiple reaction monitoring (MRM) in positive mode (+MRM) using the following source specific parameters: IS 4500V, TEM 450°C, curtain gas (CUR = 20), nebulizer gas (GS1 = 50), heater gas (GS2 = 70) and collision gas (CAD = 10). All parameters were determined by direct infusion of standard solutions (100-300 ng/ml) in methanol at a flow rate of 10 µl/min using the quantitative optimization function of the Analyst software 1.4.2. Samples were quantified by determining the peak AUC with the quantitation function of the Analyst software 1.4.2 using the transitions as specified below (table 4-6).

analyte	transition [amu]	retention time [min]
2-EG	501→ 106	1.9
2-DHG	519→ 106	1.6
2-EET-EA	470→ 452	1.6
2-DHEA	488→ 106	1.4

Table 4-5: *Respective retention times and transitions of the analytes used in MS assay.*

analyte	transition	CE	DP
2-EG	501→ 106	77	81
2-DHG	519→ 106	75	81
2-EET-EA	470→ 452	31	66
2-DHEA	488→ 106	91	91

Figure 4-6: *Compound specific parameters for different compounds analyzed in LC-MS/MS. EP (entrance potential) value is 10 for all analytes. DP: declustering potential, CE: collision energy.*

5 RESULTS

Note: In the following chapter (5.1), the label “nEH2” refers to EH4, since the former term for the novel epoxide hydrolase EH4 was nEH2. The proteins encoded on the respective expression plasmids are labeled after the vector (example: the protein produced by plasmid pGEFHisCnEH2AB is labeled nEH2AB). The alternative term (e.g. EH4AB) is given in brackets.

5.1 Characterization of EH4

The objective of the first part of this work was to investigate the human EPHX4 gene (also known as ABHD7) and its coding protein EH4 towards epoxide hydrolase activity, in order to characterize a putative new member of the epoxide hydrolase family. The characterization of EH4 implies two main approaches: i) the recombinant expression of enzymatically active protein in prokaryotic and eukaryotic cells, for analysis of enzymatic activity, and ii) the generation of an antibody against EH4 for detection of the protein in recombinant lysates and tissues.

5.1.1 In silico characterization of EH4

The human EPHX4 gene (GeneID: 253152, HGNC: 23758) is located on human chromosome 1p.22.1. Other names referring to this gene are ABHD7, EPHXRP and FLJ90341. The gene contains 7 exons and 6 introns and the resulting mRNA is 1635 bp long. The predicted protein consists of 362 aa with a molecular weight of 42.3 kDa (pI 8.0) (http://www.ncbi.nlm.nih.gov/IEB/Research/Acembly/index.html?human) {Thierry-Mieg, 2006 #7}. 335 bp of the gene are antisense to spliced gene prada (GenBank: BM723110.1). The EH4 protein (UniProtKB/Swiss-Prot Q8IUS5) is encoded with two amino acid variations Y321F and F285I, of which the first one is likely a natural variant (SNP, single nucleotide polymorphism) {Gerhard, 2004 #9} and the latter one is based on a sequence conflict {Ota, 2004 #8}. The protein investigated in this work contains a phenylalanine residue at position 321 and 285 (see appendix 8.3.1). Residues 17 – 37 indicate a potential signal-anchor for type II membrane proteins, based on results from protein sequence analysis software tools (http://www.uniprot.org/uniprot/Q8IUS5). Other *in silico* analyses using the database MitoProt II (v1.101; {Claros, 1996 #16}) and the NetCGlyc 1.0 Server (http://www.cbs.dtu.dk/services/NetNGlyc/) point towards a mitochondrial targeting sequence (cleavage site at position 58), and predict C mannosylation at position 106. The EPHX4 gene is present in chimpanzee (99%), dog (94%), mouse (98%), rat (89%), chicken (82%), and zebra fish (67%) and shares high sequence identity with the human protein (% identity given in brackets). The closest *c. elegans* gene is ceeh-1 (42%; UniProt: Q21147). The overall expression of EPHX4 is low. A comparison of the available expression data indicates, that the gene is mostly expressed in the central and peripheral nervous system, mainly brain, eye and dorsal root. Moreover, expression is detected in intestine, blood and adipose tissue.

5.1.2 EH4 expression constructs

To investigate the putative enzymatic activity of the protein, enzymatically active EH4 was recombinantly expressed by different eukaryotic and prokaryotic expression systems. To further obtain a sensitive and specific detection tool for identification of the protein in cell lysates and/or tissues, different EH4 fragments were expressed in *E. coli* for production of an antibody. All vector, primer and protein sequences, and also PCR conditions used in the following experiments, are listed in the appendix (see 8.1).

5.1.2.1 E. coli expression constructs

In this study, following constructs were produced: His-tagged constructs were generated for production of an EH4 specific antibody, and to investigate if specific peptides of the protein are critical for expression. The plasmid pGEFGSTNnEH2 was constructed for investigation of the enzymatic activity of EH4 in E. coli, whereas pGEFGSTNnEH2AB was produced to investigate the influence of GST fusion on expression and solubility of the recombinant protein. All His-tagged EH4 fragments (see table 5-1) were generated through cloning into the pGEF-HisC Vector. Since production and expression of functional eukaryotic membrane proteins is difficult in bacterial expression systems, the membrane anchor (aa 1 – 59) was deleted in the nEH2AB (EH4AB) protein. Furthermore, the two putative active sites D307 and H336 were removed to avoid any toxicity of the protein to the bacterial host, which would lead to negative selection. The primers used for amplification of the respective cDNA contained restriction sites for BglII and BspHI, which were used for insertion of the cDNA into the MCS of pGEF-HisC by NcoI and BglII II restriction sites. Since the expression of His-tagged nEH2AB (EH4AB) protein in *E. coli* failed, two parts of the protein sequence were expressed separately to identify if any of the protein parts includes critical peptides that prevent expression. The different protein parts contain either the membrane anchor (1/3) or C-terminal parts of the α/β hydrolase fold (3/3). The PCR product of both inserts for construction of nEH2_1/3 (aa 1-118; EH4_1/3) and nEH2_3/3 (aa 267-362; EH4_3/3) contained NcoI I and BglII restriction sites, which were introduced with the respective primers and allowed cloning into the NcoI I/BglII digested pGEF-HisC vector. The mammalian expression construct pIRESneonEH2 was used as template for the amplification of the respective cDNAs (see 5.1.2.2).

expression plasmid	template	vector	primer	restriction sites
pGEFHisCnEH2AB	IRAK	pGEF-HisC	# 3 # 4	BspHI BglII
pGEFHisCnEH2_1/3	pIRESneonEH2	pGEF-HisC	# 5 # 6	NcoI BglII II
pGEFHisCnEH2_3/3	pIRESneonEH2	pGEF-HisC	# 7 # 8	NcoI BglII II

Table 5-1*: Overview of C-terminal His-tagged E. coli expression constructs (see appendix for primer sequences).*

Parallel to the generation of the His-tagged EH4 fragments, two different N-terminal tagged expression constructs were produced (table 5-2). Both constructs are deficient in the membrane anchor (aa 1-59) but differ in the presence of the putative active sites D307 and H336. The GST-nEH2 (GST-EH4) protein covers aa 60 - 354 of the EH4 protein and was constructed to investigate enzymatic activity of EH4. The respective construct (incl. D307 and H336; GSTnEH2/GSTEH4) was constructed by EcoRI/NdeI restriction of the pGEFnEH2HisC plasmid. This plasmid contains the complete 3` sequence of EH4. The resulting EcoRI/NdeI fragment was subcloned into pGEFGSTNnEH2AB (described below) by using the same restriction sites. GST-nEH2AB (GST-EH4AB) lacks 60 C-terminal amino acids and corresponds to the protein encoded by pGEFHisCnEH2AB. The construct was used to investigate the influence of N-terminal fusion with GST on the expression of truncated EH4. For production of the C-terminal truncated expression construct (pGEFGSTNnEH2AB), an intermediate construct – ToponEH2AB – was digested with BspHI andBglII and subcloned into NcoI/BamHI digested pGEF-GSTN vector, employing the compatibility of NcoI/BspHI and BglII/BamHI restriction sites.

expression plasmid	donor plasmid A	receiving plasmid B	restriction A	restriction B
pGEFGSTNnEH2AB	TOPOnEH2AB	pGEFGSTN	BspHI/Bgl II	NcoI/BamHI
pGEFGSTNnEH2	pGEFnEH2HisC	pGEFGSTNnEH2AB	EcoRI/NdeI	EcoRI/NdeI

Table 5-2: *Overview of N-terminal GST-tagged E. coli expression constructs and cloning details.*

5.1.2.2 Mammalian cells expression constructs

Eukaryotic expression constructs provide posttranslational modification, which may be critical for expression of enzymatically active proteins. In terms of functional characterization of EH4, an expression construct for recombinant expression in mammalian cells was prepared (table 5-3). The cDNA coding for the complete sequence of EH4 was amplified from the IRAK plasmid and cloned into pIRESneo using EcoRV and BamHI restriction sites.

expression plasmid	template	vector	primer	restriction sites
pIRESneo-nEH2	IRAK	pIRESneo	# 1 # 2	EcoRV/BamHI

Table 5-3: *Generation of the pIRESneo expression construct for expression in mammalian cells (see appendix for primer sequences and PCR conditions).*

5.1.2.3 Sf-9 expression constructs

Besides mammalian cells, insect cells are another eukaryotic expression system used for recombinant expression of heterologous proteins. Previous work in our lab showed that EH3 can be enzymatically active expressed in Sf9 cells. Therefore EH4 expression constructs for Sf9 cells were generated (containing the complete cDNA) to investigate enzymatic activity of EH4. As demonstrated by Pendergast and Luckow {Pendergast, 1989 #6; Luckow, 1988 #7}, GC rich 5` non - coding sequences can affect the expression level and mRNA stability of heterologous proteins that are recombinantly expressed in Sf9 cells. For this reason, a modified shuttle vector (pFastBacmod) was generated,

where the ATG start codon of the novel introduced NdeI restriction site corresponds to the native Polyhedrin wild-type start codon. Hence the original 5`GC rich sequence was eliminated. The pFastBacmod was constructed as follows: primer #13 bound upstream of the PolH and formed a BspEI restriction site, whereas primer #14 bound within the PolH and was equipped with an MCS that contained an NdeI recognition sequence. The resulting PCR amplificate was then cloned into pFastBacHis vector by using BspEI and PstI restriction endonucleases.

To build the expression constructs that encode for His-tagged EH4, the respective PCR products (primer and PCR conditions see 8.1) were cloned into either the original (pFastBacHis) or modified (pFastBacmod) vector. Cloning into the original vector by BamHI/ PstI restriction resulted in the plasmid labeled Y, whereas cloning into the modified vector by NdeI/PstI restriction resulted in Bmod. In order to then clone the expression construct that produced non-tagged EH4 (Amod), the cDNA was inserted by NdeI/BamHI restriction. This resulted in a frameshift that included a stop codon before the His (6x) sequence.

expression plasmid	template	vector	primer	restriction sites
pFastBacmod	pFastBacHis	-	# 13 # 14	(BspEI)/MCS
Y (nEH2His)	IRAK	pFastBacHis	# 9 # 10	BamHI/Pst I
Amod (nEH2)	IRAK	pFastBacmod	# 11 # 2	NdeI I/BamHI
Bmod (nEH2His)	IRAK	pFastBacmod	# 11 # 10	NdeI/Pst I

Table 5-4: *Overview of Sf-9 expression constructs (see appendix for primer sequences).*

5.1.3 Expression of EH4 for antibody production

For the generation and production of an antibody, the respective antigen and epitope needs to be present in high amount and purified. To produce the required fragments, an attempt to recombinantly overexpress EH4 in *E. coli* and purify the protein using the corresponding His-Tag was made. Expression of EH4 was performed using the constructs described in chapter 5.1.2.1. The expression of nEH2-3/3 (EH4-3/3) yielded detectable amounts of recombinant protein in *E. coli* lysate, and was used for immunization.

5.1.3.1 Expression of His-tagged EH4

Previous work in our lab showed that the expression of the full length EH4 is not possible. Therefore, two truncated EH4 proteins were expressed in bacteria to generate an antibody against EH4. In addition to that, the proteins were expressed to investigate if any of the two parts is critical and prevents expression. The C-terminal His-tagged EH4 protein that contains aa 267-362 was successfully overexpressed in *E. coli*, as demonstrated by coomassie staining (figure 5-1). Neither coomassie gel analysis nor western blot allowed detection of anchorless EH4 (pGEFHisCnEH2AB) and truncated EH4 protein containing aa 1-118 (nEH2-1/3; EH4-1/3). The fact, that EH4-3/3 is

overexpressed in *E. coli* and expression of EH4 1/3 failed, suggests that at least the first N-terminal amino acids are critical for expression in E. coli.

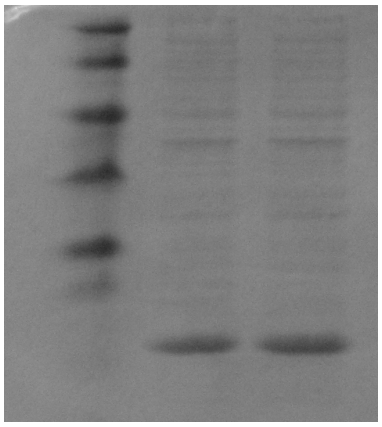

Figure 5-1: *Expression of EH4-3/3 (nEH2-3/3; 12.5 kDa) in BL21AI. Expression was induced with 20µM at OD_{600}~0.4 and continued ON at 18℃. Bacterial cells were disrupted by French® press and analyzed by SDS-PAGE. Lane 1: Marker, Lane 2 and 3: lysates of EH4-1/3 expressing E.coli.*

Expression of EH4-3/3 (nEH2-3/3) in BL21AI indicated formation of inclusion bodies. For affinity chromatography, the proteins needed to be resolved. To analyze whether the protein is present in protein aggregates or insoluble inclusion bodies, the pellet obtained after centrifugation of bacterial

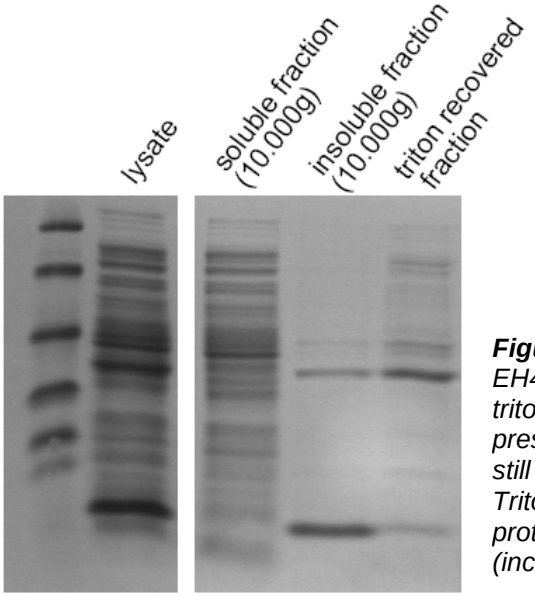

Figure 5-2: *Resolving protein aggregates. EH4-3/3 containing pellets were washed with triton buffer to resolve any protein aggregates present in the pellet. The majority of protein is still present in the pellet after treatment with TritonX wash buffer, indicating that the protein is present in insoluble aggregates (inclusion bodies).*

lysate was washed with Triton containing buffer (100mM Tris, 200mM NaCl, 1mM EDTA, 0.5% Triton, 0.02% NaN3, pH 7.8). Figure 5-2 shows that the majority of the protein is still present in the pellet after washing with Triton wash buffer. This indicates that the most of EH4-3/3 was present in insoluble inclusion bodies and not in protein aggregates (figure 5-2).

5.1.3.2 Purification of His-tagged EH4

In order to purify EH4-3/3 by affinity chromatography, the protein needs to be resolved from the inclusion bodies. The pellet was resolved in ib-buffer (6M Urea, 100mM Tris, NaN_3, pH 8.5) at room temperature ON, prior to affinity chromatography. Although denaturing conditions generally do not affect binding of histidine residues to chelating sepharose, there was no specific binding of EH4-3/3

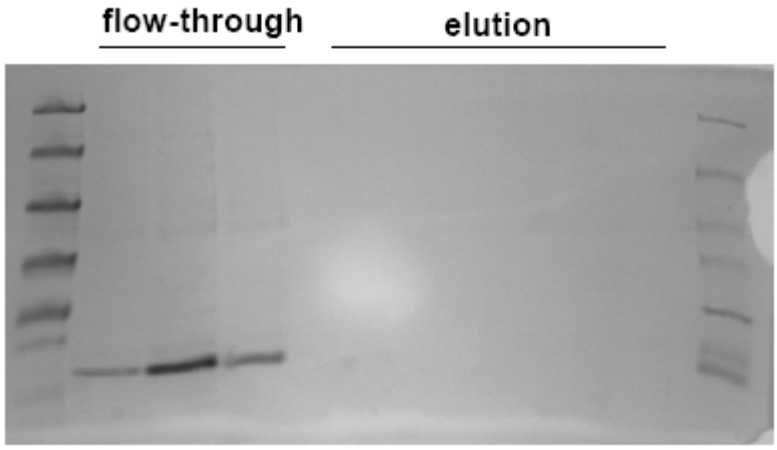

Figure 5-3: *Purification of His tagged EH4-3/3 (nEH2-3/3) by affinity chromatography. Resolved EH4-3/3 inclusion bodies were submitted to affinity chromatography as described in materials and methods. There is no binding of EH4-3/3 to the His-Trap column and the protein is present in the flow-through (unbound proteins).*

(nEH2-3/3) to the matrix, as demonstrated by coomassie gel analysis of the different elution fractions (figure 5-3). Analysis of the remaining fractions revealed that all protein was present in the flow-through.

Several other approaches to purify the protein by size exclusion or anion exchange failed. Yet, the protein present in the above fraction was pure enough to be used for immunization.

5.1.3.3 Production of specific antibodies using EH4-3/3

The protein fractions were concentrated by VIVA spin technique, submitted to SDS-Page (0.4 mg total, 0.1 mg per band) and the protein was excised from the PAA gel and sent for immunization. Immunization followed a 3-month protocol with 4 injections (day 0, 14, 28 and 56) of which each contained 0.1 mg protein. The antibody was raised in rabbit. Pre-immune serum (2ml, day 0), serum from small bleed (2ml, day 38), large test bleed (20ml, day 66) and final bleed (day 87, 50ml) were obtained and tested for immuno reactivity against EH4 expressed in Sf9 cells and GST-tagged EH4 expressed in *E. coli*. Figure 5-4 A shows a coomassie staining of GST and GST-EH4 expressed in *E. coli*. Samples of the same lysate (GST and GST-EH4) were blotted onto PVDF membrane and incubated with EH4 - antiserum (final bleed) at a dilution of 1:1000 (figure 5-4 B). There was no specific detection of EH4 compared to the negative control (GST-lysate only) observed. Altering the dilution of the antiserum (1:500, 1:2000 and 1:10.000) as well as the antigen (EH4-3/3) showed unspecific binding of the antibody in the EH4 sample and the negative control.

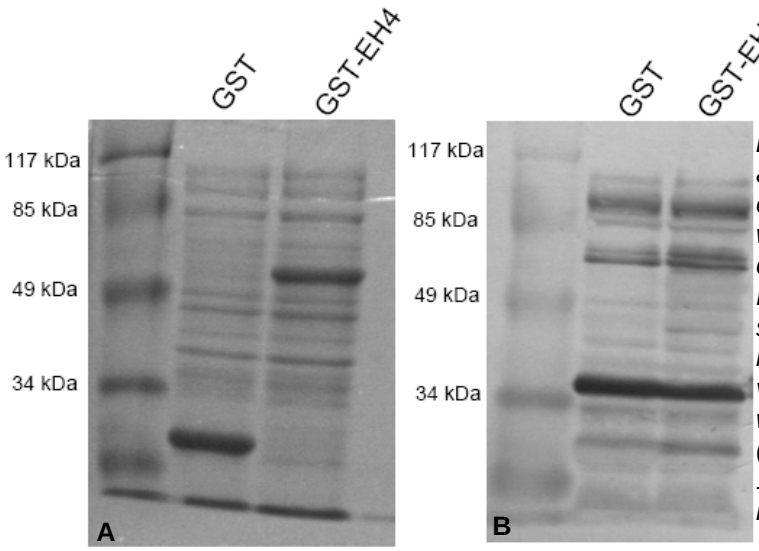

Figure 5-4: *Test of EH4 antiserum (rabbit, final bleed) obtained after immunization with EH4-3/3 (nEH2-3/3). Over expression of GST and GST-EH4 is visible after coomassie staining (A). There is no specific immuno reaction with GST-EH4 visible in western blot analysis with the EH4 immune serum (B). Dilution of EH4 antiserum: 1:1000. GST-lysate served as negative control.*

Since the protein for immunization was expressed in *E. coli* and excised from a PAA gel, the unspecific binding and the background might arise from crossover reaction with other *E. coli* proteins present in the lysate. Therefore, the immune serum was also tested against EH4 protein that was recombinantly expressed in Sf9 cells. His-tagged EH4 was analyzed by western blot (using α-His antibody) to confirm the presence of EH4 in the cell lysate (figure 5-5). The same samples were

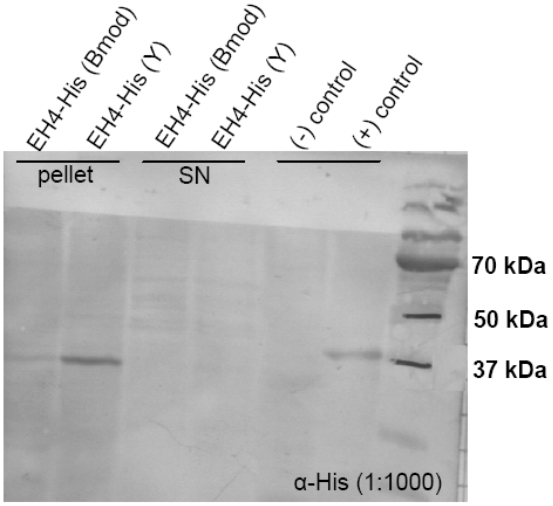

Figure 5-5: *Western blot analysis of EH4 -His expressed in Sf9 cells using α-His antibody (1:1000). There is specific detection of EH4-His protein visible in the pellet. There is no protein present in the SN. (-) control: control infected Sf9 cells. (+) control: His tagged mycoVI (39kDa). Bmod and Y refer to different expression constructs that encode for EH4-His, but differ in the upstream DNA sequence (see materials and methods).*

blotted again and incubated with the EH4 immune serum (1:1000) to test for specific immuno reactivity with EH4 (figure 5-6). A band is visible at the expected molecular weight, however the immune reactivity was far too unspecific and the negative control showed a band at the same height, which disallows differentiation between EH4 specific and Sf9 unspecific signals.

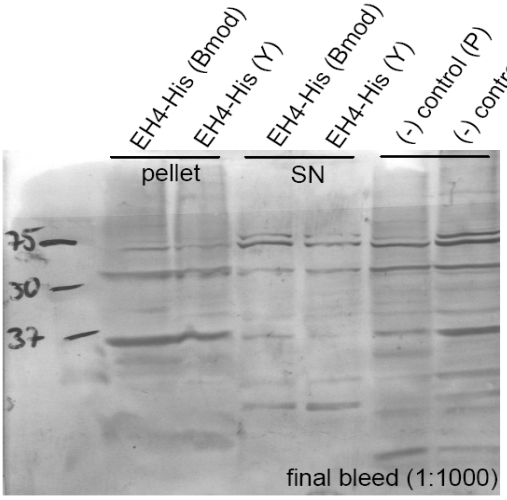

Figure 5-6: *Western blot analysis of EH4-His expressed in Sf9 cells using EH4 antiserum (final bleed). There is no specific immuno reactivity of the antiserum with EH4 visible. Bmod and Y refer to different expression constructs that encode for EH4-His, but differ in the upstream DNA sequence (see materials and methods).*

Alternatively, two synthetic peptides (DPSLGTHCYVRIKDS and EGSHWLQQDQPDIVN) corresponding to the EH4 from mouse, were used for generation of an antibody. The sequence similarity is sufficient to expect a cross reaction with EH4 from human.

Figure 5-7 shows the immunoreactions of one generated peptide antibody (DPSLGTHCYVRIKDS) against lysate of EH4 expressing Sf9 cells. There was no specific detection of EH4 visible. The above results showed that the EH4 immune sera obtained after immunization with truncated protein as well as synthetic peptides cannot be used for specific detection of EH4 protein in *E. coli* and Sf9 cell lysate.

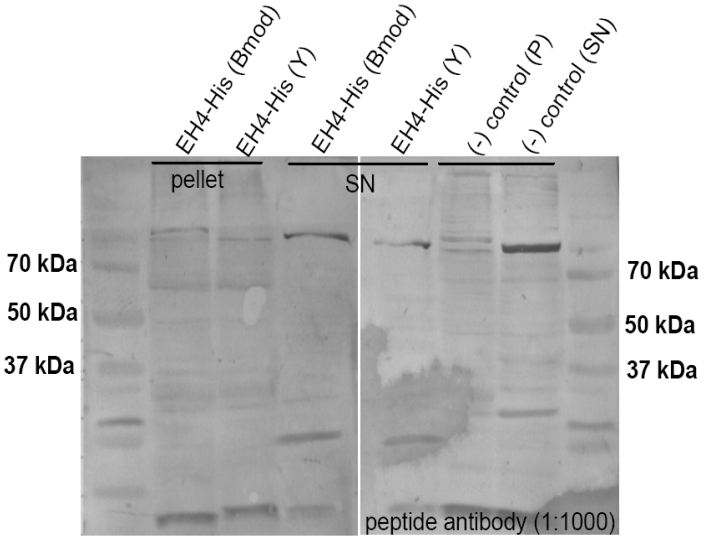

Figure 5-7: *Western blot analysis of EH4 expressed in Sf9 cells, using immune serum generated against a synthetic peptide. There is no specific detection of the peptide antibody with EH4 visible. Bmod and Y refer to different expression constructs that encode for EH4-His, but differ in the upstream DNA sequence (see materials and methods).*

5.1.3.4 Peptide analysis by LC-MS/MS

Since the different immune sera failed to specifically detect EH4 protein, an alternative method based on peptide analysis by LC-MS/MS was established for detection of (untagged) EH4 in Sf9 cell lysates. For this purpose, proteins were isolated by methanol extraction from pelleted EH4 expressing insect cells and analyzed by LC-MS/MS as described in materials and methods. The obtained peptide spectrum was blasted against a human protein database, and the resulting matches were analyzed. The best match was in fact human EH4. This was a significant result as indicated by the high

probability based mowse (molecular weight search) score of 310 (figure 5-8). The score indicates the probability that the observed match is a random event. The green region indicates the significance level and scores within this region are of no significance (in this case a probability score of 42). Hence the score of 310 confirmed the presence of EH4 in the investigated sample. This method could be used as an alternative to detect specific proteins independent from immunoblotting.

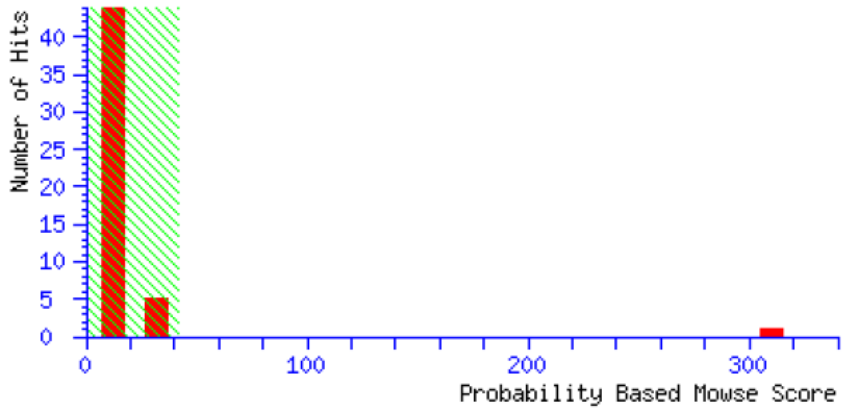

Figure 5-8: *Probability based MOWSE (molecular weight search) score of the Mascot search results. The best match observed was human EH4 with a probability score of 310. This result is significant. The green shaded region marks the significance level. Scores within the green region are not significant.*

Figure 5-9 shows the amino acid sequence of EH4 and the matching peptides (highlighted in bold red). Altogether, 9 different peptides matched with the human protein database and resulted in the identification of EH4 (figure 5-9). Both EH4 and His-tagged EH4 were detected in methanol extracts from pelleted insect cells but not from the supernatant of Sf9 cultures. This indicates that EH4 is most likely not secreted.

```
  1 MARLRDCLPR LMLTLRSLLF WSLVYCYCGL CASIHLLKLL WSLGKGPAQT
 51 FRRPAREHPP ACLSDPSLGT HCYVRIKDSG LRFHYVAAGE RGKPLMLLLH
101 GFPEFWYSWR YQLREFKSEY RVVALDLRGY GETDAPIHRQ NYKLDCLITD
151 IKDILDSLGY SKCVLIGHDW GGMIAWLIAI CYPEMVMKLI VINFPHPNVF
201 TEYILRHPAQ LLKSSYYYFF QIPWFPEFMF SINDFKVLKH LFTSHSTGIG
251 RKGCQLTTED LEAYIYVFSQ PGALSGPINH YRNIFSCLPL KHHMVTTPTL
301 LLWGENDAFM EVEMAEVTKI FVKNYFRLTI LSEASHWLQQ DQPDIVNKLI
351 WTFLKEETRK KD
```

Figure 5-9: *Primary sequence of EH4.The peptides that matched in a BLAST search against human proteins are shown in bold red.*

5.1.4 Expression of EH4 for functional characterization in *E. coli*

In order to investigate and characterize enzymatic activity of EH4, prokaryotic and eukaryotic cell lysates containing theoretically active protein (including all putative catalytic residues) were submitted to activity assays. Expression and activity measurements of EH4 from *E. coli*, Cos-7, V79 and Sf9 cells are described below.

5.1.4.1 Expression of GST-tagged EH4 (E. coli)

Anchorless EH4 was expressed with an N-terminal GST-tag to investigate enzymatic activity of EH4. A truncated EH4 protein (GST-EH4AB), lacking the putative catalytically active residues D307 and H336, was parallel expressed. This was done in order to investigate the influence of GST fusion on expression and solubility of truncated EH4. As figure 5-10 depicts, N-terminal fusion with GST led to

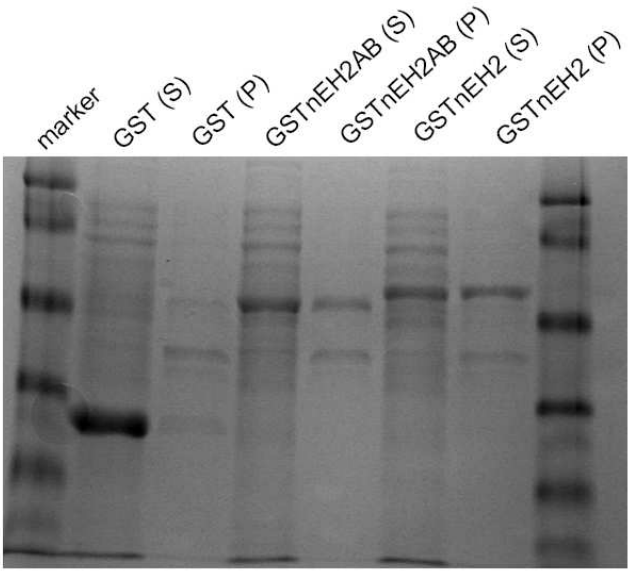

Figure 5-10: *Expression of N-terminal GST-tagged EH4. Expression of GST, GST-nEH2AB (GST-EH4AB) and GST-nEH2 (GST-EH4) in Bl21AI was induced with 20µM arabinose at OD_{600}~0.4 and continued over night at 18℃. Bacterial pellet was resuspended in 0.1M $NaPO_4$, pH 7.4 and disrupted by French® pressure cell press. Molecular weights are 28kDa (GST), 56kDa (GST-nEH2AB) and 62kDa (GST-nEH2). (P): pellet (10 min, 13.000 rpm) and (S): Supernatant.*

visible overexpression of both EH4 proteins, the truncated protein deficient in D307 and H336 (GSTnEH2AB/GST-EH4AB) and the protein only lacking the membrane anchor (GSTnEH2/GST-EH4). This result showed that N- terminal fusion influences and improves the expression of EH4 in bacteria, because previous attempts to express the C-terminal tagged (His) truncated EH4 protein (nEH2ABHis, EH4ABHisC) for antibody generation in *E. coli* was not possible. The majority of both recombinant proteins was present in the supernatant, most likely as a result of GST fusion. Fusion with GST is known to increase probability of directing the recombinant protein into the cytosol.

5.1.4.2 CDNB assay

For affinity purification of GST-tagged proteins, it is necessary that the GST fusion protein is folded correctly. Since the enzymatic activity of GST correlates with the correct folding of the protein, a CDNB assay was performed to analyze the activity of GST. The assay measures the conjugation of the synthetic GST substrate CDNB (1-chloro-2,4-dinitrobenzene) with reduced glutathione, and was performed as described under materials and methods. Native glutathione transferase (GST) shows

the highest activity in CDNB conjugation (table 5-5). However, the EH4 fusion proteins showed a significant GST activity as compared to the negative control, which indicated the presence of properly folded fusion protein. Figure 5-11 shows the corresponding graphs.

	GST	GST-EH4	GST-EH4AB
change in absorption	0.069	0.019	0.030
specific activity [nmol/min*mg]	95.5	26.7	41.7

Table 5-5: *Conjugation of CDNB with glutathione by GST, GST-EH4 and GST-EH4AB. The specific activity is calculated as the increase in absorption per minute and mg total protein. Change in absorption at 340nm corresponds to 0.0096 /µM (CDNB) * cm*

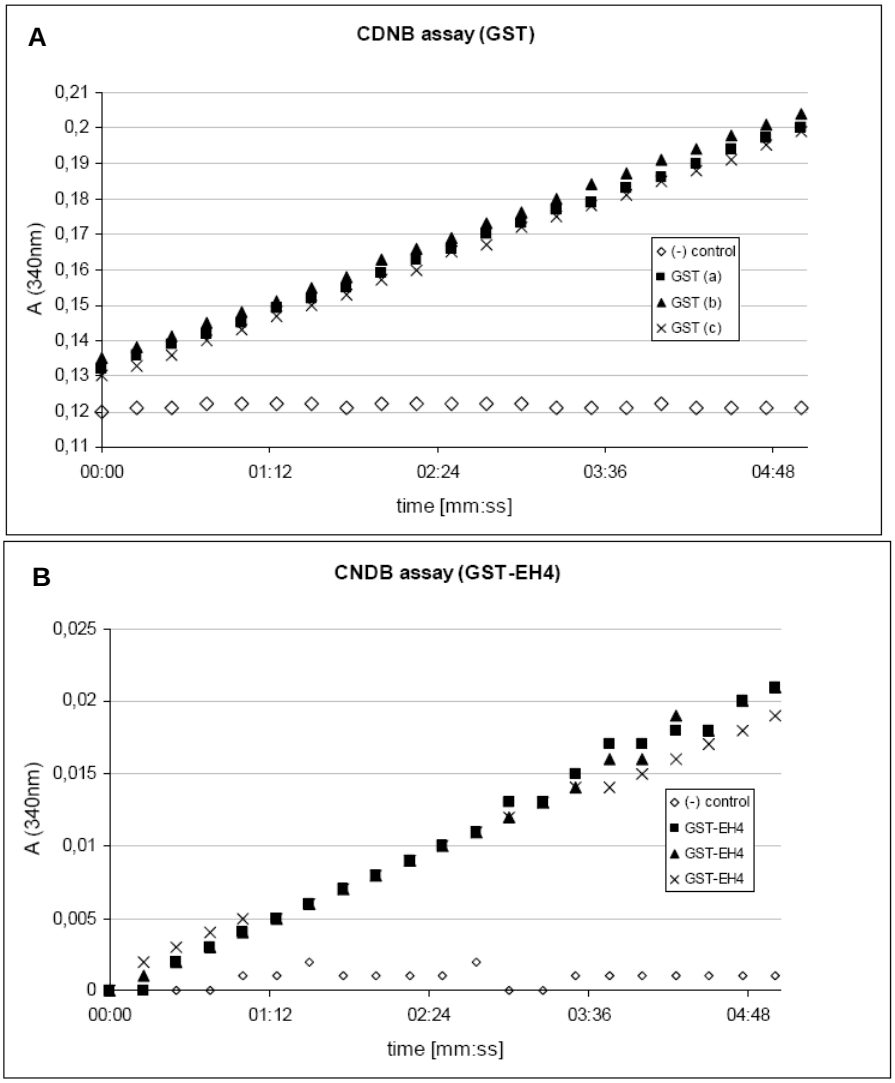

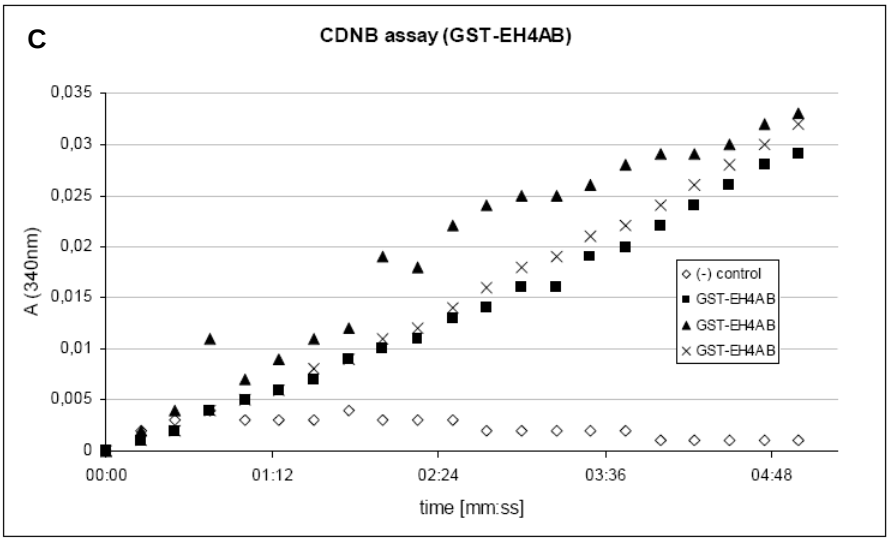

Figure 5-11: *CDNB assay with different bacterial GST constructs (A: GST, B: GST-EH4, C: GST-EH4AB). CDNB assay was performed with French® press lysates of BL21AI. GSH 1mM, CDNB 50µM, total protein was 5µg in all three samples. Samples were measured in triplicate every 15 sec. neg control: GSH and CDNB only.*

5.1.4.3 Purification of GST-tagged EH4

Since the results of the CDNB assay indicated a correct folding of the GST fusion protein, the GST tagged proteins were submitted to affinity chromatography. To purify the GST tagged EH4, the supernatant of bacterial lysate was incubated with GSH sepharose, and affinity chromatography was performed as described in materials and methods. Figure 5-12 shows the SDS-Page analysis of the different fractions obtained. Although not all GST proteins bind to GSH sepharose, a considerable amount was selectively eluted from the matrix after incubation with elution buffer.

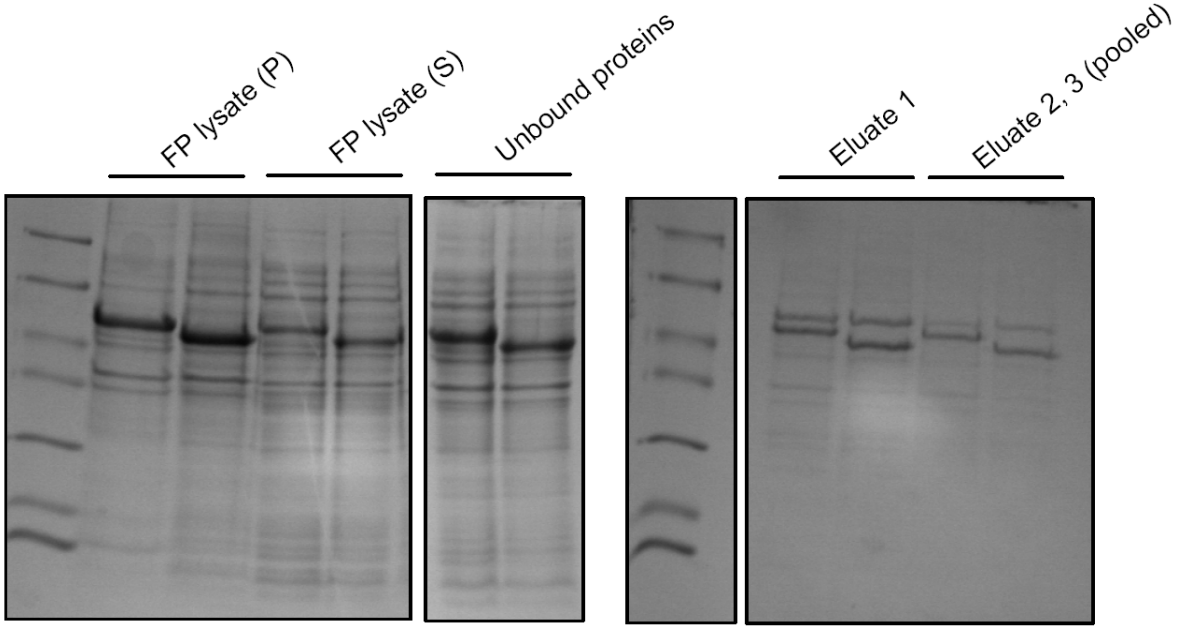

Figure 5-12: *Batch purification of GST-nEH2 (GST-EH4; 62kDa) and GST-nEH2AB (GST-EH4AB; 56kDa). Proteins were recombinantly expressed in E. coli BL21AI (18℃, ON), disrupted by using French® Pressure Cell Press and purified as described in materials and methods. (20µg protein per lane)*

In addition to the GST fusion proteins, the coomassie gel (figure 5-12) shows an additional band at 70kDa, which is copurified and present in the elution fraction. The protein most likely corresponds to the bacterial Hsp70 DnaK (Pharmacia 1997). This bacterial molecular chaperone binds to the peptide sequence on the matrix that fuses with the GST protein and may be eliminated by washing the bound fusion protein with either Triton or MgATP (Pharmacia 1997; Rial and Ceccarelli 2002).

In order to increase the amount of soluble GST-EH4 and hence the yield of purified protein, the pellet (4000rpm, 45 min) of the cell lysate was washed with TritonX (1%) to resolve any protein aggregates present in the pellet. Approximately 80% of the pelleted GST tagged EH4 proteins was resolubilised and present in the resulting supernatant. The Triton soluble fraction was incubated with GSH sepharose and purified as described in materials and methods.

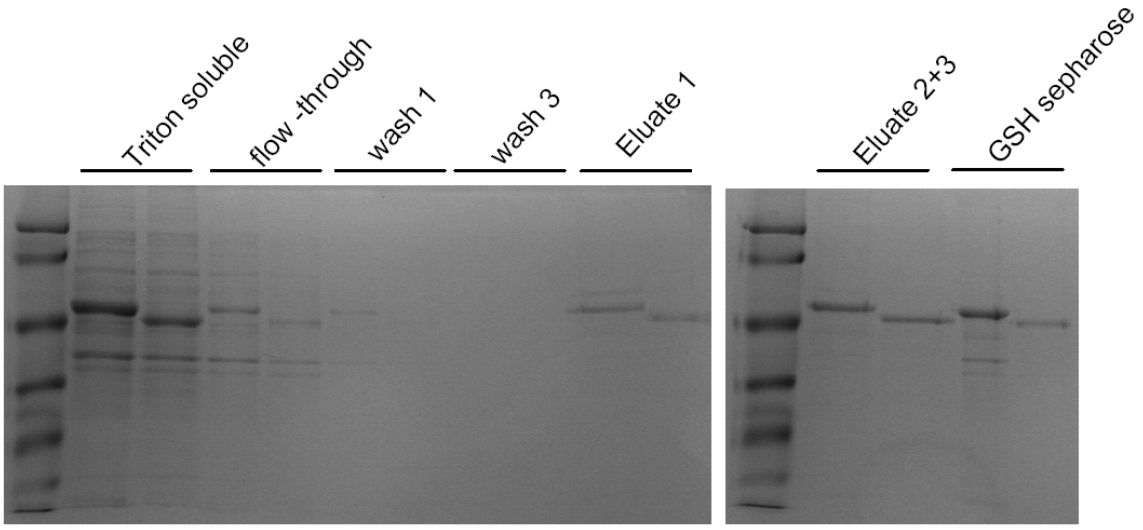

Figure 5-13: *Batch purification of TritonX soluble proteins. Proteins were recombinantly expressed in BL21AI (18℃, ON). The pellet obtained after French Press disruption was washed in Triton buffer. Resolubilised protein was submitted to affinity chromatography. MW: GST-nEH2 (GST-EH4): 62kDa) and GST-nEH2AB (GST-EH4AB): 56kDa*

Figure 5-13 shows the SDS-Page analysis of the resulting protein fractions. As in the previous experiment, not all GST tagged proteins were bound to the sepharose material. Yet, there was a visible concentration and purification of GST-EH4 as well as GST-EH4AB visible. Some amount of protein was still bound to the sepharose matrix (not eluted), which is most probably a result of the short incubation with GSH (10 minutes). There was no copurification of bacterial chaperones visible, since washing with TritonX led to dissociation of these complexes and hereby prevented interaction with the chromatography matrix.

A CDNB assay was performed in order to test for activity and proper folding of the eluted proteins. The purified GST fusion proteins showed a GST activity comparable to the crude lysate.

5.1.4.4 Enzymatic activity of GST- EH4

GST-EH4 containing all putative catalytically active residues was successfully expressed in bacteria. Therefore, the purified fusion protein was tested for activity towards the radioactively [1-^{14}C] labeled

substrates 9, 10-epoxystearic acid (ESA) and styrene 7, 8-oxide (STO) as described in materials and methods.

As table 5-6 shows, there was notable activity of the bacterial lysates (GST, GST-EH4) compared to the negative control (buffer). On average, the radioactivity measured in the aqueous phase of GST lysate was 3 times higher than in the samples that contain the GST fusion protein. This approximately reflects the ratios measured in the CDNB assay, indicating that the radioactive compound present in the aqueous phase is most likely a GSH conjugate of styrene 7, 8-oxide.

sample	mean (dpm)	[1-^{14}C] STO [nmol]
Buffer (phosphate buffer 0.1M, 7.4)	1371	-
Lysate GST	30553	0,88
Lysate GSTEH4	10473	0,28
Lysate GST (BSA (1mg/ml))	33038	0,96
Lysate GSTEH4 (BSA (1mg/ml)	11986	0,32
Lysate GST (Glycerol 2-5%)	32228	0,94
Lysate GSTEH4 (Glycerol 2-5%)	13124	0,36

Table 5-6: *Enzymatic activity of GST against [1-^{14}C] labeled styrene 7, 8-oxide. GST expressed in BL21AI has higher activity towards styrene-oxide as compared to the fusion protein. [1-^{14}C] STO corresponds to 15 mCi/mmol.*

It has been shown that glutathione transferases conjugate GSH to styrene oxide (Hayakawa, Lemahieu et al. 1974; Hiratsuka, Yokoi et al. 1989), which leads to formation of the more hydrophilic GSH conjugate and is therefore extracted into the aqueous phase. It remains unclear if any contribution to styrene turnover was due to EH4, because the distinction between conjugate and diol is not possible with this assay. There was no radioactively labeled diol product detectable by TLC, when using [1-^{14}C] labeled 9, 10-epoxystearic acid (ESA) as substrate.

5.1.5 Expression of EH4 for functional characterization in mammalian cells

Since investigation of EH4 enzymatic activity with GST tagged protein from *E. coli* turned out to be inapplicable, an eukaryotic expression system using Cos-7 and V79 cells was established as alternative method. Activity measurements were performed with ESA and other fatty acid derived epoxides.

5.1.5.1 Stable expression of EH4

EH4 mRNA was present in stably transfected Cos-7 cells. This was confirmed by RT - PCR and subsequent sequencing (figure 5-14). Since Cos-7 cells turned out to have endogenous EH activity towards the initial screening substrate 9 (10) epoxystearic acid (see 5.1.5.2), an additional cell line (V79) was transfected with EH4 cDNA (figure 5-15). V79 cells are deficient of at least endogenous

mEH, as shown by western blot analysis and activity measurements of mock transfected control cells towards STO turnover (Herrero, Arand et al. 1997). These cells also show very low endogenous sEH activity (Glatt, Gemperlein et al. 1987).

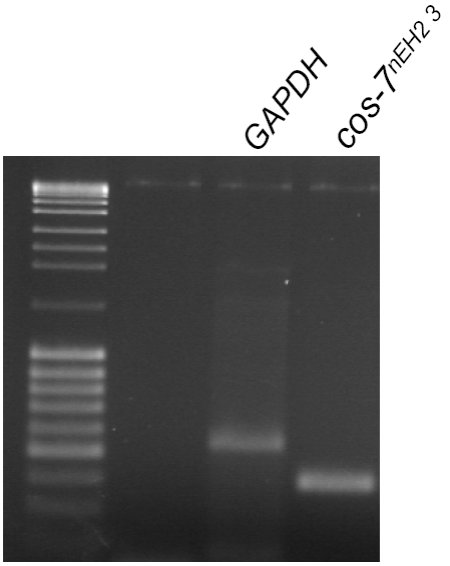

Figure 5-14: *Expression of EH4 in Cos-7 cells (clone 3). mRNA was isolated from stable transfected Cos-7 cells and RT PCR was performed with EH4 (nEH2) specific primer. The sequence of the amplificate (390bp) was confirmed by sequencing. GAPDH (523bp) was used as positive control.*

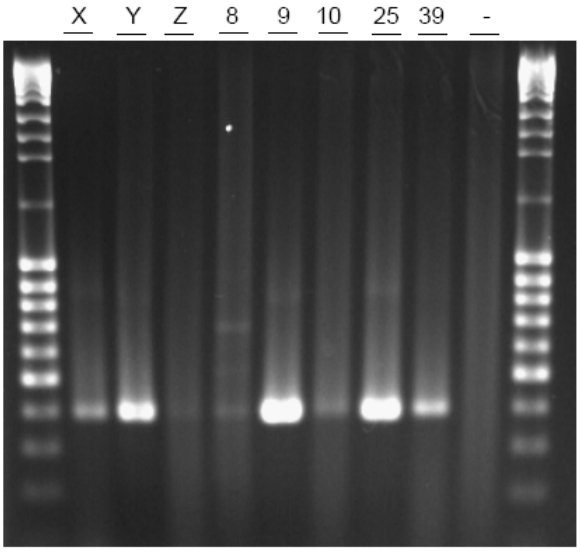

Figure 5-15: *Expression of EH4 (nEH2) in different V79 stable transfected cell clones. mRNA was isolated from stable transfected V79 cells and RT PCR was performed with EH4 (nEH2) specific primer. The sequence of the amplificate was confirmed by sequencing. (-): negative control.*

5.1.5.2 EH4 activity analysis in transfected mammalian cell lines

Radiolabeled substrates were used to test for activity of EH4 towards styrene 7, 8- oxide (STO), a substrate known to be turned over by most of the investigated EHs. Furthermore, turnover of 9(10) epoxystearic acid (ESA), another EH substrate that structurally refers to fatty acid derived signaling molecules, was investigated as described in material and methods.

The results of the radioactivity assay with Cos-7 cells indicated an endogenous activity towards 9(10) epoxystearic acid (figure 5-16). In this assay, the hydrolysis product can be identified by its different

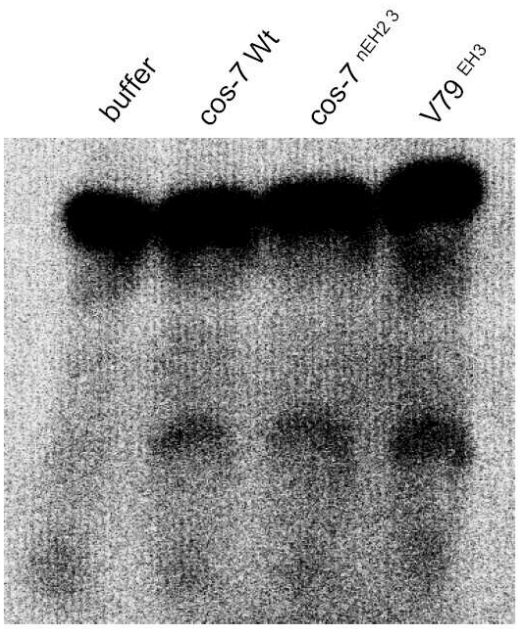

Figure 5-16: *Endogenous turnover of 9(10) epoxystearic acid by Cos-7 cells. 5.4x10^4 (Cos-7 Wt), 6x10^4 (Cos-7 $^{nEH2\ 3}$) and 4.5x10^4 (V79^{EH3}, positive control) cells were incubated with [1-14C] ESA for 10 minutes at 37°C and analyzed by TLC.*

migration distance. The corresponding diol is more polar and thus shows a shorter migration distance than the epoxide. As indicated in figure 5-16, the turnover of ESA by EH4 (nEH2) transfected cells was about the level of Cos-7 Wt cells.

To investigate if there was a low EH4 activity that cannot be detected by this assay, further experiments using LC-MS/MS analysis were performed (see appendix 8.6.1). The LC-MS/MS assay is a more sensitive method with higher resolution. The assay was performed in order to verify or exclude EH4 activity in EH4 infected cells compared to control cells. The data confirmed the results obtained from TLC and could not demonstrate a significant activity of EH4. Turnover of EETs as well as EpoMEs and cis/trans ESA (data not shown) did not exceed the level of endogenous activity observed in control cells. Endogenous sEH activity of Cos-7 cells has been reported by other groups measuring *t*-SO turnover (Sandberg, Hassett et al. 2000) and has also been detected by western blot analysis (Fang, Hu et al. 2006). For that reason, Cos-7 cells are not applicable for enzymatic activity assays that should investigate hydrolase activity of EH4 towards epoxy lipids, and therefore were excluded from the experiments.

As alternative mammalian cell system, V79 cells were stably transfected with EH4 (figure 5-15) and activity measurements using LC-MS/MS were performed. Experiments with V79 Wt cells using LC-MS/MS showed that V79 Wt cells did not have endogenous activity towards the tested epoxy lipids. Activity measurements did not prove hydrolysis of Hepoxilins, EETs, EpOMEs and cis/trans ESA by EH4 (see appendix 8.6.2).

5.1.5.3 Expression of EH4 for functional characterization in Sf9 cells

Recombinant expression of the highly related EH3 in Sf9 cells resulted in the expression of enzymatic active protein. Therefore, a baculovirus expression system for expression of EH4 in insect cells was established.

Expression of His-tagged EH4 protein was detected after infection with a multiplicity of infection (MOI) of 5 (figure 5-17). The MOI indicates the ratio of infectious virus particles to targeted cells, in this case 5 virus particles per cell. In comparison, an infection with MOI 1 did not yield any detectable amounts of EH4 protein as indicated by WB analysis (figure 5-17).

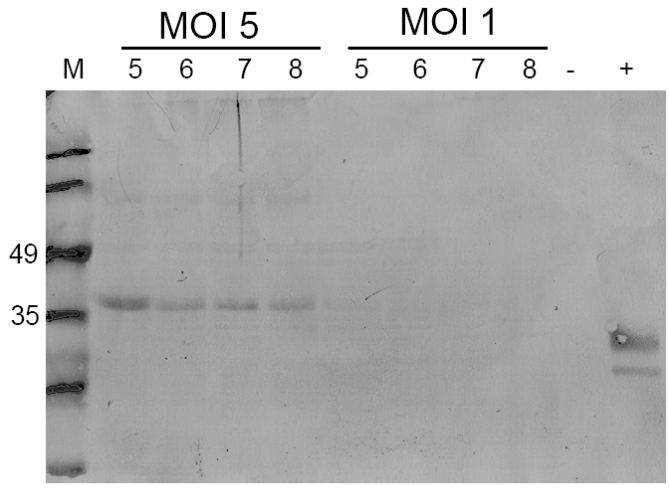

Figure 5-17: *Expression of EH4-His (Bmod) with infection of MOI1 and MOI5 at days 5-8 post infection. 5x10^6 cells were pelleted daily and resolved in 150 µl PBS. 1x10^5 cells were mixed with laemmli and analyzed by Western Blot using α-His antibody. negative control (-) Sf9 Wt, positive control (+) PknG (32kDa).*

First signs of expression were detectable on day 3 post infection (dpi), and the highest expression was reached on day 5 and 6 (figure 5-18 A). The coomassie analysis of Sf9 proteins of Wt cells compared to infected cells showed an altered expression pattern (see 5.1.5.4). Yet, a clearly visible overexpression of the recombinant protein (figure 5-18 B) was not possible after infection with the

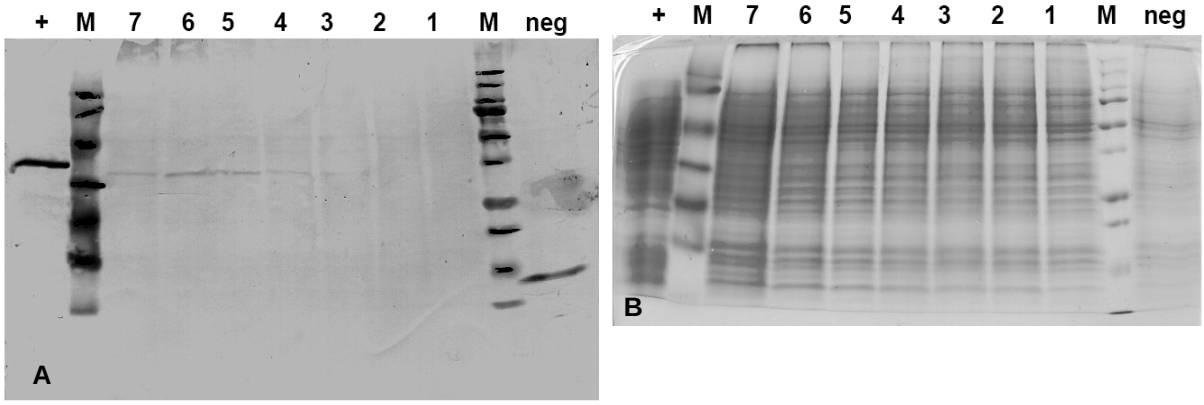

Figure 5-18: *Expression of EH4-His (nEH2-His; Bmod) 1-7 days after infection with MOI 5. 1x10^6 cells were pelleted daily and analyzed by western Blot (A). There is no overexpression detectable in the corresponding coomassie gel (B). neg: Sf9 Wt; +: His tagged mycoVI (39kDa), 1-7: days after infection.*

modified bacmid (Bmod). Likewise, there was no sign of overexpression after infection with the unmodified bacmid (Y) visible. The bacmid Y encodes for the same His-tagged EH4 protein, but displays upstream GC rich non-coding sequences, which have been reported to influence and reduce

heterologous expression. However, the results indicated that removing of GC rich non-coding regions upstream of the gene did not improve expression of EH4.

5.1.5.4 Analysis of Sf9 expression pattern

Coomassie analysis of recombinant expressed proteins in Sf9 cells led to altered expression pattern and to the occurrence of an additional band in recombinant EH3 and EH4 lysates, as compared to Sf9 Wt cells (5-19). To test whether this band corresponds to EH3 and EH4, and therefore would allow the quantification of the recombinant expressed protein, the appropriate band was excised and analyzed by LC-MS/MS as described in materials and methods .

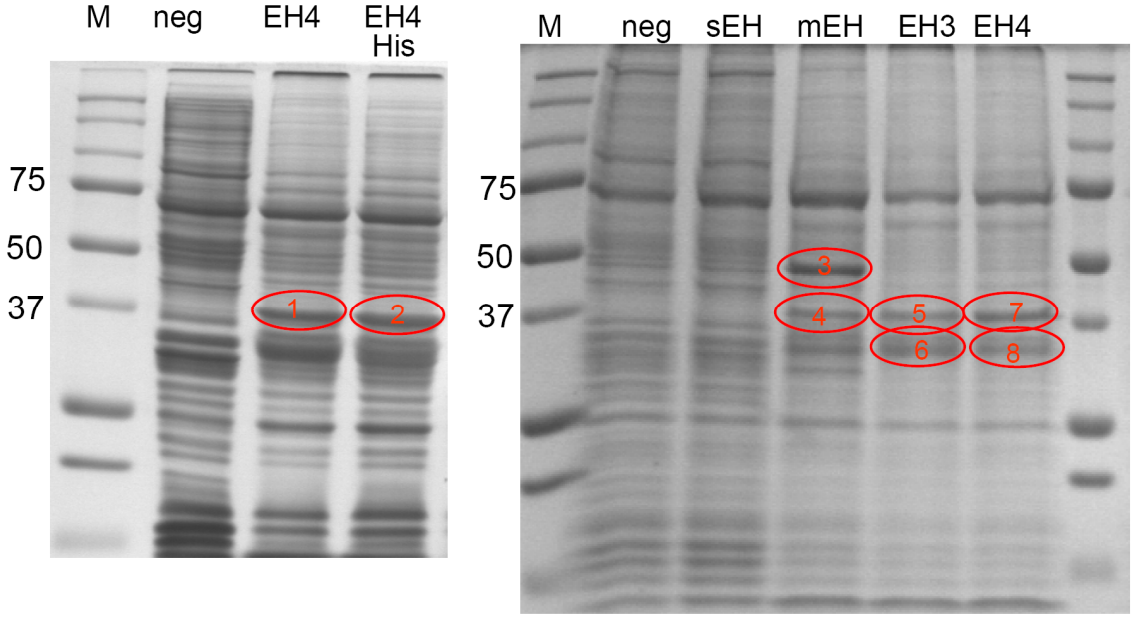

Figure 5-19: *Coomassie analysis of different proteins recombinantly expressed in Sf9 cells. Expression of native and His-tagged EH4 protein resulted in an additional band as compared to the negative control (A). Expression and coomassie analysis of expression pattern from novel epoxide hydrolases compared to sEH and mEH (B). Protein bands encircled in red were excised from the gel and analyzed by LC-MS/MS.*

The bands # 1, 2, 4, 5 and 7 are not present in Wt cells. To clarify if these bands correspond to the respective recombinant expressed protein, the bands were excised and analyzed by LC-MS/MS. Band # 3 was tested for presence of mEH since it is the dominant band at approx. 50kDa, which corresponds to the molecular weight of mEH (53kDa; #4 was used as negative control). The two protein bands # 6 and 8 were also analyzed for presence of EH3 and EH4, in case both proteins would have lower MW due to degradation or posttranslational modification. Peptide analysis of the different gel pieces resulted in significant positive results in samples # 3 (mEH; probability score 55, significance level 39) and 8 (EH4; probability score 274, significance level 41; see figure 5-20 (A) and (B)), whereas sample 1 and 6 indicated presence of EH4 and EH3, but not significantly (EH4: probability score 22, significance level 41 and EH3: probability score 25, significance level 43).

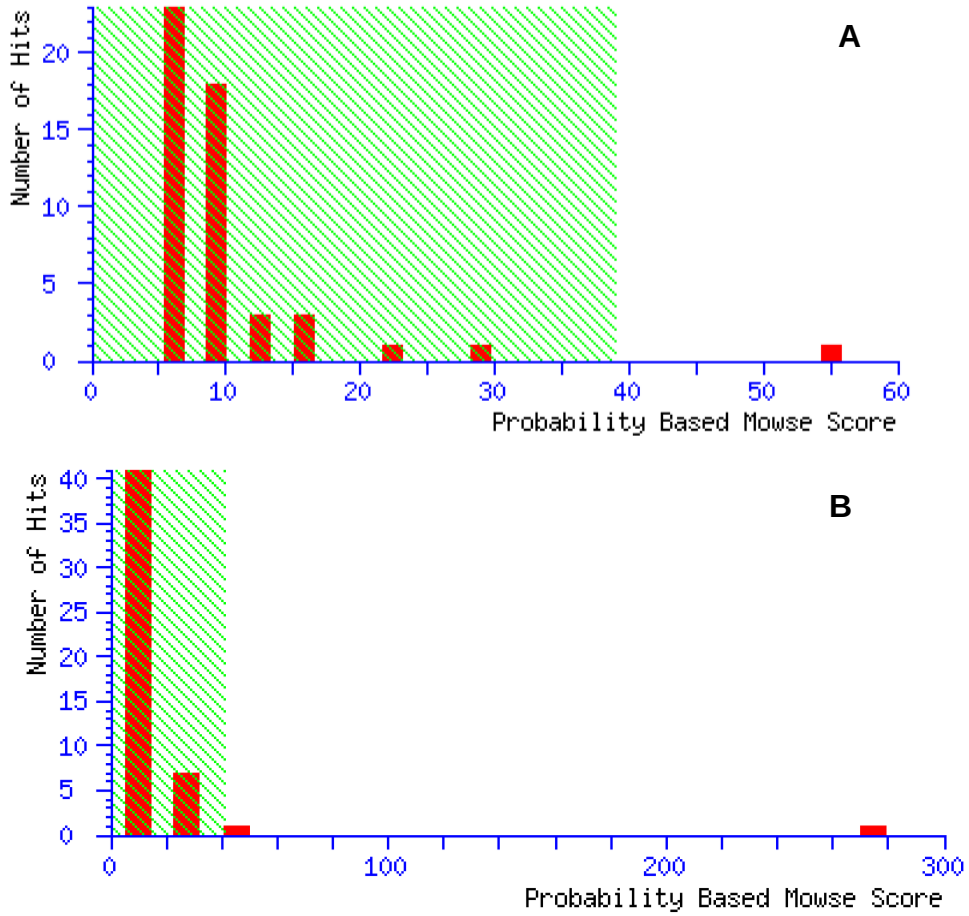

Figure 5-20: *Probability Score for peptide analysis of mEH (#3, (A)) and EH4 (#8, (B)). Both scores are significant since they are above significance level (green shade).*

Samples 2, 4, 5 and 7 resulted in the match of different proteins as expected at least for sample 4. Most probably, the additional band (37kDa) observed in coomassie gel did not correspond to the recombinant expressed protein, but rather was an effect of infection and expression of membrane bound proteins. Figure 5-21 shows the coomassie analysis of Sf9 cells transfected with a putative bacterial Oxidoredutktase (Rv3790) compared to Sf9 Wt cells. The Rv3790 infected cells also show an additional band at ~ 37kDa.

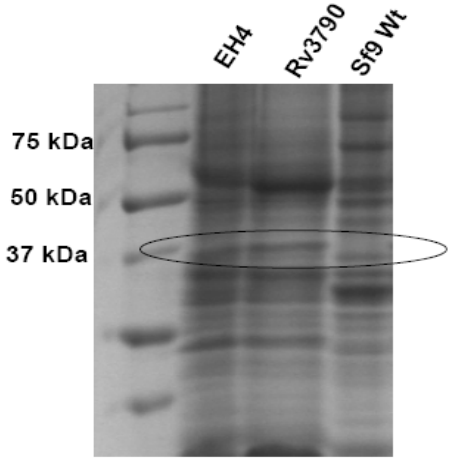

Figure 5-21: *Coomassie gel of Sf9 Wt cells and Sf9 cells infected with EH4 and Rv3790 (control cells). The additional band at 37kDa observed in EH4 expressing cells is also present in control infected cells, but not in Sf9 Wt cells.*

These results demonstrate that EH3, as well as EH4, were only expressed to a low amount and that the additional band does not correspond to the recombinant protein. Furthermore, it was possible to identify peptides from proteins separated by SDS-Page and directly digested in the gel by LC-MS/MS. This shows that the method could be applied for detailed analysis of specific bands.

5.1.5.5 EH4 activity assay in Sf9 cell lysates

Activity measurements with Sf9 cell lysates were performed using LC-MS/MS. There was no significant and reproducible turnover of EETs (5(6) EET, 8(9) EET, 11(12) EET, 14(15) EET), EpoMEs (leukotoxin 9(10) EpoME, isoleukotoxin 12(13) EpoME), Hepoxilins (HxA3, HxB3), 19(20) EDPE, 17(18) EETeE, 2(14(15) EET)-EG and 14(15) EET-EA by EH4, when compared to control infected cells.

To investigate whether there was a slight enzymatic activity of EH4 in the lysate, that was masked by the background activity of Sf9 cells, a screening for potential inhibitors of endogenous hydrolase activity was performed. This inhibitor should block background activity in order to reveal putative hydrolase activity of EH4. It was shown that juvenile hormone epoxide hydrolase (JHEH) from *manduca sexta* has 64% similarity to human mEH (Wojtasek and Prestwich 1996). Therefore, Sf9 endogenous EH is most likely a membrane associated enzyme. Screening for endogenous inhibitors was carried out with different mEH inhibitors. As figure 5-22 shows, valpromide is a potent inhibitor of endogenous hydrolase activity in Sf9 cells, and incubation with 5mM valpromide reduces endogenous activity about 98%. First experiments aiming at the determination of IC_{50} values indicated an inhibition of 50% at approximately 500µM (figure 5-23).

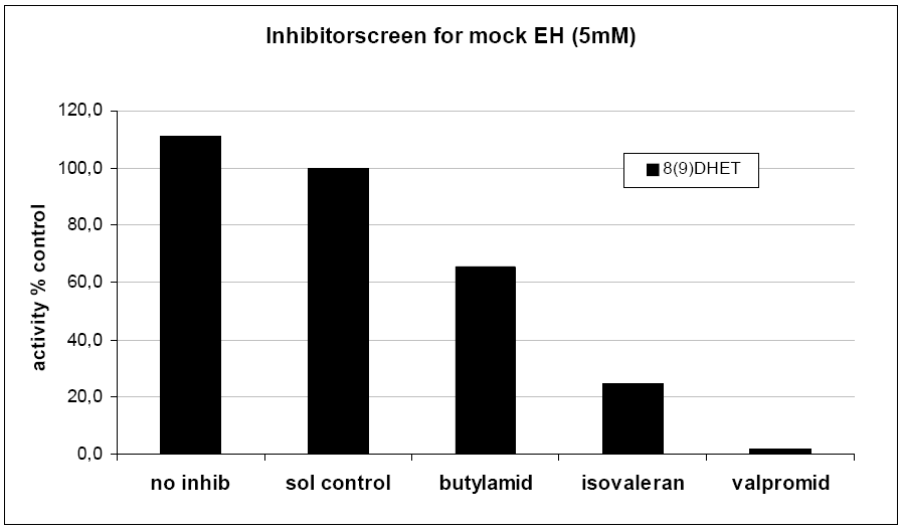

Figure 5-22: *Inhibitor screen for endogenous EH in Sf9 cells. Mock transfected Sf9 cells were disrupted by French® Pressure Cell press and preincubated with different inhibitors (5mM) for 5 minutes on ice. Turnover of 8(9) EET (5µM) for 30 minutes was measured by LC-MS/MS.*

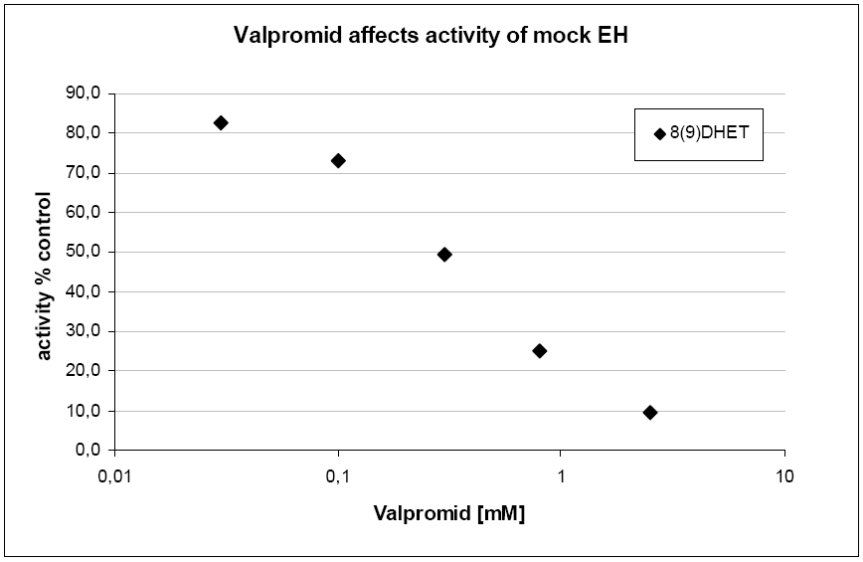

Figure 5-23: *IC_{50} determination of Valpromide. Sf9 cells infected with mock virus were preincubated with valpromide at different concentrations for 5 minutes on ice, before adding 5µM substrare (8(9) EET). Enzymatic reaction was continued for 30 min at 37℃ before an alysis in LC-MS/MS.*

Attempts to measure EH4 activity at simultaneous inhibition of endogenous activity with 5mM valpromide could not demonstrate EH4 specific turnover of EETs (5(6) EET, 8(9) EET, 11(12) EET, 14(15) EET), EpOMEs (leukotoxin 9(10) EpOME, isoleukotoxin 12(13) EpOME) and Hepoxilins (HxA3, HxB3). The level of diol detected in EH4 infected cell lysate was the same as observed in the control. Furthermore, the activity in EH4 cell lysate towards EET regioisomers and EpOMEs was inhibited by valpromide, indicating that the activity measured in recombinant lysates was a result of endogenous EH.

5.1.5.6 Attempts to purify EH4-His from Sf9 lysate

Western Blot analysis and peptide analysis of Sf9 cell lysates confirmed the presence of EH4-His after infection of insect cells as described above. Although EH4 was not overexpressed in Sf9 cells (see 5.1.5.4) and although the protein is assumed to be membrane bound, attempts to enrich and concentrate possible minimal amounts of EH4 from the soluble fraction were made. It is possible that the immunological method to detect His-tagged EH4 was not sensitive enough to detect small amounts of EH4 in the soluble fraction. EH4 expressing Sf9 cell lysates were submitted to immobilized metal-affinity chromatography (IMAC; (Porath, Carlsson et al. 1975) using Ni2+ (BioRad DuoFlow). Figure 5-24 shows the histogram of the respective run.

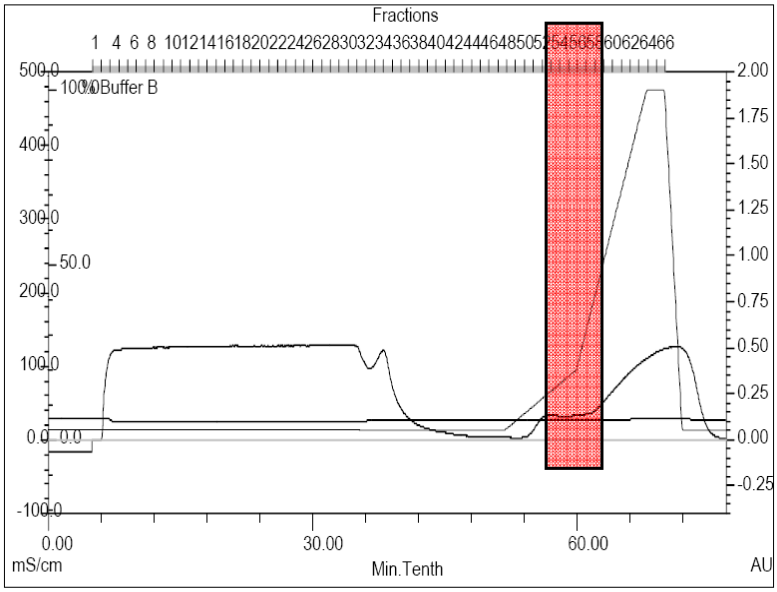

Figure 5-24: *Affinity chromatography of His-tagged EH4 recombinantly expressed in Sf9 cells.*

15µl of the different 1ml fractions (flow-through 2-4 and 32-36, elution 51-66) were analyzed by coomassie staining. As illustrated in figure 5-25, fractions 53 to 56 showed a specific eluted band at approx. 45kDa, that was also immuno reactive to α-His antibody. However, activity measurements with the respective fractions towards EET regioisomers did not show any signs of specific turnover. To further confirm the presence of EH4-His and to test whether the eluted protein corresponds to EH4, the fractions were digested with trypsin and analyzed by LC-MS/MS. Because the subsequent MRM scan failed to detect EH4 specific peptides in the sample, an EMS scan that analyses all peptides that are present in the sample was performed. The following BLAST analysis resulted in the detection of the endogenous protease Cathepsin L (figure 5-26).

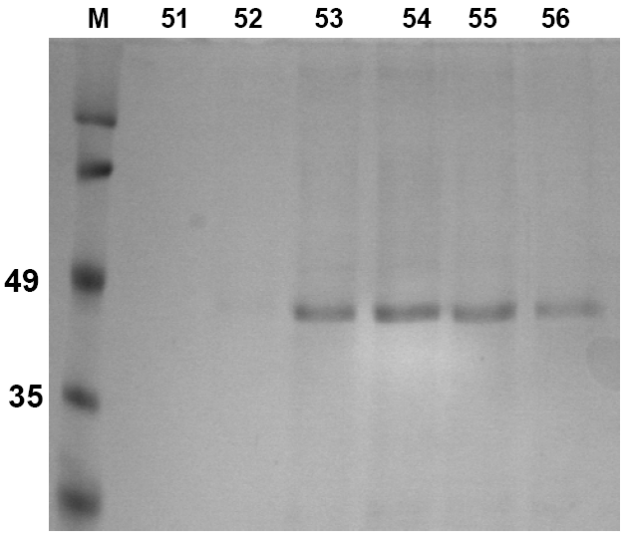

Figure 5-25: *Coomassie analysis of the elution fraction marked in red (see figure 5-22). Affinity chromatography resulted in the purification of Cathepsin L.*

Results of the mascot Blast search (www.matrixscience.com) pointed towards a Cathepsin L like protease from *Helicoverpa armigera* (Cotton bollworm; Q6UB44_HELAM) with a probability based

mowse score of 144 (significance level 53) based on three matching queries (peptides shown in red; figure 5-26)

```
  1 MKSIAVLLCV VGAACAVSLL DLVREEWSAF KLEHSKRYDS EVEDKFRMKI
 51 YLENKHRIAK HNQRFEQGAV SYKLRPNKYA DMLSHEFVHV MNGFNKTLKH
101 PKAVHGKGRE SRPATFIAPA HVTYPDHVDW RKKGAVTEVK DQGKCGSCWA
151 FSTTGALEGQ HFRKTGYLVS LSEQNLIDCS AAYGNNGCNG GLMDNAFKYI
201 KDNGGIDTEK AYPYEGVDDK CRYNAKNSGA DDVGFVDIPQ GDEEKLMQAV
251 ATVGPVSVAI DASQESFQFY SDGVYYDENC SSTDLDHGVM VVGYGTDEQG
301 GDYWLVKNSW GRTWGDLGYI KMARNKNNHC GIASSASYPL V
```

Figure 5-26: *Mascot search results of the purified protein analyzed by LC-MS/MS. Peptides that match with the primary sequence of Cathepsin L like protease of Heliothis armigera are shown in red.*

The results suggest that the purified protein is a Sf9 analogue of the Sf21 protease, which was purified and characterized by Johnson et al (Johnson and Jiang 2005). The protease is expressed in Sf21 at high levels and shares properties with cystein proteases of the papain family. This protein copurifies with histidine tagged proteins from Ni^{2+} affinity columns.

5.1.6 Subcellular localization of EH4

In order to investigate the subcellular localization and confirm the predicted membrane localization of EH4 obtained by *in silico* analysis, EH4 was analyzed by differential centrifugation as described under materials and methods. Figure 5-27 shows the western blot analysis of different subcellular fractions and clearly demonstrates that EH4 is present and enriched in all membrane containing fractions. This indicates that EH4 is membrane associated.

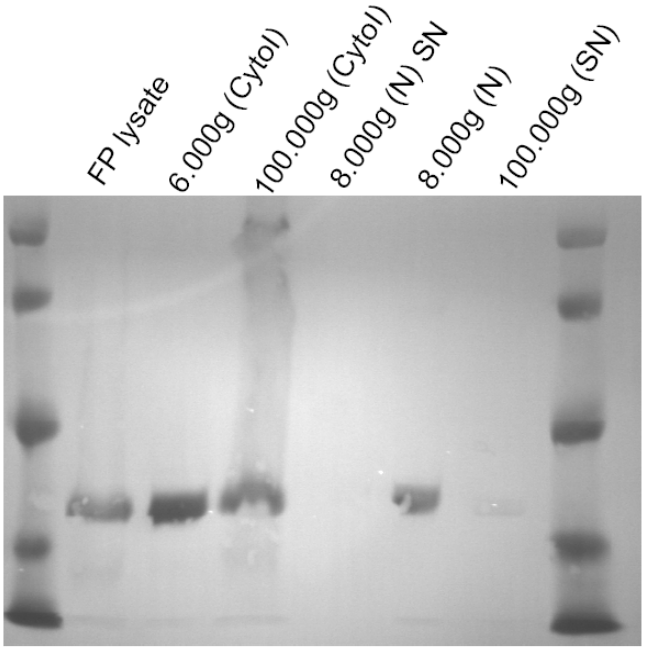

Figure 5-27: *Western Blot analysis of subcellular localization of EH4-His recombinantly expressed in Sf9 cells. The sample was centrifuged at 800g for 15 minutes to separate the nucleic fraction (N) from the cytosolic fraction (CytoI). SN: supernatant. (for details see 4.7.6)*

Figure 5-27 shows that EH4 was enriched and present in membrane fractions. Therefore, activity assays with homogenized pellets of EH4 infected Sf9 cells were performed. The objective was to

detect enzymatic activity of EH4, which so far might have been missed due to a low enzyme concentration. However, LC-MS/MS based activity assays using homogenized pellets failed to prove hydrolase activity of EH4 towards EET regioisomers and EpOMEs.

5.1.7 Expression of EH4 *in vivo*

In silico analysis of EH4 indicated expression mainly in the central nervous system. In addition, expression is present in the respiratory system, the hematological system and the gastro intestinal system, as well as in its associated organs.

To investigate the *in vivo* expression of EH4, and to confirm the *in silico* expression data, different tissues from mice were analyzed by RT PCR. The tested organs belong to the respiratory system (lung), hematological system (blood, spleen), central nervous system (brain), urogenital system (kidney), cardiovascular system (heart), muscular system (muscle) and the GI tract (liver). As figure 5 - - 28 shows, EH4 is clearly expressed in whole brain homogenate. Other experiments also indicated expression in cultured astrocytes, olfactory bulb, blood, liver and lung. However this was less clear and validated. Identity of the amplificate obtained by RT PCR from brain was confirmed by sequence analysis.

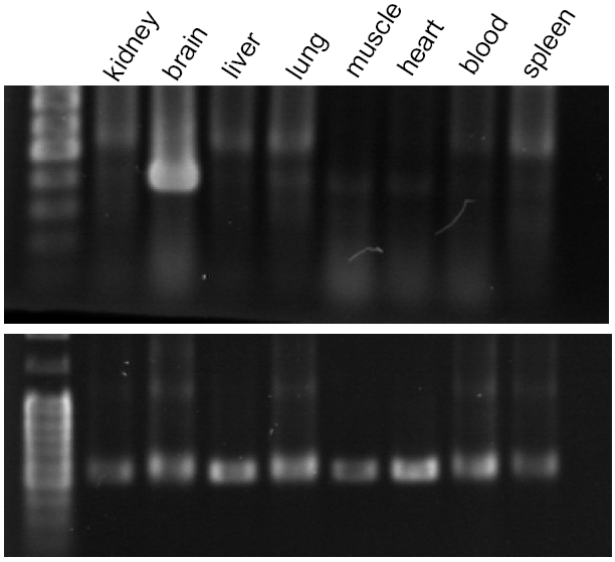

Figure 5-28: *Agarose gel analysis of EH4 expression in different tissues from mice by RT-PCR. A: Amplification of EH4 (390 bp), B: Amplification of GAPDH (positive control; 523bp).*

5.2 Functional characterization of EH3

The second part of this thesis comprises a characterization of the enzymatic activity of EH3 by i) analyzing the substrate profile and ii) determination of the kinetic parameters of 8(9) EET, 11(12) EET, 14(15) EET and 9(10) EpOME turnover. In addition to that, the effects of established sEH and mEH inhibitors on EH3 activity were investigated.

5.2.1 In silico characterization of EH3

The human EPHX3 gene (GeneID: 79852, HGNC: 23760) is located on human chromosome 19, at 19p13.12 according to Entrez Gene. Other names of this gene are ABHD9, FLJ22408 and MGC131519. The gene contains 7 exons and 6 introns and produces a 1891bp mRNA that encodes for a 360 aa protein (40.9kDa) (Thierry-Mieg and Thierry-Mieg 2006). The protein studied in this work refers to Q9H6B9 (UniProtKB/Swiss-Prot) and displays an N-terminal signal peptide (aa 1- 35) and a predicted glycosylation site at aa 267 (N-linked glycosylation; http://www.uniprot.org/uniprot/Q9H6B9). Other in silico analyses point towards a mitochondrial targeting sequence (cleavage site at position 62) and C-mannosylation at position 110. The EPHX3 gene is present in chimpanzee (99%), dog (87%), mouse (83%) and zebra fish (49%) and all share high sequence identity with the human protein (% identity given in brackets). The closest *c. elegans* genes are ceeh-1 (42%) (UniProt accession number Q21147) and ceeh-2 (38%) (UniProt: Q21277). The gene is expressed in human tissues, mostly in lung, skin, placenta, kidney and brain (Thierry-Mieg and Thierry-Mieg 2006).

5.2.2 Activity assays using LC-MS/MS

LC-MS/MS was used to demonstrate enzymatic activity of EH3 towards different substrates and to determine kinetic parameters.

5.2.2.1 Direct precipitation in acetonitrile

For LC-MS/MS analysis, the respective analytes need to be solved in acetonitrile. The general method was to extract the compounds with ethyl acetate, evaporate the solvent and resolve the analytes in acetonitrile. However, the efficacy of extraction with ethyl acetate is a subject to considerable variations and thus turned out to be impractical for quantitative analysis and validation of experiments in this work. To bypass this problem, a protocol using direct precipitation in acetonitrile was established. By using this protocol, the measurement errors based on varying extraction efficacy were eluded. Figure 5-29 shows that the precipitation in acetonitrile sufficiently inhibits enzymatic activity of EH3. EH3 was incubated with three different EET regioisomers and precipitated after 1 and 10 minutes. Precipitation inhibits EET hydrolysis as seen in the different amounts of DHETs produced after 1 minute as compared to DHET amount produced after incubation for 10min. The ratio (10min/1min) for 8(9) EET is 19, for 11(12) EET and 14(15) EET the ratio is 14 and 16, respectively. The value obtained is higher than 10, which can be explained by an initial lower temperature. The

samples were kept on ice until the substrate was added. This implicates that the assay temperature in the first minute might have been lower than 37℃.

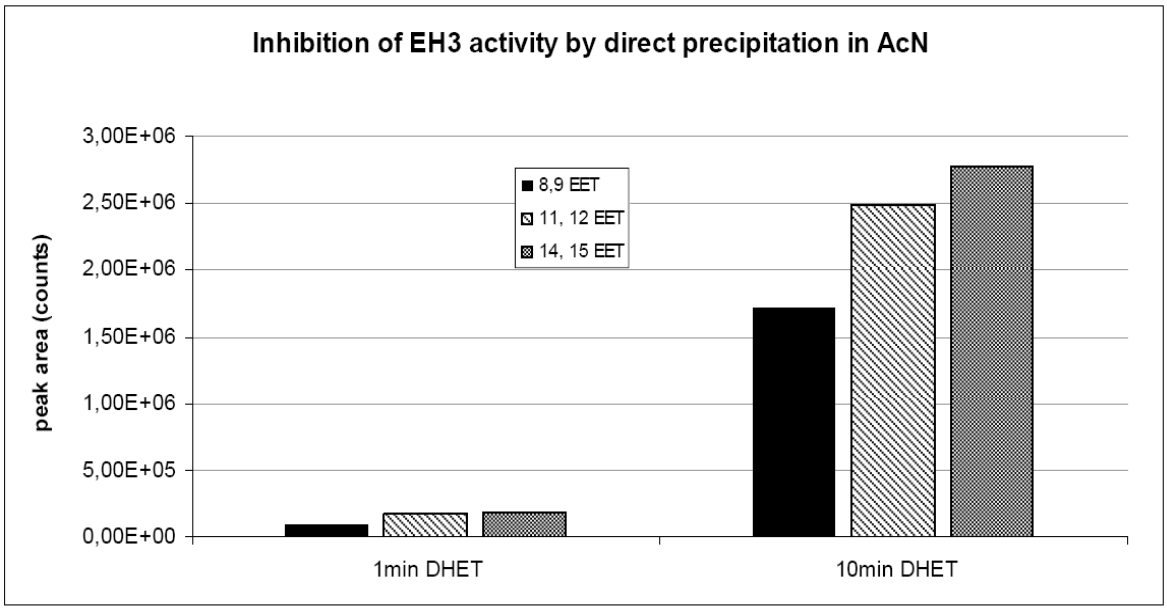

Figure 5-29: *EH3 was recombinantly expressed in Sf9 cells. FP lysate was incubated with 20µM 8(9)-, 11(12)- and 14(15) EET at 37℃. After 1 and 10 minutes, 1 volume acetonitrile was added to the sample before centrifugation and analysis by LC-MS/MS. In the meantime, the 1 minute sample was further incubated at 37℃ to test for en zymatic activity in 50% acetonitrile.*

5.2.2.2 Precision of EET/DHET quantitation

For quantitative analysis and determination of kinetic parameters, linearity of DHET detection and the calibration curve of the respective transition signals in LC-MS/MS, at least in the field of the investigated concentration range, is a basic requirement. Measurement of different DHET amounts showed that signal intensities in the range below, as well as above 10µM DHET directly correlate. The signal rises linearly with the increase of DHET amount injected on the column (figure 5-30).

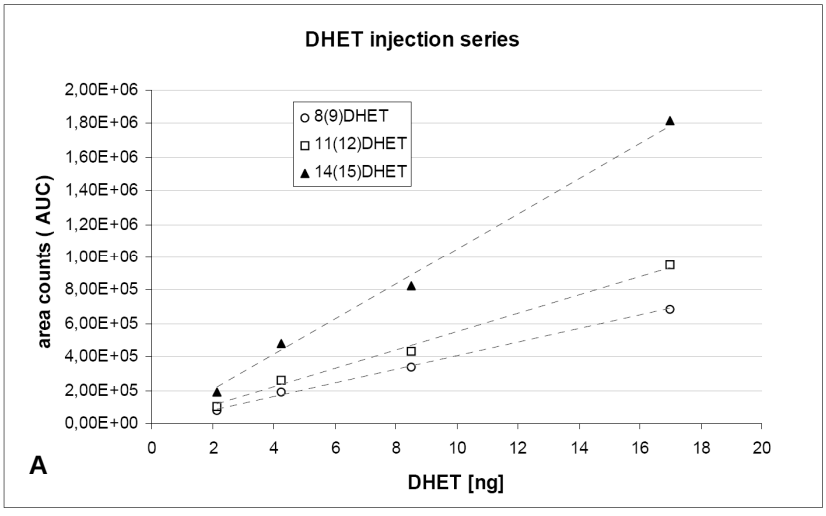

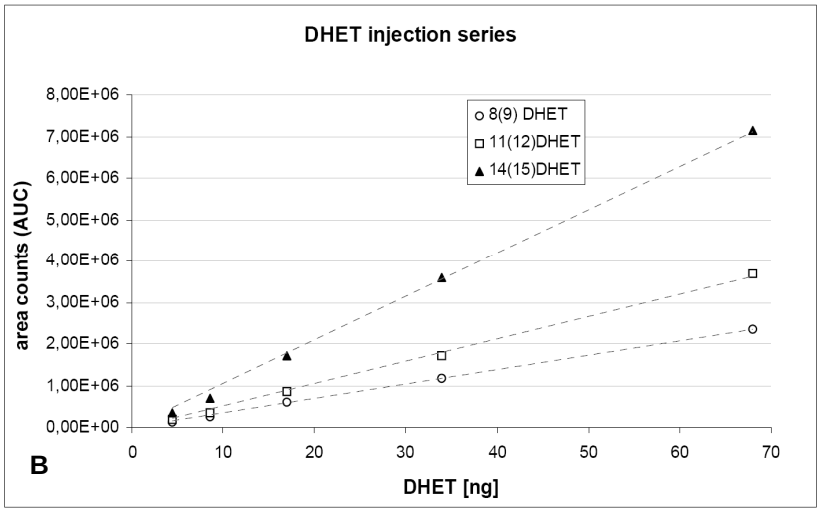

Figure 5-30: *Linearity of DHET signal intensities of different amounts injected. The signal rises linearly with the amount of DHET injected on the column.*

5.2.3 Substrate profile of EH3

Epoxyeicosatrienoic acids (EETs) are converted by EH3 to their corresponding diols. Therefore, catalytic constants of the respective turnover were determined. Activity assays using other lipid epoxides with indicated physiological function were performed in this work, to unveil different substrates by which EH3 might intervene with physiological processes.

5.2.3.1 Kinetic parameters of EET turnover

Epoxyeicosatrienoic acids are important signaling molecules and endogenous substrates of EH3. To classify the relevance of EET turnover by EH3, kinetic parameters of EET turnover were determined. These parameters were compared to the catalytic constants of sEH and mEH in order to assess the physiological impact of EH3. Figure 5-31 shows the kinetic analysis of EET turnover. The results of these analyses and a comparison with the previously obtained data of human sEH and mEH (Marowsky, Burgener et al. 2009) are given in table 5-7.

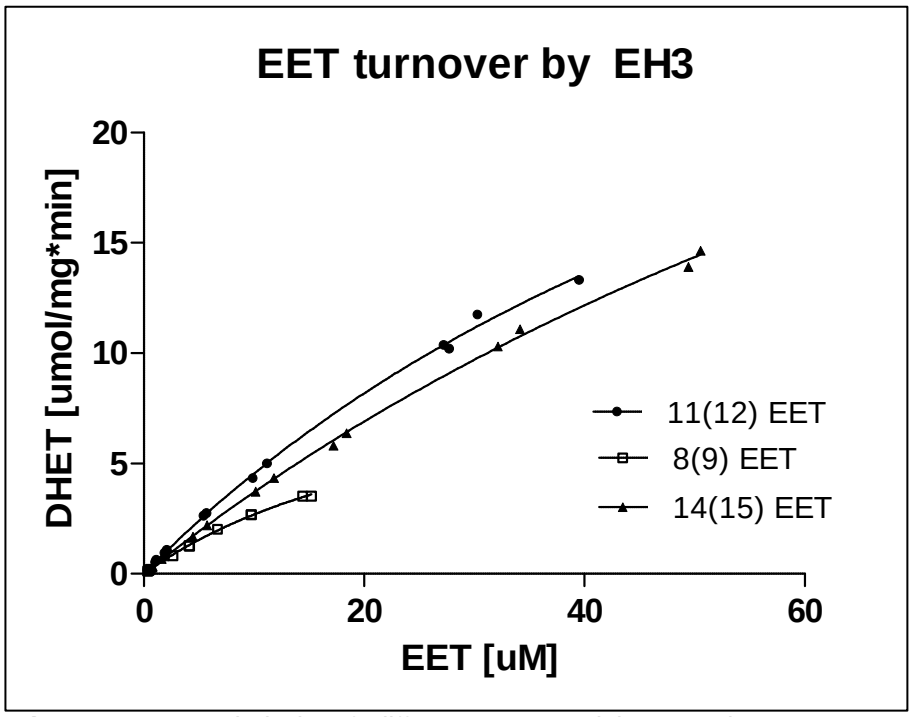

Figure 5-31: *Hydrolysis of different EET regioisomers by EH3. EH3 expressing Sf9 cells were disrupted by French® Pressure cell press and assay was performed as described in materials and methods. Results of the analysis are given in the table below.*

	EH3	sEH[a]	mEH[a]
8,9-EET			
Vmax [µmol x mg-1 x min-1]	10.47	2.4	0.1
Km [µM]	28	2	1
kcat/Km [s-1 x M-1]	2.5×10^5	5×10^5	1×10^5
11,12-EET			
Vmax [µmol x mg-1 x min-1]	40.4	11	0.3
Km [µM]	78	0.6	0.5
kcat/Km	3.53×10^5	5×10^6	2×10^5
14,15-EET			
Vmax [µmol x mg-1 x min-1]	51.2	20	0.025
Km [µM]	128	2	0.25
kcat/Km	2.75×10^5	5×10^6	1×10^5

Table 5-7: *Comparison of kinetic parameters of EET turnover by EH3, mEH and sEH. V_{max} and K_M were determined by kinetic modeling.*
[a]: Catalytic constants of EET turnover from the recombinant mouse enzyme reported previously (Marowsky, Burgener et al. 2009).

Table 5-7 shows that the catalytic efficacy of EET turnover (8(9) EET, 11(12) EET, 14(15) EET) by EH3 is in the same order of magnitude as those of mEH and sEH. In fact the V_{max} values of EH3 are higher, but since enzymes generally catalyze reactions below K_m, the ratio K_{cat} over K_m is the relevant value.

The resulst show that all analyzed substrates were converted by EH3 with high V_{max} and K_m. This resulted in catalytic efficacies that are in the range of those that were reported for mEH. Turnover of 5(6)-EET was not analyzed, because insect cell preparations displayed a significant background activity with this particular substrate. All other EET regioisomers remained essentially stable in the presence of insect cell homogenates that were infected with control virus.

5.2.3.2 Other substrates of EH3

Screening for possible epoxides as substrates for EH3 revealed other endogenous mediators that are hydrolyzed by EH3. Figure 5-32 depicts the turnover of leukotoxin and isoleukotoxin (12(13) EpOME), as well as the two hepoxilins HxA3 (Hepoxilin A3) and HxB3 (Hepoxilin B3). The diagram displays the formation of the corresponding diols (DiHOMEs and Trioxilins) in % of total turnover.
The well established sEH inhibitor AUDA (12-(3-adamantan-yl-ureido) dodecanoic acid) is an inhibitor of EH3 enzymatic activity as described below (5.2.5). This inhibitor was used to specifically ascribe the

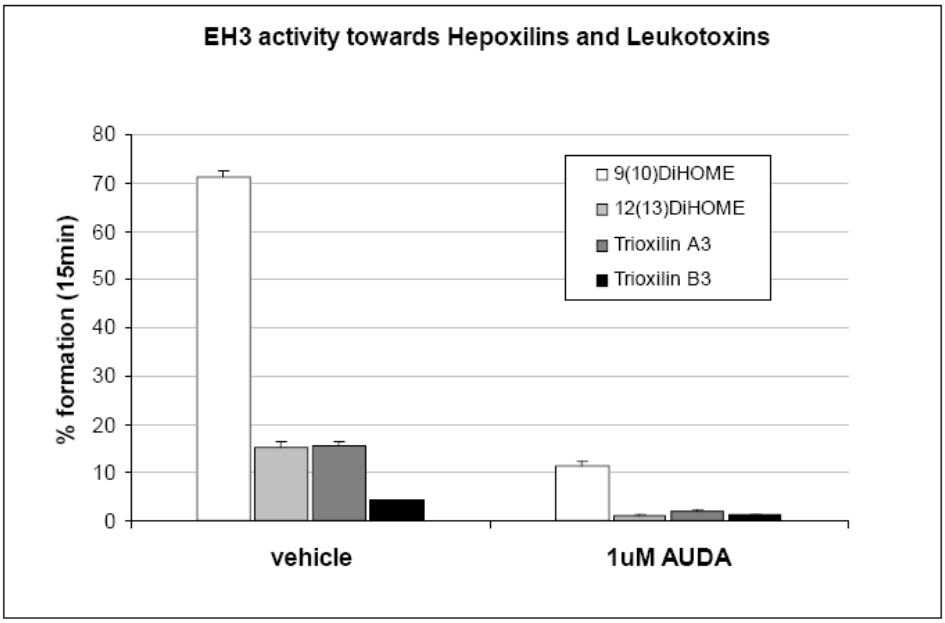

Figure 5-32: *Specific activity of EH3 towards leukotoxins (9(10) and 12(13) EpoME) and hepoxilins (Hepoxilin A3 and B3). The activity is shown as formation of the respective diols after 15min. Inhibition with the sEH inhibitor AUDA leads to significant decrease of diol formation, demonstrating that the turnover is EH3 specific.*

respective turnover to EH3, and to discriminate EH3 activity from a background activity. Within the investigated time period of 15 min, the formation of leukotoxin - diol (9(10) DiHOME) was the highest with 70% of total leukotoxins being hydrolyzed. In contrast, only 4% Hepoxilin B3 was converted to the corresponding Trioxillin B3. Both substrates, isoleukotoxin and Hepoxilin A3, were hydrolyzed to the same amount (15%).
Finally a series of other lipid derived epoxides was investigated. First experiments in this study indicated that EH3 is also capable of hydrolyzing the 14(15) epoxide of arachadinoyl ethanol amide 14(15) EET-EA. This is a potential CYP450 metabolite of the cannabinoid receptor agonist

anandamide (figure 5-33). Turnover of 14(15) EET-EA by EH3 resulted in 40 times the formation of the respective diol than in control cells. Hydrolysis with hsEH served as positive control.

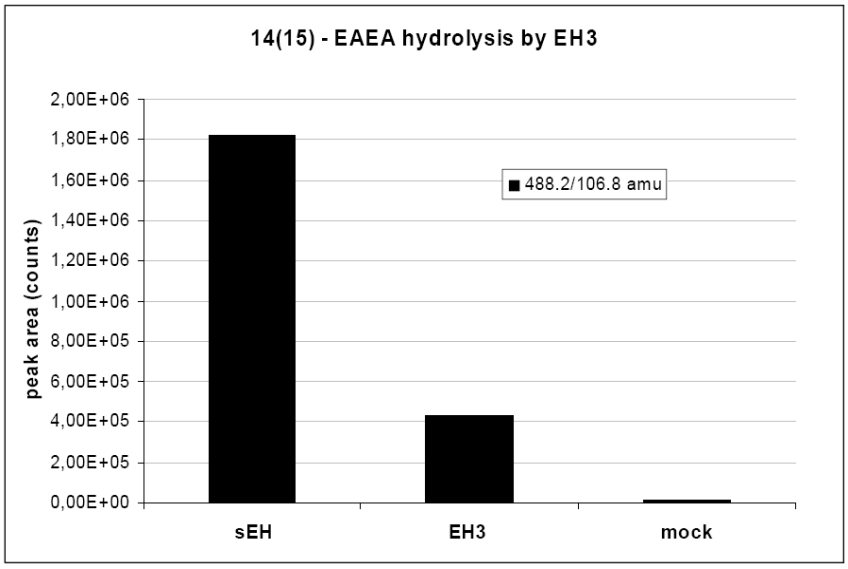

Figure 5-33: *Hydrolysis of the epoxy metabolite of arachadinoyl ethanol amide, 14(15) epoxy arachadinoyl ethanol amide (14(15) EET-EA). Control cells only show marginal amounts of the respective diol compared to EH3 expressing Sf9 cells.*

In contrast to the above investigated substrates, EH3 wasn't capable of hydrolyzing 17(18) EpETE, 19(20) EDPE and 2-14(15)-epoxy glycerol (2-14(15) EG, data not shown). There was no difference between EH3 expressing cells and control infected Sf9 cells in turnover of 17(18) EpETE and 19(20) EDPE. In addition to that, inhibition with 1µM AUDA had not effect on the amount of diol produced. This indicates that EH3 is not involved in the formation of the respective diol. Results from 2(14(15)-EET) EG turnover indicated, that Sf9 cells display endogenous 2-EG esterase activity. 14(15) EET as well as 14(15) DHET were detected in the cell lysates after incubation with the glycerol ester derivate. Most probably, endogenous esterases hydrolyze 2(14(15)-EET) EG into 14(15) EET. 14(15) EET in turn is hydrolyzed by EH3 to the corresponding diol 14(15) DHET. This is an explanation for the detection of 14(15) EET and 14(15) DHET in this assay. Hence the analysis of hydrolase activity of EH3 towards this particular substrate is not possible in Sf9 cell lysates.
A detailed determination of kinetic parameters of 14(15) EET-EA turnover in the given time frame was not considered due to the high costs of the respective substrate.

5.2.3.3 Kinetic parameters of Leukotoxin turnover

Leukotoxin is an endogenous lipid mediator and a substrate of EH3 that is efficiently hydrolyzed by EH3 (70% turnover after 15 min) as shown above (5.2.3.2). As it displays important physiological function in development of ARDS, the respective kinetic parameters of leukotoxin turnover by EH3 were determined (figure 5-34). Leukotoxin is converted by EH3 with a V_{max} of 20.67 µmol mg^{-1} x min^{-1} and a K_m of 25.2 µM.

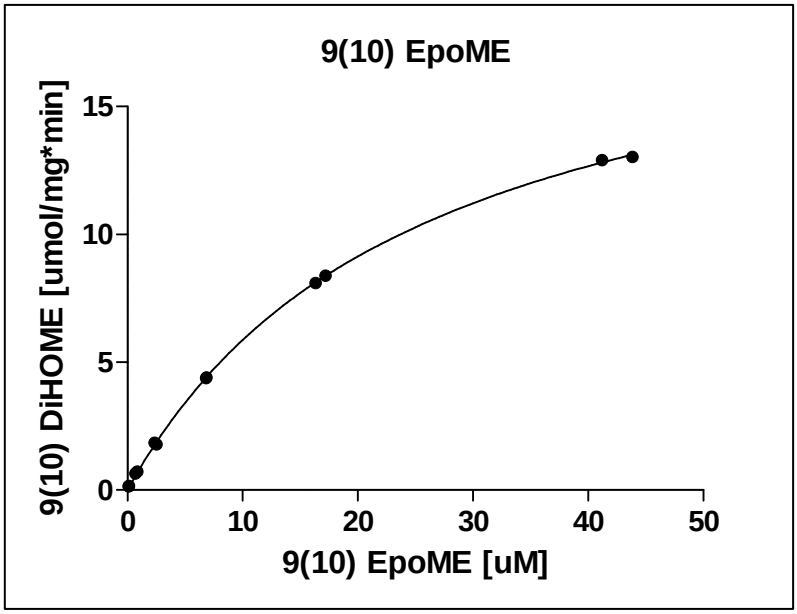

Figure 5-34: *Hydrolysis of leukotoxin (9(10) EpoME) by EH3. EH3 expressing Sf9 cells were disrupted by French® Pressure cell press and assay was performed as described in materials and methods. Results of the analysis are given in the table below.*

Table 5-8 shows a comparison of the catalytic constants of EH3 with those of sEH and two *c. elegans* enzymes, which were investigated by Harris and colleagues recently (Harris, Aronov et al. 2008).
The catalytic efficacy (K_{cat} / K_m) of 9(10) EpOME turnover by EH3 is slightly higher than that of sEH and about an order of magnitude higher than that of ceeh-1. Ceeh-2 shows only very low turnover of leukotoxin with a catalytic efficacy of 1.2 x 10^3 M^{-1}x s^{-1}.

	EH3	sEH[c,b]	ceeh-1[b]	ceeh-2[b]
Leukotoxin (9(10) EpOME)				
V_{max} [µmol x mg^{-1} x min^{-1}]	20.67	2.78	0.137	6.7 x 10^{-3}
K_m [µM]	25	6.15	7.5	8.4
k_{cat}/K_m [M^{-1}x s^{-1}]	5.6 x 10^5	4.5 x 10^5	2.9 x 10^4	1.2 x 10^3

Table 5-8: *Kinetic parameters of leukotoxin (9(10) EpOME) turnover by EH3, sEH and the c. elegans orthologous ceeh-1 and ceeh-2. V_{max} and K_m of EH3 were determined by kinetic modeling as described in materials and methods. Values of sEH, ceeh-1 and ceeh-2 are taken from the results published by Harris et al. (b) (Harris, Aronov et al. 2008) and Greene (c) (Greene, Williamson et al. 2000).*

5.2.4 Quantification of EH3

For determination of the kinetic parameters of EET turnover by EH3, in particular V_{max} and k_{cat}, the amount of EH3 present in the investigated cell lysate needs to be determined. To calculate the protein concentration, EH3 was first expressed in bacteria. The concentration of recombinant EH3 was calculated based on serial dilutions of BSA. Secondly, a western blot with known EH3 concentration was performed to calculate western blot signals from the Sf9 cell lysates.

5.2.4.1 Expression of EH3 in E. coli

For recombinant expression of EH3 in *E .coli*, a pRSETb expression vector that contains the full length EH3 cDNA (EH3 (FL)) was generated by EcoRI / NcoI cloning, using an EH3 containing plasmid (provided by Michael Arand). This vector was used as template for amplification of anchorless EH3 (primer #15 and #16; details and PCR conditions see appendix). The resulting PCR fragment was subcloned into PCR4 Topo vector. Since the NcoI restriction site in this EH3 containing vector turned out to be spontaneously mutated during PCR amplification and therefore was not applicable for further cloning into pRSETb, the vector was digested with EcoRI and alternatively cloned into pRSETc. For generating the respective pRSETb construct, a KasI/EcoRI fragment of Topo-EH3 was cloned into a pRSETb construct that was produced earlier (pRSETb EH3 frameshift; figure 5-35).

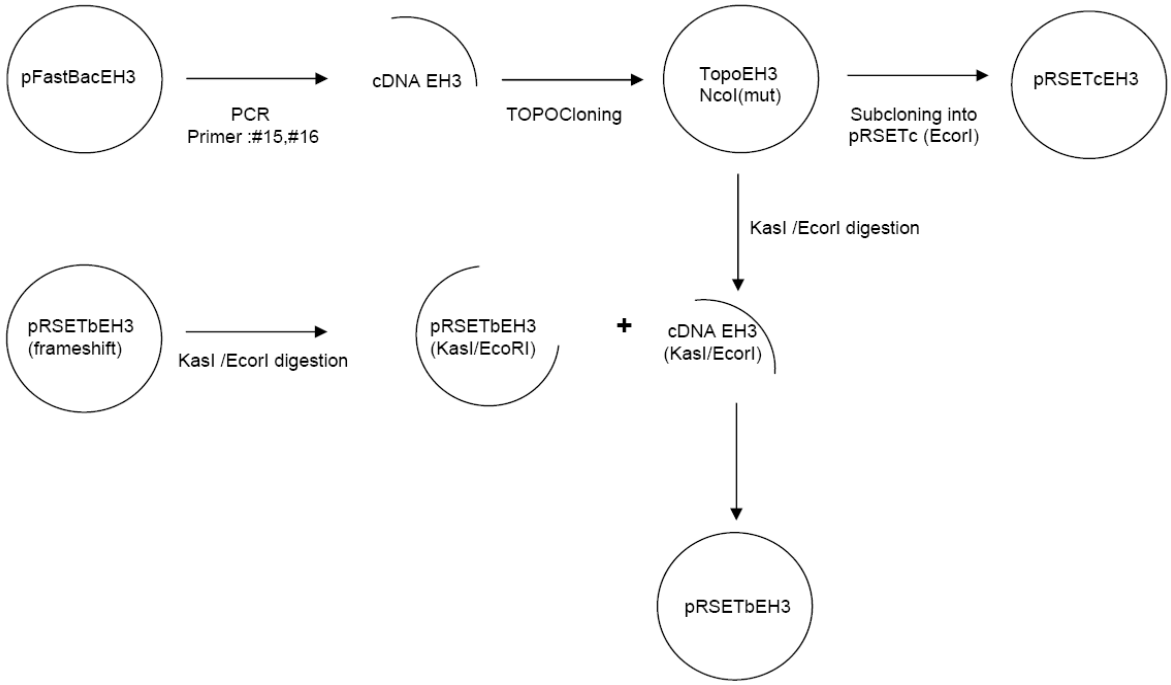

Figure 5-35: *Cloning diagram for generation of EH3 expression constructs.*

This earlier produced construct includes a single mutation at position 528, which leads to a frameshift and thus premature termination of translation. This finally results in a truncated EH3 protein with 146 aa (sequence see appendix). Both anchorless proteins (pRSETbEH3, pRSETcEH3) were overexpressed (figure 5-36), whereas the full length protein was not.

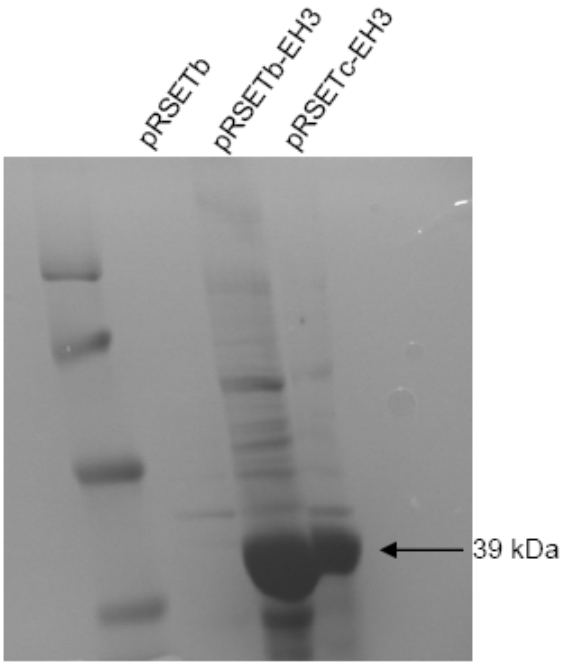

Figure 5-36: *Expression of anchorless EH3 in BL21DE3. Expression was induced at OD_{600}~ 0.4 with 1mM IPTG and continued for 4h at 37℃. Bacterial cells were resuspended in assay buffer and disrupted by French® Pressure Cell Press. Lysate was centrifuged for 20min at 4000 rpm to spin down inclusion bodies.*

5.2.4.2 Determination of EH3 amount present in Sf9 cell lysate

For quantifying the EH3 amount that is present in Sf9 lysates, His- tagged EH3, that was expressed in *E. coli,* was used as a standard to calibrate Western Blot signals of Sf9 lysates. The amount of His-tagged EH3 present in bacterial inclusion bodies was calculated based on a BSA calibration curve (figure 5-37).

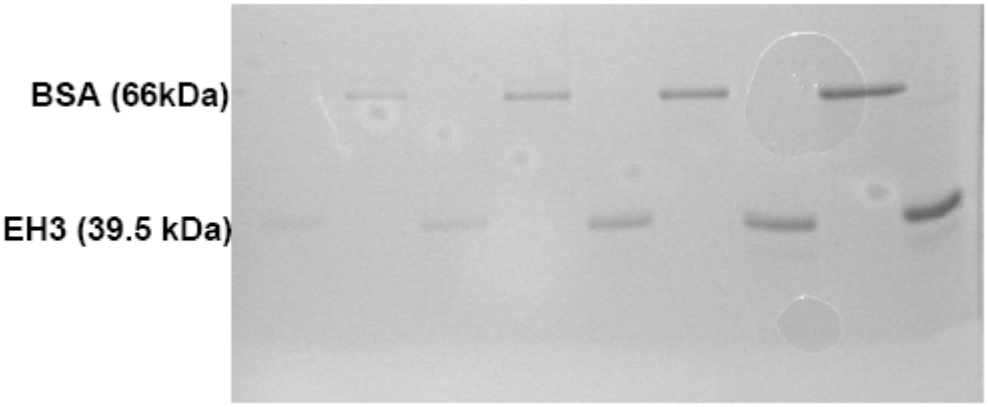

Figure 5-37: *Coomassie staining of BSA and EH3 separated on SDS-Page (12.5%). A dilution series of 0.25µg – 2µg BSA was loaded on the gel to quantify the amount of EH3 present in different dilutions of inclusion bodies.*

Calibration of BSA signals (figure 5-38) revealed 1.6 area counts per ng BSA. This value was used to quantify the protein amount of EH3 expressed in *E. coli* (figure 5-39).

Different dilutions of EH3 inclusion bodies (in 10 µl endvolume each) were analyzed by coomassie staining (5-39 A) and density was measured by ImageJ (figure 5-39 B). Signal intensity increased with dilution factor (R^2=0.9934). Calculation of density signals revealed a concentration of 0.6 µg/µl of EH3 in the above used inclusion body suspension.

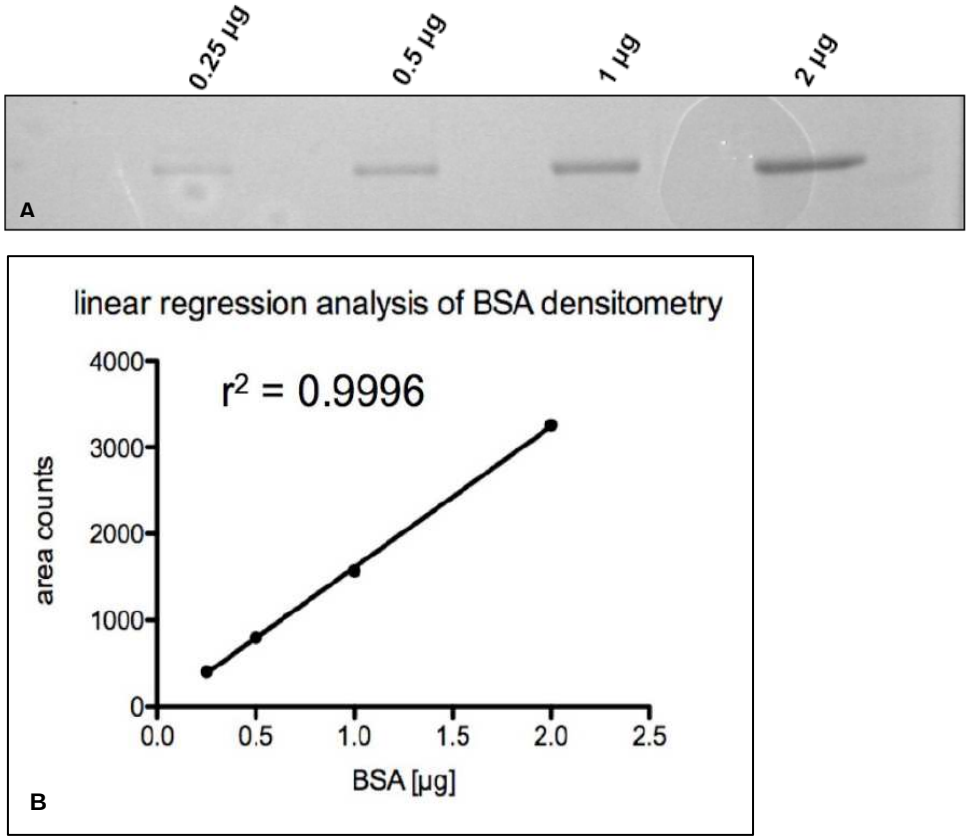

Figure 5-38: *Calibration of BSA density signals from coomassie staining using ImageJ. BSA (0.25 µg - 2 µg) was loaded on 12.5% PAA gel and stained with coomassie (A). Calibration curve of BSA density signal after analysis with ImageJ (B).*

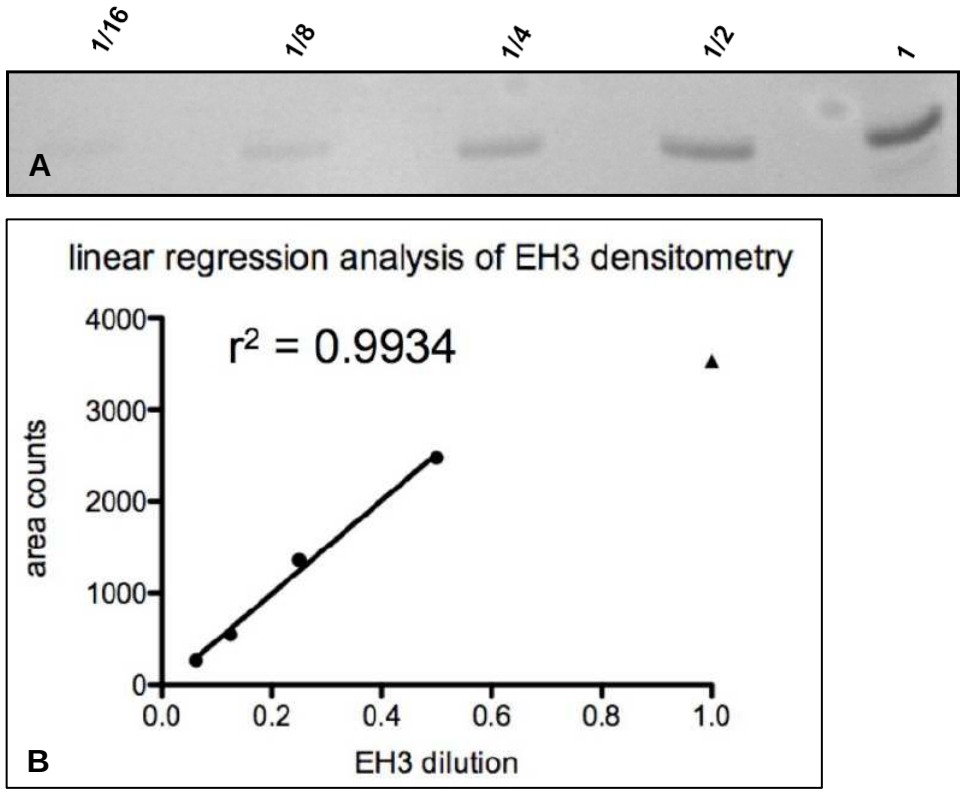

Figure 5-39: *Quantification of EH3 expressed in E. coli. Inclusion bodies were washed in 20mM TE buffer and different dilutions were submitted to SDS-Page (12.5%) and analyzed by coomassie staining (A). Evaluation of signal density was performed using ImageJ (B).*

Subsequently, different amounts (1.25 ng - 20 ng) of EH3 protein were analyzed by western blot, and density signals of EH3 were evaluated by ImageJ. Comparison of the signals from Sf9 cell lysates with the signals of known EH3 concentration was used to determine the concentration of EH3 present in the samples that were used for activity assays and determination of kinetic parameters.

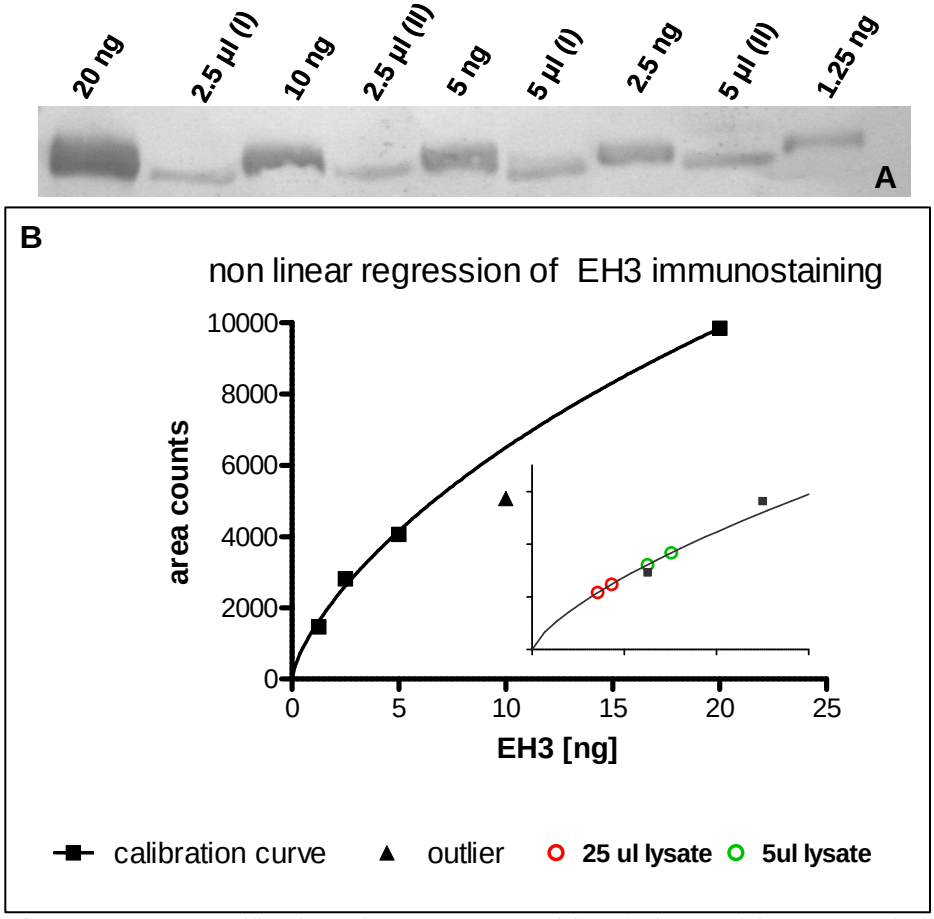

Figure 5-40: *Quantification of EH3 expressed in Sf9 lysate (charge I and II) using ImageJ. Different amounts (1.25 – 20ng) of EH3 were immunoblotted (A) to calibrate density signals for quantification of EH3 present in Sf9 lysates (B). The outlier was not included in linear regression.*

	area counts	ng on blot	ng/µl
charge II (2.5 µl)	1082	0.7	0.28
charge II (5µl)	1609	1.3	0.27
charge I (2.5µl)	1239	0.8	0.32
charge I (5µl)	1833	1.5	0.3

Table 5-9: *Calculation of the EH3 protein amount present in the Sf9 cell lysate.*

Figure 5-40 shows the western blot used to quantify the respective amount of EH3 present in the insect cell lysate. Different amounts (1.25ng – 20ng) of EH3 were used as a standard to quantify the protein amount of Sf9 lysates (charge I and II). The calibration curve of EH3 was best described by non linear regression of an allosteric sigmoid modeling (5-40 B). This is a routine modeling provided by the PRISM® software. Based on this modeling and the signal density obtained for Sf9 samples, the

amount of EH3 present in the Sf9 lysate was calculated. This resulted in a concentration in the insect cell lysates of 0.31 ng/µl EH3 (charge I) and 0.27 ng/µl (charge II) respectively (table 5-9).

5.2.5 Inhibitor profile of EH3

Inhibition of EET turnover by sEH is regarded as a promising tool for maintaining the beneficial effects of EETs and hence for application in treatment of diverse EET linked diseases like hypertension and inflammation. Various inhibitors have been developed and tested for their potential as marketable drug. Several representative sEH inhibitors (sEHi) and mEH inhibitors (mEHi) have been analyzed towards their inhibitory effect on EH3 enzymatic activity.

5.2.5.1 AUDA and structure related sEHi inhibit EH3 enzymatic activity

To investigate the effect of established sEHi and mEHi on enzymatic activity of EH3, cell lysates were preincubated with different inhibitors and turnover of 8(9) EET was measured after 10 minutes. As table 5-10 shows, enzymatic activity of EH3 is affected and reduced by AUDA and by the structurally related sEH inhibitors # 950 and # 1214 to 5.5%, 18% and 38% respectively. The established sEHi ACU and # 1675 (t-AUCB) did not affect EH3 activity. Likewise elaidamide, a well known mEH inhibitor, did not show any effect on turnover of 8(9) EET by EH3. As expected, all sEHi significantly reduced enzymatic activity of hsEH. However, the apparent stimulating effect of elaidamide on hsEH is surprising and cannot be explained.

As illustrated in table 5-10, compounds #950 (1-Adamantan-1-yl-3-{5-[2-(2-ethoxyethoxy)ethoxy]pentyl}-urea) and #1214 (8-(3-Adamantan-1-yl-ureido)-octanoic acid) share fatty acid like structure with AUDA (12-(3-adamantan-yl-ureido) dodecanoic acid) and are potent inhibitors of EH3 activity. These findings may give a hint to the substrate spectrum and preference of EH3 for slim, fatty acid derived epoxy compounds displaying an aliphatic chain. The inhibition of EH3 enzymatic activity by elaidamide is not significant (p-value: 0.071) due to the high variation in the vehicle control (22%).

	EH3	sEH
	residual	activity [%]
elaidamide 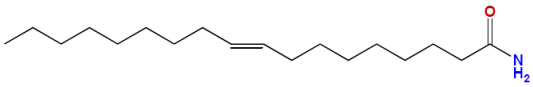	75 ± 6.0	130± 3.4*
12-(3-Adamantan-1-yl-ureido)-dodecanoic acid (AUDA) 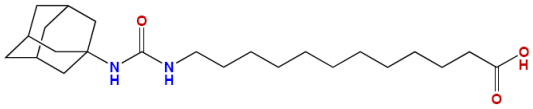	5.5 ± 0.1**	1.6 ± 0.5**
1-Adamantan-1-yl-3-{5-[2-(2-ethoxyethoxy)ethoxy]pentyl}-urea 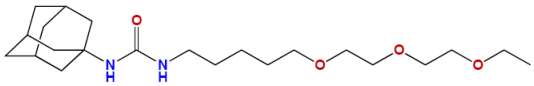	18± 0.7 **	4 ± 1.5**
8-(3-Adamantan-1-yl-ureido)-octanoic acid 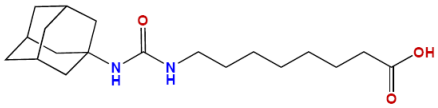	38 ± 3.9**	14 ± 2.6**
1-Adamantan-1-yl-3-{4-[1-(4-oxo benzoic acid)cyclohexyl}-urea 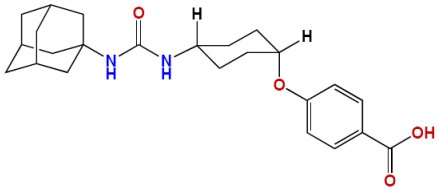	97 ± 4.6	0.2 ± 0.1**
1-adamantan-1-yl-3-cyclohexyl urea (ACU) 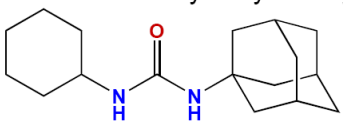	103 ± 10.4	8.1 ± 2.2**

Table 5-10: *Inhibitory effects of different sEH and mEH inhibitors on enzymatic activity of EH3 and hsEH. EH3 (0.3 ng/µl) and hsEH (0.5 ng/µl) was preincubated with the respective inhibitor before addition of 8(9) EET (5 µM) for 10 min at 37℃. The residual activity in % of the vehicle control was determined in triplicate (± standard deviation; students t-test: * p<0.05, **p<0.005).*

5.2.5.2 IC50 determination of AUDA

Since treatment with 1µM AUDA strongly inhibits EH3 and almost completely diminishes the formation of 8(9) DHET, the IC_{50} of AUDA was determined (figure 5-41). AUDA inhibits EH3 enzymatic activity with an IC_{50} of 100nM, which is well in the range to have the enzyme affected under the experimental conditions usually employed for *in vivo* sEH inhibition (e.g. Dorrance, Rupp et al. 2005).

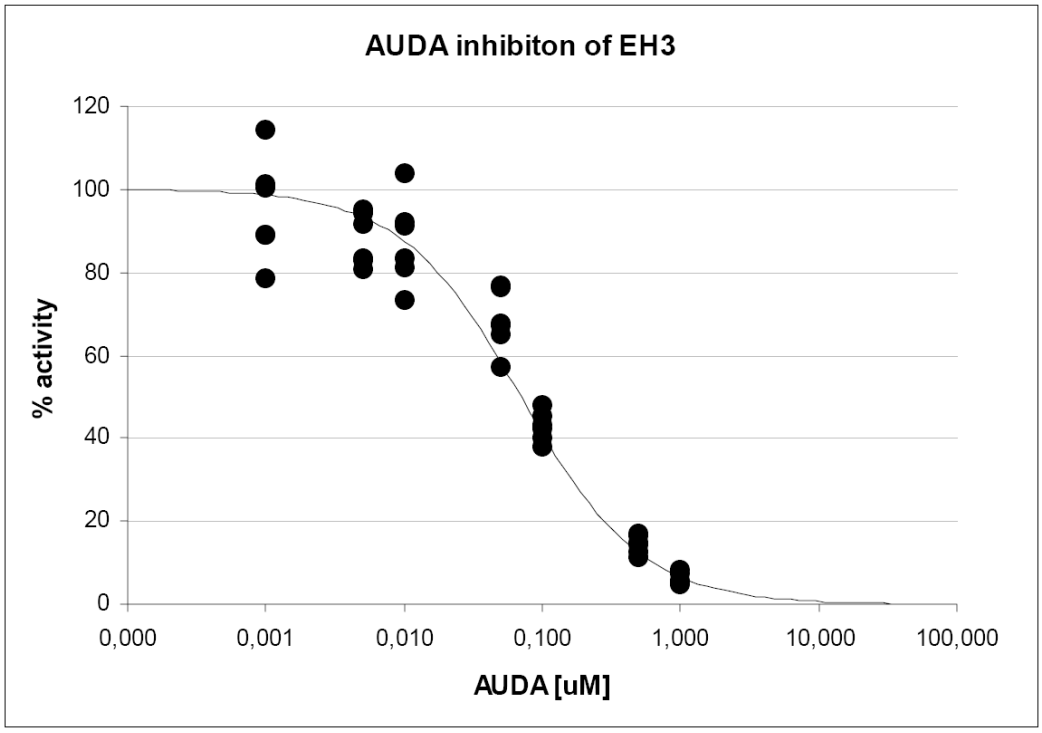

Figure 5-41: *IC_{50} determination of AUDA on enzymatic activity of EH3. Inhibition was analyzed in two independent experiments in duplicates. EH3 expressing Sf9 cells were preincubated with AUDA in different concentrations for 5 minutes before 8(9) EET was added and hydrolysis was enabled for 10min at 37℃. Samples were analyzed by LC-MS/MS and activity compared to vehicle control (100%) was calculated.*

5.2.6 Expression of EH3 in vivo

To investigate the expression pattern of EH3 in the mammalian organism, mRNA was isolated from different mouse organs and analyzed for EH3 expression. In addition, human total protein western blots with samples from brain, uterus, lung, kidney, spleen and placenta, were submitted to immunoblotting with EH3 specific antibody. Reverse transcriptase PCR revealed strongest expression of EH3 in lung and heart. Moreover expression in kidney, muscle and brain was detectable. However this was less significant and reproducible.

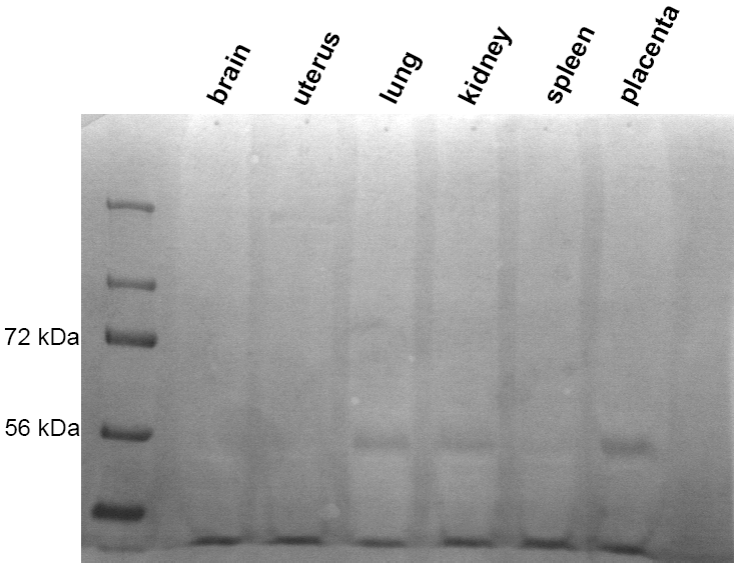

Figure 5-42: *Western blot of different human protein lysates against EH3. There is a distinct band at 56kDa visible in lung, kidney and placenta.*

Western blot analysis of total human protein lysates showed a single immunoreactive band in lung, kidney and placenta (figure 5- 42). Although the band seems to be specific, the molecular weight of 56kDa is higher than expected for EH3 (40.1 kDa) and could be explained by glycosylation of EH3. However, expression of EH3 in lung, kidney and placenta is in line with available human expression data (www.genesapiens.org).

6 DISCUSSION

6.1 Expression of EH4 and EH3 in E. coli

The expression of EH3 as well as EH4 in *E. coli* turned out to be difficult during this work. Two different observations were made: i) proteins that contain the membrane anchor are not expressed in *E. coli* and ii) N - terminal fusion of truncated protein promotes overexpression in bacteria. The only C-terminal tagged protein that could be expressed in *E. coli* was EH4-3/3. This protein consists of 95 C-terminal amino acids and lacks the membrane anchor and most of the α/β - hydrolase fold structure. This suggests that the membrane anchor and/or features of the N-terminal amino acids inhibit proper expression and folding of the protein.

The fact that anchorless N-terminal tagged EH3 protein led to visible overexpression in bacteria, whereas the N-terminal tagged full length EH3 protein (including the membrane anchor) was not expressed in *E. coli,* indicates that the putative membrane anchor is critical for protein expression. A direct comparison between the two expression constructs pGEFGSTN-EH4AB and pGEFHisCEH4AB further shows, that the N-terminal tag promotes expression. Both constructs only differ in the location of the tag, but encode for the same protein. Yet only the N-terminal tagged protein was expressed in *E. coli*.

The two enzymes, EH3 and EH4, are membrane associated and display a membrane anchor within the N-terminal amino acids. It is commonly known that bacterial expression of proteins, in particular membrane proteins, can involve difficulties (Baneyx and Mujacic 2004; Wagner, Bader et al. 2006). The correct folding of newly synthesized proteins is supported by molecular chaperones, molecules that mediate refolding or unfolding as well as solubilization of proteins, by shielding hydrophobic domains from the cytoplasmic environment. It has been shown that some membrane proteins require membrane-specific chaperones, which might not be present in bacterial cells. If the protein does not rapidly reach native conformation or interacts with a folding modulator, the consequence is either proteolytic degradation or deposition into inclusion bodies (Baneyx and Mujacic 2004). Proteolytic degradation might be one reason why the expression of full length EH3 and EH4 protein is not possible in *E. coli.* Other explanations are negative selection by the recombinant protein, mRNA instability or hindrance of the translation initiation. A negative selection of the *E. coli* cells that express EH3 or EH4 is not very likely, because GST-EH4 and His-EH3 contain all catalytically active amino acids and yet they are overexpressed in bacterial cells. Difficulties in translation, either on the level of mRNA stability or initiation of translation are more likely. Protein synthesis is often regulated at the level of translation initiation, which depends on the binding of initiation factors and ribosomal subunits. In prokaryotic cells, natural mRNA contains so called Shine-Dalgarno (SD) sequences that form base pairs with specific bases in the 16S rRNA, and thereby augment translation initiation by anchoring the 30S rRNA (Kozak 1999). In absence of such interaction the translation initiation might be inefficient and protein synthesis is hindered. Besides the upstream SD sequences, there are also downstream sequences that influence translation initiation by interacting with 16S rRNA. It was demonstrated, that the so called DB (Downstream Box) sequence can likewise stimulate translation, independent form the SD sequences (Sprengart, Fuchs et al. 1996). It is feasible that N-terminal fusion to GST or Histidine

might enhance interaction of the 16S rRNA with the start codon and thus promote translation initiation of EH3 and EH4. This would explain why the N-terminal fusion of EH4 resulted in overexpression, whereas the C-terminal tagged EH4 could not be expressed.

Both proteins, EH3 and EH4 were also expressed in eukaryotic expression systems. In contrast to recombinant expression in *E. coli*, the expression of full length C-terminal tagged and non-tagged EH3 and EH4 was possible in insect cells. The baculovirus based expression system is an established system for overexpression of heterologous proteins in insect cells. Yet, expression of EH3 and EH4 was rather low (approx. 0.1%), although other EHs were successfully overexpressed in this expression system (oral communication with Prof. Arand). Since the expression of EH4 in Cos-7 and V79 cells was verified only at mRNA level, it is not clear whether the expression of non-tagged full length protein implicates difficulties in these cells.

6.2 Detection of EH4

The rabbit immunization with either truncated protein or synthetic peptides failed to obtain an immune serum that specifically detects EH4 from *E. coli* and insect cell lysates. This might be due to the high conservation of the amino acid sequence between human EH4 and rabbit EH4. The ensemble rabbit genome assembly contains an EPHX4 related gene (www.ensembl.org) for which one transcript is recorded (ENSOCUP00000015012). This transcript encodes for a 159 amino acid peptide that aligns with aa 201-362 of the human EH4 protein and shows a sequence identity of 94% (see 8.7). The truncated protein used for immunization contained aa 267-362 and therefore is highly similar to the rabbit protein. A highly conserved sequence might not trigger the expected immune reaction. Alternatively, an LC-MS/MS based method was established to detect EH4. The analysis of methanol extracted peptides resulted in more significant hits, compared to the peptides obtained after tryptic digestion and extraction from PAA gel. Most probably the tryptic in gel digest is less sufficient, since the trypsin has to diffuse into the gel first. In addition to that, there might be a loss of peptides during the extraction process of the peptides from the PAA gel.

Several experiments aimed at the detection of the peptide that contains the putative catalytic nucleophile. This would open the possibility to screen for genuine substrates by LC-MS/MS. EH4 expressing tissue homogenates, e.g. brain homogenates, could then be directly denatured in methanol and peptides could be analyzed by the specific MRM scan. The increase in mass of the specific peptide would then give information on the nature of the substrate that is covalently bound and “trapped” to the catalytic nucleophile. In principal, this method has been applied in the work of Dr. Annette Cronin in our group, to identify the catalytic aspartate of sEH phosphatase domain (Cronin, Homburg et al. 2008).

6.3 Activity assays of EH3 and EH4

The N-terminal fusion of GST to EH4 enabled overexpression of the theoretically active protein in *E.coli.* Thus the enzymatic activity towards styrene 7, 8 oxide (STO) was investigated in recombinant *E. coli* lysates. Activity measurements towards STO showed that GST itself has enzymatic activity

because radioactivity was detected in the aqueous phase of recombinant GST lysates. Most likely this is a result of GSH conjugation to STO. It has been shown that glutathione transferases conjugate GSH to styrene oxide (Hayakawa, Lemahieu et al. 1974; Hiratsuka, Yokoi et al. 1989) and that GSH is present in *E. coli* (Apontoweil and Berends 1975). Although rather few research exists on bacterial GST enzymes, Iizuka et al. (Iizuka, Inoue et al. 1989) purified GST from *E. coli* B, which showed specific activity towards CDNB. However, they are not quantitatively prominent enzymes in these cells and the activity was significantly lower than those from mammals, plants and fungi. It is conceivable that the radioactivity measured in the aqueous phase originated from a GSH conjugate of STO, either catalyzed by recombinant expressed GST or endogenous GST from *E. coli*. It is not possible to discriminate between endogenous and recombinant GST with the performed assay. However, thin layer chromatography with radiolabeled phenylglycol as standard and preceding incubation with e.g. CDNB to deplete GSH, would be an approach to identify the product in the aqueous phase as either conjugate or possible hydrolysis product. There is one reference that describes a bacterial enzyme from *Mesorhizobium loti,* called FosX , that is likewise able to hydrolyze the natural antibiotic fosfomycin and to form a GSH conjugate in the presence of GSH (Fillgrove, Pakhomova et al. 2003). Although it is very unlikely that the GST from *S. japonicum* used for fusion to EH4 displays similar activity, the expression system was excluded from further activity experiments, because a clear discrimination between GST produced diol and EH4 produced diol would not have been possible. An alternative expression system that was used for recombinant expression in this work was stable transfection of the mammalian cell lines Cos-7 and V79. A variety of experiments to detect enzymatic activity of EH4 in mammalian cells failed. The system was excluded from activity experiments, because Cos-7 cells exhibited endogenous activity towards EETs. The background activity is most likely mediated by sEH, which is present in these cells as reported and observed in different studies (Sandberg, Hassett et al. 2000; Fang, Hu et al. 2006). Furthermore it must be taken into account that presence of EH4 in Cos-7 as well as V79 cells was only demonstrated on mRNA level.

The use of Sf9 cells as expression system for enzymatically active EH4 was the most promising approach, since EH3 has been successfully expressed in Sf9 cells in active form. Yet, the performed experiments did not allow to demonstrate hydrolase activity of EH4 towards various substrates. Attempts to detect significant EH4 specific turnover in whole recombinant Sf9 cell lysates as well as in fractions of membrane proteins failed. Based on the assumption that EH4 has epoxide hydrolase activity, there are three possible explanations for the absence of enzymatic activity: (i) the enzyme is lacking cofactors which are required for catalysis, (ii) the enzyme is inactively expressed or (iii) the enzyme has a restricted substrate spectrum and the relevant compound has not been tested yet. It is very unlikely that EH4 requires a cofactor for enzymatic conversion, since all known α/β hydrolase fold EHs mediate cofactor independent hydrolysis. In contrast, it cannot be excluded that the enzyme is expressed in inactive form. It is possible that the protein is present in protein aggregates, which would also be an explanation for the results obtained by differential centrifugation. It is not possible to differentiate native membrane association from protein aggregates with this experiment. If the protein is indeed located in the mitochondria as predicted by *in silico* analysis, the correct folding and activity might depend on adequate targeting and/or organelle specific proteins. In absence of these proteins the recombinant expressed enzyme cannot acquire proper folding. Hydrophobic residues are then

exposed to the aqueous phase, which results in clustering of the proteins and the subsequent formation of aggregates. However, protein aggregation has not been observed for recombinant expression in Sf9 cells of any epoxide hydrolase so far.

Regarding the possible substrates for EH4, there are many different fatty acid derived epoxides present in the organism, and the elucidation of novel pathways constantly reveals alternative molecules, which might be substrates for EH4. The clear expression of EH4 in the brain and eye suggested DHA derived epoxides as possible substrates, since DHA is one of the most abundant fatty acids in the brain and enriched in synapses and retina (Hong, Gronert et al. 2003; Mukherjee, Marcheselli et al. 2007). However, the 19(20) epoxide of DHA was not turned over by EH4. Yet, there are other possible compounds arising from novel pathways of DHA to docosatriens and resolvins, e.g. 4(5), 7(8) and 16(17) epoxy intermediates that still might be relevant substrates for EH4 (Hong, Gronert et al. 2003).

It can be excluded that the His-Tag is responsible for the lack of enzymatic activity, because all activity assays were likewise performed with full length non-tagged EH4. It is also possible that endogenous enzymes present in the insect cell lysate show higher activity than EH4, and thus EH4 activity can not be detected. Blocking of endogenous activity was an approach to unveil possible marginal EH4 activity. Insect cell lysates were preincubated with valpromide, which turned out to reduce the endogenous turnover of Sf9 cells. However, it must be taken into account that in those experiments EH4 might have been equally affected by valpromide. In this case EH4 activity still remained undetected. In terms of EH3, endogenous activity of Sf9 cells did not affect determination of EH3 kinetic parameters, since the background activity was in the range of 0.5% - 1.5% of EH3 turnover. This had no relevant influence on the obtained catalytic constants. Another possible reason for inactivity of EH4 might be an amino acid exchange at position 321. The NCBI Ace View database annotates a SNP (single nucleotide polymorphism) that leads to a Y321F variant of EH4. The EH4 protein investigated in this work contains a phenylalanine residue at position 321, which is not present in other mammalian species. Extensive sequence comparison during writing of this thesis showed, that Y321 is highly conserved in other species like chimpanzee, cow, mouse, dog, chicken and zebra fish (an alignment is given in 8.7). There are also human cDNA clones that contain a tyrosine residue at position 321. A detailed analysis of the underlying cDNA clones revealed, that only one human reference sequence (NM_173567, BC041475) showed the amino acid exchange. This argues against a polymorphism of EH4 and rather points towards a mutation in the respective cDNA clone. However, this was not expected, since the officially available IMAGE clone is based on this mutated reference sequence. It is not very likely that F321 has an effect on the catalytic activity of the enzyme. F321 is positioned between the α/β hydrolase fold and the lid domain, a region which should not influence the catalytic site. However, it must be taken into account that the amino acid exchange might lead to conformational changes and thereby affects enzymatic activity. One approach to investigate the relevance of Y321 for enzymatic activity of EH4 would be a respective nucleotide exchange in the expression plasmid by use of QuickChange® PCR. Recombinant expression of the resulting EH4 Y321 and subsequent enzymatic activity assays should unveil the relevance of Y321 for enzymatic activity of EH4.

6.4 Subcellular localization of EH4

To investigate the subcellular localization and the predicted membrane localization, His- tagged EH4 was submitted to differential centrifugation and analyzed by western blot. The western blot results of the experiment can only be interpreted qualitatively and not quantitatively, since cellular fractionation as performed in this work is not able to clearly isolate the different subcellular compartments from each other. There is a tendency to a higher concentration of EH4 in mitochondrial membranes observed, which coincides with the *in silico* results that indicate a mitochondrial target sequence. Yet, a clear mitochondrial location still needs to be demonstrated, since there was no mitochondrial marker used in this experiment. As already mentioned above, formation of protein aggregates could also be an explanation for the results obtained in western blot analysis. Likewise, immuno reactive bands would be observed in all membrane associated fractions, because protein aggregates are insoluble and thus present in the respective pellet. Since aggregated proteins are denatured and hence inactive, this would also explain an absence of enzymatic activity.

6.5 Expression of EH3 and EH4 in vivo

EH4 mRNA was detected in whole brain homogenate from adult mice, which is in line with the *in vivo* expression data available at the Allen Mouse Brain Atlas (Lein, Hawrylycz et al. 2007). A detailed analysis of the expression summary shows highest expression of EH3 in cortex, hippocampus and olfactory bulb. Furthermore, Stansberg et al. generated a global expression map in rat brain and showed that Abhd7 (now designated *EPHX4*, see (Decker, Arand et al. 2009) is significantly enriched in the cortex (Stansberg, Vik-Mo et al. 2007). A close examination of the cDNAs underlying the data available on expression databases (e.g. EST Profile at UniGene) showed that most reference sequences derive form cortical probes (e.g. CJ059344, CJ059344, CJ059315, BY255071) of neonates (Okazaki, Furuno et al. 2002; Carninci, Kasukawa et al. 2005). The expression of EH4 is clearly focused on the central nervous system and not to the liver or other xenobiotic metabolizing organs, which indicates a physiological role of EH4 rather than a function in detoxification.

In vivo expression of EH3 in mice was demonstrated in lung and heart in previous work in our group. *In silico* analysis furthermore indicated significant expression of EH3 in skin and tongue of mice. Detailed examination of the available expression data points towards restricted expression of the gene to a particular cell type within these organs. Toulza et al. (Toulza, Mattiuzzo et al. 2007) investigated the human epidermal transcriptome and demonstrated that EH3 is highly expressed only in late granular keratinocytes. Granular keratinocytes comprise the most terminally differentiated, viable cell layer. These cells are characterized by the expression of numerous genes that are involved in skin barrier formation, which suggests a role of EH3 in cornification. Furthermore, available reference sequences from tongue of adult mice were extracted only from taste buds (e.g. EH105600), which points towards a role of EH3 in taste reception. Attempts to demonstrate EH3 mRNA in skin and tongue of adult mice failed during this work. This might be the result of the restricted expression pattern or an altered expression depending on the developmental state.

Since there is no specific antibody against EH4 available, protein analysis was only performed in terms of EH3 expression. There was a single immuno reactive band visible in human samples from lung, kidney and placenta, but the expected molecular weight differs from the one observed in the western blot. The bands were detected at 56 kDa instead of 40 kDa. One explanation for the shift in molecular weight is glycosylation. Glycosylation of EH3 was also indicated by *in silico* analysis. A possible approach to investigate glycosylation of proteins is the treatment with PGNaseF. This is an endoglycosidase that removes all N-linked glycosylation. Since western blot in human tissues indicated expression in placenta, commercially available total protein and membrane protein fractions of human placenta were analyzed towards glycosylation of EH3. Unfortunately, it was not possible to confirm the expression of EH3 in the placenta samples. Therefore it remains to be investigated if EH3 is indeed glycosylated in lung, kidney and placenta, and if glycosylation causes the molecular weight shift.

6.6 What is the role of EH3 in the human organism?

The initial question was if EH3 is a detoxifying enzyme or a physiological regulator. Previous experiments have shown that EH3 hydrolyzes the fatty acid derived 9(10) epoxystearic acid, but not the generic EH substrate STO and the steroid epoxides 5(6) and 24(25) cholesterolepoxide. This led to the assumption that EH3 is more likely involved in the turnover of fatty acid derived endogenous epoxides. This work shows that 8(9) EET, 11(12) EET, 14(15) EET and 9(10) EpOME (leukotoxin) are converted by EH3 with a catalytic efficacy comparable to that of sEH. In addition to that, EH3 is capable to hydrolyze 12(13) EpOME (isoleukotxin), Hepoxilin A3 as well as B3 and 14(15) EET-EA to their corresponding diols. This spectrum of substrates, together with that of inhibitors, suggests that slim, fatty acid derived molecules are preferentially converted by EH3. The fact that EH3 does not convert 19(20) EDPE and 17(18) EET indicates that the distance between the epoxide and the carboxylic head of the substrate might be critical for proper binding to the active site, and thus affects the catalytic turnover. The tested substrate spectrum raises no claims to completeness since it might well be that there are other structurally related epoxides which are converted by EH3 but have not been tested yet.

To date, research only focused on sEH as major player in the turnover of endogenous epoxides to regulate physiological processes. The hydrolysis of hepoxilins by EH3 is a possible indicator towards a role of EH3 in human hepoxilin metabolism. Hepoxilins are involved in differentiation of the skin and in skin barrier function (Brash, Yu et al. 2007; Epp, Furstenberger et al. 2007; Yu, Schneider et al. 2007). Moreover mutations in the coding regions of hepoxilin generating enzymes correlate with a congenital form of ichthyosis, a genetic skin disorder which is characterized by dry, thickened and scaly skin (Jobard, Lefevre et al. 2002; Eckl, Krieg et al. 2005). The *in silico* expression analysis of EH3 points towards expression in the skin which is in line with the study from Toulza et al., that demonstrated expression of EH3 in human late granular keratinocytes (Toulza, Mattiuzzo et al. 2007). An association of EH3 with skin disorder was shown by a comparative study of human disease genes, which predicts EH3 as a candidate gene for ichthyosis (Ala, Piro et al. 2008). There are also reports that point towards an EET mediated function of EH3 in granular keratinocytes. As proved in the

present work, EH3 is able to efficiently hydrolyze 11(12) EET and 14(15) EET to their corresponding diols. Both EET regioisomers are present in murine late skin keratinocytes (Keeney, Skinner et al. 1998) and have been suggested to regulate epidermal cornification by the activation of transglutaminase *in situ* (Ladd, Du et al. 2003). Transglutaminase mediates the cross linking of scaffold proteins and keratin filaments to form the cornified cell envelope. In this study, 14(15) EET increased formation of the cornified envelope by activating transglutaminase in mouse and human epidermal keratinocytes. It is feasible that the hydrolysis of 14(15) EET by EH3 might lead to decreased transglutaminase activity and hence reduce cornification. On the contrary, inactivation and null mutations in the human transglutaminase gene can cause a form of lamellar ichthyosis. The sum of these findings suggest a role of EH3 in skin differentiation and the construction of the water impermeable barrier in the cornified layer of the epidermis.

Aberrant *de novo* methylation of CpG islands is a characteristic of human cancers and is found early during carcinogenesis (Jones and Baylin 2002). The CpG islands in the promoter region of EPHX3 have been shown to be methylated in melanoma cell lines compared to cultured human epidermal melanocytes (Furuta, Nobeyama et al. 2006), as well as in primary gastric cancer and multiple gastric cancer cell lines (Yamashita, Tsujino et al. 2006). Furthermore, the gene EPHX3 is considered as prognostic marker for prostate cancer with aggressive growth properties. The methylation level of CpG islands of the EPHX3 promoter is increased in patients with early recurrence of prostate cancer compared to those patients who did not suffer from recurrence (Cottrell, Jung et al. 2007). This suggests a cancer promoting effect of EH3, yet the role of EH3 in prostate cancer has not been investigated. All available data regarding the role of arachidonic acid derivatives in prostate cancer is limited to the COX and LOX pathways, which is the prostaglandins and the enzymes themselves.

Not only decreased or absent activity, but also excessive activity of EH3 could present a problem, because the hydrolysis of leukotoxin to leukotoxin-diol seems to be an activating process. As different in vitro and in vivo studies demonstrate, leukotoxin-diol is the more toxic reagent and responsible for the severe outcome of ARDS in leukotoxin diol treated mice (Moghaddam, Grant et al. 1997; Moran, Weise et al. 1997; Zheng, Plopper et al. 2001). A role of EH3 in the genesis of ARDS is feasible, because the catalytic efficacy of leukotoxin turnover is in the range of sEH and EH3 is well expressed in the lung. This was shown by western blot analysis of human total lung protein as well as RT PCR analysis and *in silico* data. So far, the impact and relevance of EH3 in turnover of lipid derived epoxides was unregarded in research. Therefore most AUDA sensitive effects are ascribed to sEH. Theoretically, the observed AUDA sensitive *in vivo* effects could at least be partly mediated by EH3, as long as plasma concentrations are sufficiently high to affect EH3. Smith et al. showed that tobacco induced lung inflammation in rat is reduced by AUDA when given before and after exposure (Smith, Pinkerton et al. 2005). The blood concentration of AUDA after 3 days of daily injection was between 152 nM and 325 nM, a concentration that is sufficient to affect EH3 enzymatic activity. Hence it cannot be excluded that EH3 also plays a role in attenuation of tobacco smoke induced lung inflammation, because EH3 equally hydrolyzes anti - inflammatory EETs and is inhibited by AUDA.

EH3 becomes important for the development of sEHi and the human organism. The enzyme is affected by a subclass of sEHi and involved in physiological processes by hydrolysis of endogenous biologically active epoxides. For this reason, the so far sEH specific inhibitors must be divided into

sEH specific and sEH/EH3-mixed inhibitors. The degree to which EH3 has impact on the development of sEHi based therapeutics remains to be seen, because the exact physiological relevance of this novel enzyme is not clear yet.

EH3 gained interest as marker for early cancer prognosis, in particular prostate cancer. The fact that EH3 is hypermethylated in many cancers suggests, that a decreased or absent activity of EH3 has tumor promoting effects. Once the enzymatic activity and physiological role of EH3 is more elucidated and investigated in detail, the development of novel therapeutics that increase or maintain EH3 activity might represent a promising approach towards the treatment of cancer

The results of the substrate screening, the inhibitor profiling and the fact that catalytic efficacies are in the same range as those of sEH, strongly suggests a role of EH3 in physiological regulation.

6.7 Is EH4 a novel epoxide hydrolase?

Two recently reported characterized epoxide hydrolases from *c. elegans* are similar to the novel EH s that were identified in humans. Ceeh-1 and ceeh-2 share 40% sequence identity and have significant similarity to human sEH. The enzymes display enzymatic activity towards EETs as well as leukotoxin 9(10) EpOME and isoleukotoxin 12(13) EpOME (Harris, Aronov et al. 2008). Interestingly, the catalytic efficacy of ceeh-1 and ceeh-2 differ by factor 24 (leukotoxin) and 10 (isoleukotoxin), respectively. Likewise the Vmax towards turnover of 14(15), 11(12) and 8(9) EET by ceeh-2 is much lower than that of ceeh-1 (factor 80, 29 and 20 respectively). It seems possible that similar to ceeh-2 and ceeh-1, EH4 only shows very low enzymatic activity towards the tested substrate as compared to EH3. The only study that points towards physiological relevance of EH4 states that the gene is directly regulated and repressed by ZNF217, an oncogene that is overexpressed in many cancer types and thought to act as transcriptional repressor (Krig, Jin et al. 2007). The high sequence identity to EH3 and the comparatively high conservation of EH4 among different species strongly suggest that EH4 is an epoxide hydrolase with physiological function. It is feasible that the protein has a very narrow substrate spectrum and only converts few substrates with particular structure, since expression of EH3 is also rather restricted to the central nervous system.

6.8 Conclusion and outlook

The two novel identified epoxide hydrolases EH3 and EH4 are closely related (45%), but obviously differ in their substrate spectrum and enzymatic activity towards endogenous derived epoxides.

Various experiments could not prove enzymatic activity of EH4 with the tested substrates and the expression systems used in this work. It seems possible that EH4 shows very low enzymatic activity towards the tested substrates and only displays efficient turnover towards a particular substrate of so far unknown structure. Identification of EH4 substrates, in order to elucidate the function and the role of EH4 in the human organism, presents the future challenge. One approach could be the identification of the physiological substrate by “trapping“ the substrate to the catalytic nucleophile. An LC-MS/MS analysis of the respective peptide could then give information on the covalently bound substrate. For this approach, a method to detect the peptide that contains the catalytic nucleophile has

to be established first. The increase in mass of this peptide can then provide information about the compound that is bound to the nucleophile. Furthermore, the generation of an antibody against EH4 would enable protein analysis in different tissues from mice and at the same time allow validating the results that were observed by differential centrifugation. The cellular localization of EH4 in stable transfected cells could be directly investigated by immuno fluorescence. The optimization of expression and purification of GST-EH4 would be a promising approach for the generation of an antibody.

It has been shown that EH3 is rather a physiological regulator like sEH, than a detoxifying epoxide hydrolase similar to mEH. Present results are compatible with the substrate spectrum of EH3 being restricted to fatty acid derived epoxides. Furthermore, hitherto sEH specific inhibitors need to be classified into sEH specific and sEH/EH3 mixed inhibitors. The effects of mixed sEH/EH3 inhibitors used as therapeutics need to be investigated and evaluated in the future. In terms of ARDS, inhibition of EH3 might have positive effects. In terms of cancer development, a decrease in EH3 activity also might have negative effects, as suggested by the hypermethylated CpG islands which are observed in different cancer cells. Differences in expression pattern, regulation and substrate preference between sEH and EH3 are likely and need to be further investigated in order to evaluate the *in vivo* effects of sEH/EH3 mixed inhibitors. The generation of an EH3 knock out mouse would provide a useful tool for analysis of the different inhibitor effects and to investigate the physiological role of EH3. Further investigations are needed to fully understand the role of EH3 for the human organism and to unveil the signaling pathways that are involved. This would help to further understand diseases like ARDS, ichthyosis or cancer. Eventually this might enable the development of novel therapeutics that specifically target at EH3 and can be used for treatment of these diseases.

7 REFERENCES

Ala, U., R. M. Piro, et al. (2008). "Prediction of human disease genes by human-mouse conserved coexpression analysis." PLoS Comput Biol **4**(3): e1000043.

Anton, R., L. Puig, et al. (1998). "Occurrence of hepoxilins and trioxilins in psoriatic lesions." J Invest Dermatol **110**(4): 303-10.

Apontoweil, P. and W. Berends (1975). "Glutathione biosynthesis in Escherichia coli K 12. Properties of the enzymes and regulation." Biochim Biophys Acta **399**(1): 1-9.

Arand, M., A. Cronin, et al. (2005). "Epoxide hydrolases: structure, function, mechanism, and assay." Methods Enzymol **400**: 569-88.

Arand, M., A. Cronin, et al. (2003). "The telltale structures of epoxide hydrolases." Drug Metab Rev **35**(4): 365-83.

Arand, M., D. F. Grant, et al. (1994). "Sequence similarity of mammalian epoxide hydrolases to the bacterial haloalkane dehalogenase and other related proteins. Implication for the potential catalytic mechanism of enzymatic epoxide hydrolysis." FEBS Lett **338**(3): 251-6.

Arand, M., B. M. Hallberg, et al. (2003). "Structure of Rhodococcus erythropolis limonene-1,2-epoxide hydrolase reveals a novel active site." Embo J **22**(11): 2583-92.

Arand, M., H. Hemmer, et al. (1999). "Cloning and molecular characterization of a soluble epoxide hydrolase from Aspergillus niger that is related to mammalian microsomal epoxide hydrolase." Biochem J **344 Pt 1**: 273-80.

Arand, M., H. Wagner, et al. (1996). "Asp333, Asp495, and His523 form the catalytic triad of rat soluble epoxide hydrolase." J Biol Chem **271**(8): 4223-9.

Arete Therapeutics Inc (2009). Arete Therapeutics Presents Positive Clinical and Preclinical Data for AR9281. SOUTH SAN FRANCISCO, CA, ARETE THERAPEUTICS INC.

Argiriadi, M. A., C. Morisseau, et al. (2000). "Binding of alkylurea inhibitors to epoxide hydrolase implicates active site tyrosines in substrate activation." J Biol Chem **275**(20): 15265-70.

Argiriadi, M. A., C. Morisseau, et al. (1999). "Detoxification of environmental mutagens and carcinogens: structure, mechanism, and evolution of liver epoxide hydrolase." Proc Natl Acad Sci U S A **96**(19): 10637-42.

Aringer, L. and P. Eneroth (1974). "Formation and metabolism in vitro of 5,6-epoxides of cholesterol and beta-sitosterol." J Lipid Res **15**(4): 389-98.

Armstrong, R. N. and C. S. Cassidy (2000). "New structural and chemical insight into the catalytic mechanism of epoxide hydrolases." Drug Metab Rev **32**(3-4): 327-38.

Astrom, A., S. Maner, et al. (1987). "Induction of liver microsomal epoxide hydrolase, UDP-glucuronyl transferase and cytosolic glutathione transferase in different rodent species by 2-acetylaminofluorene or 3-methylcholanthrene." Xenobiotica **17**(2): 155-63.

Baneyx, F. and M. Mujacic (2004). "Recombinant protein folding and misfolding in Escherichia coli." Nat Biotechnol **22**(11): 1399-408.

Blonder, J., K. C. Chan, et al. (2006). "Identification of membrane proteins from mammalian cell/tissue using methanol-facilitated solubilization and tryptic digestion coupled with 2D-LC-MS/MS." Nat Protoc **1**(6): 2784-90.

Brash, A. R., Z. Yu, et al. (2007). "The hepoxilin connection in the epidermis." Febs J **274**(14): 3494-502.

Carninci, P., T. Kasukawa, et al. (2005). "The transcriptional landscape of the mammalian genome." Science **309**(5740): 1559-63.

Claros, M. G. and P. Vincens (1996). "Computational method to predict mitochondrially imported proteins and their targeting sequences." Eur J Biochem **241**(3): 779-86.

Cottrell, S., K. Jung, et al. (2007). "Discovery and validation of 3 novel DNA methylation markers of prostate cancer prognosis." J Urol **177**(5): 1753-8.

Cronin, A., S. Homburg, et al. (2008). "Insights into the catalytic mechanism of human sEH phosphatase by site-directed mutagenesis and LC-MS/MS analysis." J Mol Biol **383**(3): 627-40.

Cronin, A., S. Mowbray, et al. (2003). "The N-terminal domain of mammalian soluble epoxide hydrolase is a phosphatase." Proc Natl Acad Sci U S A **100**(4): 1552-7.

Decker, M., M. Arand, et al. (2009). "Mammalian epoxide hydrolases in xenobiotic metabolism and signalling." Arch Toxicol **83**(4): 297-318.

Dietze, E. C., E. Kuwano, et al. (1991). "Inhibition of cytosolic epoxide hydrolase by trans-3-phenylglycidols." Biochem Pharmacol **42**(6): 1163-75.

Dorrance, A. M., N. Rupp, et al. (2005). "An epoxide hydrolase inhibitor, 12-(3-adamantan-1-yl-ureido)dodecanoic acid (AUDA), reduces ischemic cerebral infarct size in stroke-prone spontaneously hypertensive rats." J Cardiovasc Pharmacol **46**(6): 842-8.

Draper, A. J. and B. D. Hammock (2000). "Identification of CYP2C9 as a human liver microsomal linoleic acid epoxygenase." Arch Biochem Biophys **376**(1): 199-205.

Eckl, K. M., P. Krieg, et al. (2005). "Mutation spectrum and functional analysis of epidermis-type lipoxygenases in patients with autosomal recessive congenital ichthyosis." Hum Mutat **26**(4): 351-61.

Epp, N., G. Furstenberger, et al. (2007). "12R-lipoxygenase deficiency disrupts epidermal barrier function." J Cell Biol **177**(1): 173-82.

Fang, X. (2006). "Soluble epoxide hydrolase: a novel target for the treatment of hypertension." Recent Pat Cardiovasc Drug Discov **1**(1): 67-72.

Fang, X., S. Hu, et al. (2006). "14,15-Dihydroxyeicosatrienoic acid activates peroxisome proliferator-activated receptor-alpha." Am J Physiol Heart Circ Physiol **290**(1): H55-63.

Fillgrove, K. L., S. Pakhomova, et al. (2003). "Mechanistic diversity of fosfomycin resistance in pathogenic microorganisms." J Am Chem Soc **125**(51): 15730-1.

Fisslthaler, B., R. Popp, et al. (1999). "Cytochrome P450 2C is an EDHF synthase in coronary arteries." Nature **401**(6752): 493-7.

Ford, D. K. and G. Yerganian (1958). "Observations on the chromosomes of Chinese hamster cells in tissue culture." J Natl Cancer Inst **21**(2): 393-425.

Furuta, J., Y. Nobeyama, et al. (2006). "Silencing of Peroxiredoxin 2 and aberrant methylation of 33 CpG islands in putative promoter regions in human malignant melanomas." Cancer Res **66**(12): 6080-6.

Gerhard, D. S., L. Wagner, et al. (2004). "The status, quality, and expansion of the NIH full-length cDNA project: the Mammalian Gene Collection (MGC)." Genome Res **14**(10B): 2121-7.

Glatt, H., I. Gemperlein, et al. (1987). "Search for cell culture systems with diverse xenobiotic-metabolizing activities and their use in toxicological studies." Mol Toxicol **1**(4): 313-34.

Gluzman, Y. (1981). "SV40-transformed simian cells support the replication of early SV40 mutants." Cell **23**(1): 175-82.

Greene, J. F., K. C. Williamson, et al. (2000). "Metabolism of monoepoxides of methyl linoleate: bioactivation and detoxification." Arch Biochem Biophys **376**(2): 420-32.

Guo, A., J. Durner, et al. (1998). "Characterization of a tobacco epoxide hydrolase gene induced during the resistance response to TMV." Plant J **15**(5): 647-56.

Haeggstrom, J. Z., F. Kull, et al. (2002). "Leukotriene A4 hydrolase." Prostaglandins Other Lipid Mediat **68-69**: 495-510.

Harris, T. R., P. A. Aronov, et al. (2008). "Identification of two epoxide hydrolases in Caenorhabditis elegans that metabolize mammalian lipid signaling molecules." Arch Biochem Biophys **472**(2): 139-49.

Hassett, C., S. M. Turnblom, et al. (1989). "Rabbit microsomal epoxide hydrolase: isolation and characterization of the xenobiotic metabolizing enzyme cDNA." Arch Biochem Biophys **271**(2): 380-9.

Hayakawa, M., K. Kosaka, et al. (1990). "Proposal of leukotoxin, 9,10-epoxy-12-octadecenoate, as a burn toxin." Biochem Int **21**(3): 573-9.

Hayakawa, T., R. A. Lemahieu, et al. (1974). "Studies on glutathione-S-arene oxidase transferase. A sensitive assay and partial purification of the enzyme from sheep liver." Arch Biochem Biophys **162**(1): 223-30.

Heredia, A. (2003). "Biophysical and biochemical characteristics of cutin, a plant barrier biopolymer." Biochim Biophys Acta **1620**(1-3): 1-7.

Herrero, M. E., M. Arand, et al. (1997). "Recombinant expression of human microsomal epoxide hydrolase protects V79 Chinese hamster cells from styrene oxide- but not from ethylene oxide-induced DNA strand breaks." Environ Mol Mutagen **30**(4): 429-39.

Hiratsuka, A., A. Yokoi, et al. (1989). "Glutathione conjugation of styrene 7,8-oxide enantiomers by major glutathione transferase isoenzymes isolated from rat livers." Biochem Pharmacol **38**(24): 4405-13.

Hong, S., K. Gronert, et al. (2003). "Novel docosatrienes and 17S-resolvins generated from docosahexaenoic acid in murine brain, human blood, and glial cells. Autacoids in anti-inflammation." J Biol Chem **278**(17): 14677-87.

Hwang, S. H., H. J. Tsai, et al. (2007). "Orally bioavailable potent soluble epoxide hydrolase inhibitors." J Med Chem **50**(16): 3825-40.

Iizuka, M., Y. Inoue, et al. (1989). "Purification and some properties of glutathione S-transferase from Escherichia coli B." J Bacteriol **171**(11): 6039-42.

Imig, J. D. (2005). "Epoxide hydrolase and epoxygenase metabolites as therapeutic targets for renal diseases." Am J Physiol Renal Physiol **289**(3): F496-503.

Imig, J. D., X. Zhao, et al. (2002). "Soluble epoxide hydrolase inhibition lowers arterial blood pressure in angiotensin II hypertension." Hypertension **39**(2 Pt 2): 690-4.

Janssen, D. B., F. Pries, et al. (1989). "Cloning of 1,2-dichloroethane degradation genes of Xanthobacter autotrophicus GJ10 and expression and sequencing of the dhlA gene." J Bacteriol **171**(12): 6791-9.

Jobard, F., C. Lefevre, et al. (2002). "Lipoxygenase-3 (ALOXE3) and 12(R)-lipoxygenase (ALOX12B) are mutated in non-bullous congenital ichthyosiform erythroderma (NCIE) linked to chromosome 17p13.1." Hum Mol Genet **11**(1): 107-13.

Johnson, G. D. and W. Jiang (2005). "Characterization of cathepsin L secreted by Sf21 insect cells." Arch Biochem Biophys **444**(1): 7-14.

Jones, P. A. and S. B. Baylin (2002). "The fundamental role of epigenetic events in cancer." Nat Rev Genet **3**(6): 415-28.

Jung, O., R. P. Brandes, et al. (2005). "Soluble epoxide hydrolase is a main effector of angiotensin II-induced hypertension." Hypertension **45**(4): 759-65.

Keeney, D. S., C. Skinner, et al. (1998). "Differentiating keratinocytes express a novel cytochrome P450 enzyme, CYP2B19, having arachidonate monooxygenase activity." J Biol Chem **273**(48): 32071-9.

Kim, I. H., F. R. Heirtzler, et al. (2005). "Optimization of amide-based inhibitors of soluble epoxide hydrolase with improved water solubility." J Med Chem **48**(10): 3621-9.

Kingsley, P. J. and L. J. Marnett (2003). "Analysis of endocannabinoids by Ag+ coordination tandem mass spectrometry." Anal Biochem **314**(1): 8-15.

Kiyosue, T., J. K. Beetham, et al. (1994). "Characterization of an Arabidopsis cDNA for a soluble epoxide hydrolase gene that is inducible by auxin and water stress." Plant J **6**(2): 259-69.

Kosaka, K., K. Suzuki, et al. (1994). "Leukotoxin, a linoleate epoxide: its implication in the late death of patients with extensive burns." Mol Cell Biochem **139**(2): 141-8.

Kozak, M. (1999). "Initiation of translation in prokaryotes and eukaryotes." Gene **234**(2): 187-208.

Krig, S. R., V. X. Jin, et al. (2007). "Identification of genes directly regulated by the oncogene ZNF217 using chromatin immunoprecipitation (ChIP)-chip assays." J Biol Chem **282**(13): 9703-12.

Lacourciere, G. M. and R. N. Armstrong (1993). "The catalytic mechanism of microsomal epoxide hydrolase involves an ester intermediate." J. Am. Chem. Soc. **115** (22): 10466–10467.

Lacourciere, G. M. and R. N. Armstrong (1994). "Microsomal and soluble epoxide hydrolases are members of the same family of C-X bond hydrolase enzymes." Chem Res Toxicol **7**(2): 121-4.

Ladd, P. A., L. Du, et al. (2003). "Epoxyeicosatrienoic acids activate transglutaminases in situ and induce cornification of epidermal keratinocytes." J Biol Chem **278**(37): 35184-92.

Laemmli, U. K. (1970). "Cleavage of structural proteins during the assembly of the head of bacteriophage T4." Nature **227**(5259): 680-5.

Laughlin, L. T., H. F. Tzeng, et al. (1998). "Mechanism of microsomal epoxide hydrolase. Semifunctional site-specific mutants affecting the alkylation half-reaction." Biochemistry **37**(9): 2897-904.

Lauterbach, B., E. Barbosa-Sicard, et al. (2002). "Cytochrome P450-dependent eicosapentaenoic acid metabolites are novel BK channel activators." Hypertension **39**(2 Pt 2): 609-13.

Lein, E. S., M. J. Hawrylycz, et al. (2007). "Genome-wide atlas of gene expression in the adult mouse brain." Nature **445**(7124): 168-76.

Li, J., M. A. Carroll, et al. (2008). "Soluble epoxide hydrolase inhibitor, AUDA, prevents early salt-sensitive hypertension." Front Biosci **13**: 3480-7.

Liu, Y., Y. Zhang, et al. (2005). "The antiinflammatory effect of laminar flow: the role of PPARgamma, epoxyeicosatrienoic acids, and soluble epoxide hydrolase." Proc Natl Acad Sci U S A **102**(46): 16747-52.

Luckow, V. A., S. C. Lee, et al. (1993). "Efficient generation of infectious recombinant baculoviruses by site-specific transposon-mediated insertion of foreign genes into a baculovirus genome propagated in Escherichia coli." J Virol **67**(8): 4566-79.

Luckow, V. A. and M. D. Summers (1988). "Signals important for high-level expression of foreign genes in Autographa californica nuclear polyhedrosis virus expression vectors." Virology **167**(1): 56-71.

Marowsky, A., J. Burgener, et al. (2009). "Distribution of soluble and microsomal epoxide hydrolase in the mouse brain and its contribution to cerebral epoxyeicosatrienoic acid metabolism." Neuroscience **163**(2): 646-61.

McGee, J. and F. Fitzpatrick (1985). "Enzymatic hydration of leukotriene A4. Purification and characterization of a novel epoxide hydrolase from human erythrocytes." J Biol Chem **260**(23): 12832-7.

Michaelis, U. R., B. Fisslthaler, et al. (2005). "Cytochrome P450 epoxygenases 2C8 and 2C9 are implicated in hypoxia-induced endothelial cell migration and angiogenesis." J Cell Sci **118**(Pt 23): 5489-98.

Moghaddam, M., K. Motoba, et al. (1996). "Novel metabolic pathways for linoleic and arachidonic acid metabolism." Biochim Biophys Acta **1290**(3): 327-39.

Moghaddam, M. F., D. F. Grant, et al. (1997). "Bioactivation of leukotoxins to their toxic diols by epoxide hydrolase." Nat Med **3**(5): 562-6.

Moran, J. H., R. Weise, et al. (1997). "Cytotoxicity of linoleic acid diols to renal proximal tubular cells." Toxicol Appl Pharmacol **146**(1): 53-9.

Morin, C., M. Sirois, et al. (2009). "Relaxing effects of 17(18)-EpETE on arterial and airway smooth muscles in human lung." Am J Physiol Lung Cell Mol Physiol **296**(1): L130-9.

Morisseau, C., G. Du, et al. (1998). "Mechanism of mammalian soluble epoxide hydrolase inhibition by chalcone oxide derivatives." Arch Biochem Biophys **356**(2): 214-28.

Morisseau, C., M. H. Goodrow, et al. (1999). "Potent urea and carbamate inhibitors of soluble epoxide hydrolases." Proc Natl Acad Sci U S A **96**(16): 8849-54.

Morisseau, C., M. H. Goodrow, et al. (2002). "Structural refinement of inhibitors of urea-based soluble epoxide hydrolases." Biochem Pharmacol **63**(9): 1599-608.

Mrsny, R. J., A. T. Gewirtz, et al. (2004). "Identification of hepoxilin A3 in inflammatory events: a required role in neutrophil migration across intestinal epithelia." Proc Natl Acad Sci U S A **101**(19): 7421-6.

Mukherjee, P. K., V. L. Marcheselli, et al. (2007). "Neurotrophins enhance retinal pigment epithelial cell survival through neuroprotectin D1 signaling." Proc Natl Acad Sci U S A **104**(32): 13152-7.

Muller, F., M. Arand, et al. (1997). "Visualization of a covalent intermediate between microsomal epoxide hydrolase, but not cholesterol epoxide hydrolase, and their substrates." Eur J Biochem **245**(2): 490-6.

Mullin, C. A. (1988). "Adaptive relationships of epoxide hydrolase in herbivorous arthropods." Journal of Chemical Ecology **Volume 14**(Number 10): 1867-1888.

Mullin, C. A. and B. D. Hammock (1982). "Chalcone oxides--potent selective inhibitors of cytosolic epoxide hydrolase." Arch Biochem Biophys **216**(2): 423-39.

Nakanishi, M., T. Ishizaki, et al. (2000). "Leukotoxin, 9,10-epoxy-12-octadecenoate, causes pulmonary vasodilation by stimulation of vascular eNOS and iNOS." Lung **178**(3): 137-48.

Nardini, M. and B. W. Dijkstra (1999). "Alpha/beta hydrolase fold enzymes: the family keeps growing." Curr Opin Struct Biol **9**(6): 732-7.

Nardini, M., I. S. Ridder, et al. (1999). "The x-ray structure of epoxide hydrolase from Agrobacterium radiobacter AD1. An enzyme to detoxify harmful epoxides." J Biol Chem **274**(21): 14579-86.

Newman, J. W., C. Morisseau, et al. (2005). "Epoxide hydrolases: their roles and interactions with lipid metabolism." Prog Lipid Res **44**(1): 1-51.

Nigam, S., M. P. Zafiriou, et al. (2007). "Structure, biochemistry and biology of hepoxilins: an update." Febs J **274**(14): 3503-12.

Oesch, F. (1973). "Mammalian epoxide hydrolases: inducible enzymes catalysing the inactivation of carcinogenic and cytotoxic metabolites derived from aromatic and olefinic compounds." Xenobiotica **3**: 305-340.

Okazaki, Y., M. Furuno, et al. (2002). "Analysis of the mouse transcriptome based on functional annotation of 60,770 full-length cDNAs." Nature **420**(6915): 563-73.

Ollis, D. L., E. Cheah, et al. (1992). "The alpha/beta hydrolase fold." Protein Eng **5**(3): 197-211.

Ota, T., Y. Suzuki, et al. (2004). "Complete sequencing and characterization of 21,243 full-length human cDNAs." Nat Genet **36**(1): 40-5.

Ozawa, T., S. Sugiyama, et al. (1989). "Leukocytes biosynthesize leukotoxin (9,10-epoxy-12-octadecenoate)--a novel cytotoxic linoleate epoxide." Adv Prostaglandin Thromboxane Leukot Res **19**: 164-7.

Pace-Asciak, C. R. and W. S. Lee (1989). "Purification of hepoxilin epoxide hydrolase from rat liver." J Biol Chem **264**(16): 9310-3.

Pacher, P., S. Batkai, et al. (2006). "The endocannabinoid system as an emerging target of pharmacotherapy." Pharmacol Rev **58**(3): 389-462.

Pendergast, A. M., R. Clark, et al. (1989). "Baculovirus expression of functional P210 BCR-ABL oncogene product." Oncogene **4**(6): 759-66.

Pharmacia (1997). Separation of DnaK from pGEX-GST by ion exchange chromatography. Science Tools from Pharmacia Biotech. **2**.

Pharmingen (1999). Baculovirus Expression Vector System Manual. California, USA.

Porath, J., J. Carlsson, et al. (1975). "Metal chelate affinity chromatography, a new approach to protein fractionation." Nature **258**(5536): 598-9.

Potente, M., B. Fisslthaler, et al. (2003). "11,12-Epoxyeicosatrienoic acid-induced inhibition of FOXO factors promotes endothelial proliferation by down-regulating p27Kip1." J Biol Chem **278**(32): 29619-25.

Rappaport, S. M., K. Yeowell-O'Connell, et al. (1996). "An investigation of multiple biomarkers among workers exposed to styrene and styrene-7,8-oxide." Cancer Res **56**(23): 5410-6.

Rial, D. V. and E. A. Ceccarelli (2002). "Removal of DnaK contamination during fusion protein purifications." Protein Expr Purif **25**(3): 503-7.

Rigsby, R. E., K. L. Fillgrove, et al. (2005). "Fosfomycin resistance proteins: a nexus of glutathione transferases and epoxide hydrolases in a metalloenzyme superfamily." Methods Enzymol **401**: 367-79.

Sandberg, M., C. Hassett, et al. (2000). "Identification and functional characterization of human soluble epoxide hydrolase genetic polymorphisms." J Biol Chem **275**(37): 28873-81.

Schagger, H. and G. von Jagow (1987). "Tricine-sodium dodecyl sulfate-polyacrylamide gel electrophoresis for the separation of proteins in the range from 1 to 100 kDa." Anal Biochem **166**(2): 368-79.

Schwarz, D., P. Kisselev, et al. (2004). "Arachidonic and eicosapentaenoic acid metabolism by human CYP1A1: highly stereoselective formation of 17(R),18(S)-epoxyeicosatetraenoic acid." Biochem Pharmacol **67**(8): 1445-57.

Sellers, K. W., C. Sun, et al. (2005). "Novel mechanism of brain soluble epoxide hydrolase-mediated blood pressure regulation in the spontaneously hypertensive rat." Faseb J **19**(6): 626-8.

Sisemore, M. F., J. Zheng, et al. (2001). "Cellular characterization of leukotoxin diol-induced mitochondrial dysfunction." Arch Biochem Biophys **392**(1): 32-7.

Smith, K. R., K. E. Pinkerton, et al. (2005). "Attenuation of tobacco smoke-induced lung inflammation by treatment with a soluble epoxide hydrolase inhibitor." Proc Natl Acad Sci U S A **102**(6): 2186-91.

Snider, N. T., J. A. Nast, et al. (2009). "A cytochrome P450-derived epoxygenated metabolite of anandamide is a potent cannabinoid receptor 2-selective agonist." Mol Pharmacol **75**(4): 965-72.

Snider, N. T., M. J. Sikora, et al. (2008). "The endocannabinoid anandamide is a substrate for the human polymorphic cytochrome P450 2D6." J Pharmacol Exp Ther **327**(2): 538-45.

Spector, A. A. and A. W. Norris (2007). "Action of epoxyeicosatrienoic acids on cellular function." Am J Physiol Cell Physiol **292**(3): C996-C1012.

Sprengart, M. L., E. Fuchs, et al. (1996). "The downstream box: an efficient and independent translation initiation signal in Escherichia coli." Embo J **15**(3): 665-74.

Stansberg, C., A. O. Vik-Mo, et al. (2007). "Gene expression profiles in rat brain disclose CNS signature genes and regional patterns of functional specialisation." BMC Genomics **8**: 94.

Sumner, S. J. and T. R. Fennell (1994). "Review of the metabolic fate of styrene." Crit Rev Toxicol **24 Suppl**: S11-33.

Sun, J., X. Sui, et al. (2002). "Inhibition of vascular smooth muscle cell migration by cytochrome p450 epoxygenase-derived eicosanoids." Circ Res **90**(9): 1020-7.

Thierry-Mieg, D. and J. Thierry-Mieg (2006). "AceView: a comprehensive cDNA-supported gene and transcripts annotation." Genome Biol **7 Suppl 1**: S12 1-14.

Toulza, E., N. R. Mattiuzzo, et al. (2007). "Large-scale identification of human genes implicated in epidermal barrier function." Genome Biol **8**(6): R107.

Ullmann, A., F. Jacob, et al. (1967). "Characterization by in vitro complementation of a peptide corresponding to an operator-proximal segment of the beta-galactosidase structural gene of Escherichia coli." J Mol Biol **24**(2): 339-43.

van der Werf, M. J., K. M. Overkamp, et al. (1998). "Limonene-1,2-epoxide hydrolase from Rhodococcus erythropolis DCL14 belongs to a novel class of epoxide hydrolases." J Bacteriol **180**(19): 5052-7.

van Loo, B., J. Kingma, et al. (2006). "Diversity and biocatalytic potential of epoxide hydrolases identified by genome analysis." Appl Environ Microbiol **72**(4): 2905-17.

Vanderheiden, G. J., A. C. Fairchild, et al. (1970). "Construction of a laboratory press for use with the French pressure cell." Appl Microbiol **19**(5): 875-7.

VanRollins, M. (1995). "Epoxygenase metabolites of docosahexaenoic and eicosapentaenoic acids inhibit platelet aggregation at concentrations below those affecting thromboxane synthesis." J Pharmacol Exp Ther **274**(2): 798-804.

VanRollins, M., R. C. Baker, et al. (1984). "Oxidation of docosahexaenoic acid by rat liver microsomes." J Biol Chem **259**(9): 5776-83.

Vaughn, J. L., R. H. Goodwin, et al. (1977). "The establishment of two cell lines from the insect Spodoptera frugiperda (Lepidoptera; Noctuidae)." In Vitro **13**(4): 213-7.

Verschueren, K. H., F. Seljee, et al. (1993). "Crystallographic analysis of the catalytic mechanism of haloalkane dehalogenase." Nature **363**(6431): 693-8.

Wagner, S., M. L. Bader, et al. (2006). "Rationalizing membrane protein overexpression." Trends Biotechnol **24**(8): 364-71.

Widstrom, R. L., A. W. Norris, et al. (2001). "Binding of cytochrome P450 monooxygenase and lipoxygenase pathway products by heart fatty acid-binding protein." Biochemistry **40**(4): 1070-6.

Wojtasek, H. and G. D. Prestwich (1996). "An insect juvenile hormone-specific epoxide hydrolase is related to vertebrate microsomal epoxide hydrolases." Biochem Biophys Res Commun **220**(2): 323-9.

Yamashita, S., Y. Tsujino, et al. (2006). "Chemical genomic screening for methylation-silenced genes in gastric cancer cell lines using 5-aza-2'-deoxycytidine treatment and oligonucleotide microarray." Cancer Sci **97**(1): 64-71.

Ye, D., D. Zhang, et al. (2002). "Cytochrome p-450 epoxygenase metabolites of docosahexaenoate potently dilate coronary arterioles by activating large-conductance calcium-activated potassium channels." J Pharmacol Exp Ther **303**(2): 768-76.

Yu, Z., C. Schneider, et al. (2007). "Epidermal lipoxygenase products of the hepoxilin pathway selectively activate the nuclear receptor PPARalpha." Lipids **42**(6): 491-7.

Yu, Z., F. Xu, et al. (2000). "Soluble epoxide hydrolase regulates hydrolysis of vasoactive epoxyeicosatrienoic acids." Circ Res **87**(11): 992-8.

Zheng, J., C. G. Plopper, et al. (2001). "Leukotoxin-diol: a putative toxic mediator involved in acute respiratory distress syndrome." Am J Respir Cell Mol Biol **25**(4): 434-8.

8 APPENDIX

8.1 *Primer sequences and PCR conditions*

8.1.1 Cloning of expression constructs

#	label	sequence
1	nEH2 F EcoRV 1509 *(sense)*	5`- cgccgc**gatatc**ccaatggcgaggctgcg -3`
2	nEH2 R BamHI 1509 *(antisense)*	5`- ca**ggatcc**ctcattacagaccttcatagaag -3`
3	hE for-mem *(sense)*	5`- caga**tcatg**acgcccgcgtgcctgagcgac -3`
4	nEH2 R for Ab Bgl II *(antisense)*	5`- gt**agatct**ggagtggtcaccatgtgatg -3`
5	nEH2 1/3 F 140606 *(sense)*	5`- gatatcc**ccatgg**cgaggc -3`
6	nEH2 1/3 R 140606 *(antisense)*	5`- gtgctacaact**agatct**tcact -3`
7	nEH2 3/3F *(sense)*	5`- catg**ccatgg**tcttttctcagcctggag -3`
8	nEH2 3/3R *(antisense)*	5`- gatc**agatct**ccatctttttttcttgtttcttc -3`
9	nEH2 F (BamHI) IRAK 210108 (*sense)*	5`- catg**ggatcc**gcctcccaatggcgaggctgcggga -3`
10	nEH2 R (PstI) pFastBac *(antisense)*	5`- aaagaa**ctgcag**atctttttttcttgtttcttcttttagaaatgtcc -3`
11	nEH2 F (NdeI) IRAK 200807 (*sense)*	5`- cgccgcctc**catatg**gcgaggctgcggga -3`
12	nEH2 R (PstI) pFastBac *(antisense)*	5`- aaagaa**ctgcag**atctttttttcttgtttcttcttttagaaatgtcc -3`
13	pFastModify for (*sense)*	5`- ggttggctacgtatactccg -3`
14	pFastModify rev *(antisense)*	5`- gcactgcaggatccgaattcatatgtataggttttttattacaaaactgttacg -3`
15	EH3 anchorless (*sense)*	5`- ccatgggcgggcgccgtcggag -3`
16	EH3revprset *(antisense)*	5`- tata**gaattc**agcaaggaccactagtcc -3`

Table 8-1: *Primer sequence of the primers used to generate the EH3 and EH4 expression constructs.*

PCR conditions:

primers	prim. denaturation		denaturation		annealing		elongation		final elongation		cycles
# 1 / # 2	95℃	03:00	95℃	00:45	62℃	00:45	72℃	01: 00	72℃	10:00	30
# 3 / # 4	95℃	03:00	95℃	00:45	62℃	00:45	72℃	01: 00	72℃	10:00	30
# 5 / # 6	95℃	02:00	95℃	00:45	56.4℃	00:30	72℃	0 1:20	72℃	05:00	35
# 7 / # 8	95℃	02:00	95℃	00:45	56.4℃	00:30	72℃	0 1:20	72℃	05:00	35
# 9 / # 10	95℃	01:30	95℃	00:45	64℃	00:45	72℃	01 :00	72℃	03:00	30
# 11 / # 2	95℃	01:30	95℃	00:45	60.8℃	00:45	72℃	01:00	72℃	03:00	30
# 11 / # 10	95℃	01:30	95℃	00:45	60.8℃	00:45	72℃	01:00	72℃	03:00	30
# 13/ # 14	95℃	01:30	95℃	00:45	59.7℃	00:45	72℃	01:00	72℃	03:00	30
# 15 / # 16	95℃	03:00	95℃	00:45	63℃	00:30	72℃	0 1:00	72℃	10:00	28

Table 8-2: *PCR conditions used to amplify the respective cDNA for generation of different expression constructs. The primer pair given in the first column specifies the PCR reaction as mentioned in the text (see tables 5-1, 5-3 and 5-4).*

8.1.2 RT-PCR

label	sequence
nEH2 (*sense*)	5`-GAG GCA TGA TTG CCT GGC TGA TTG C-3`
nEH2 (*antisense*)	5`-GCA GTG TTG GGG TGG TCA CCA TGT G-3`
GAPDH *(sense)*	5`-CCT GCA CCA CCA ACT GCT TA-3`
GAPDH *(antisense)*	5`-ACC ACC CTG TTG CTG TAG CC-3`

Table 8-3: *Sequences of EH4 and GAPDH specific primers used for expression analysis by reverse transcriptase PCR.*

primers	prim. denaturation		denaturation		annealing		elongation		final elongation		cycles
nEH2(RT1) / nEH2(RT2)	95℃	02:00	95℃	00:45	55℃	00 :45	72℃	01:00	72℃	10:00	25
GAPDH *sense*/GAPDH *antisense*	95℃	02:00	95℃	00:45	62℃	00:45	72℃	01:00	72℃	10 :00	30

Table 8-4: *PCR conditions for specific amplification of EH4 and GAPDH cDNA.*

8.2 *DNA sequences*

8.2.1 EH3

Figure 8-1: *cDNA sequence of EH3.*

8.2.2 EH4

Figure 8-2: *cDNA sequence of EH4 (EPHX4).*

8.3 *Protein sequences*

8.3.1 EH4

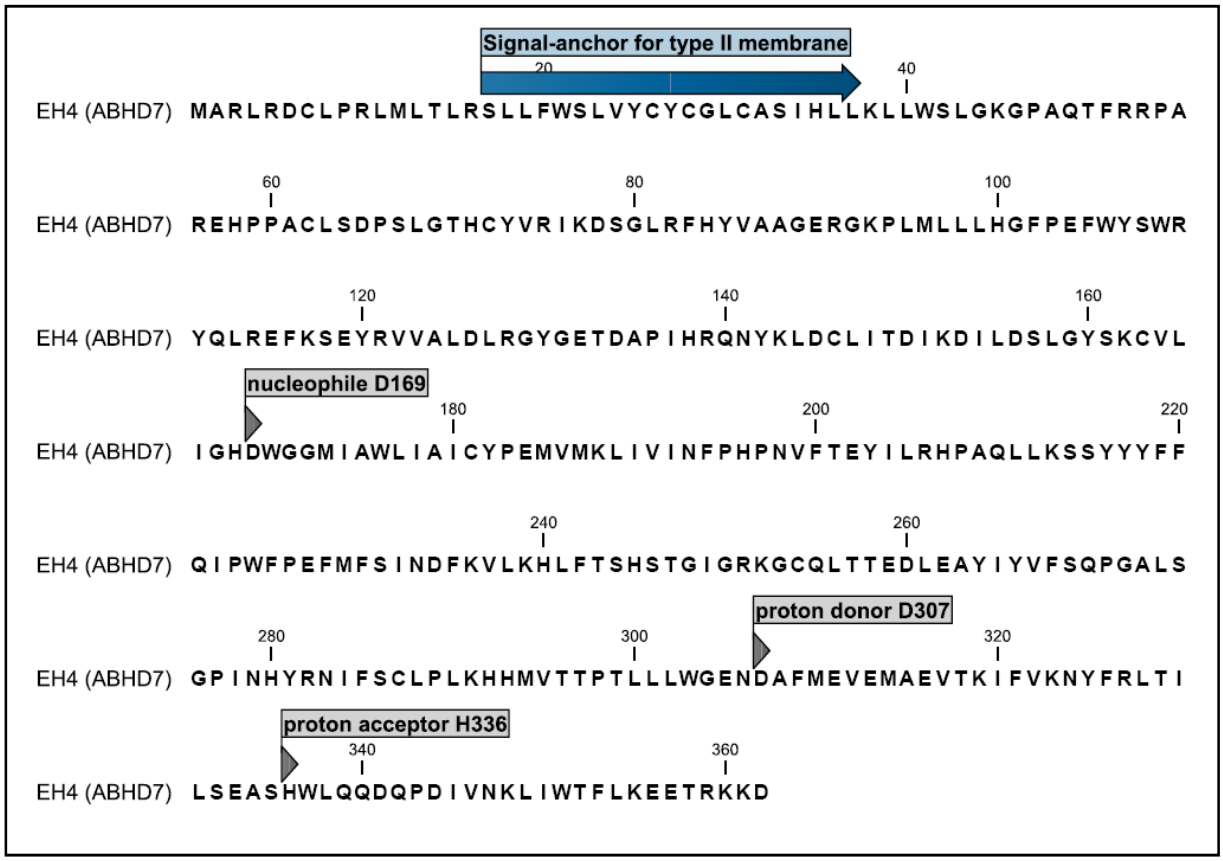

Figure 8-3: *Amino acid sequence of EH4. Indicated in blue is the putative membrane anchor, the presumed catalytically active residues are indicated in grey.*

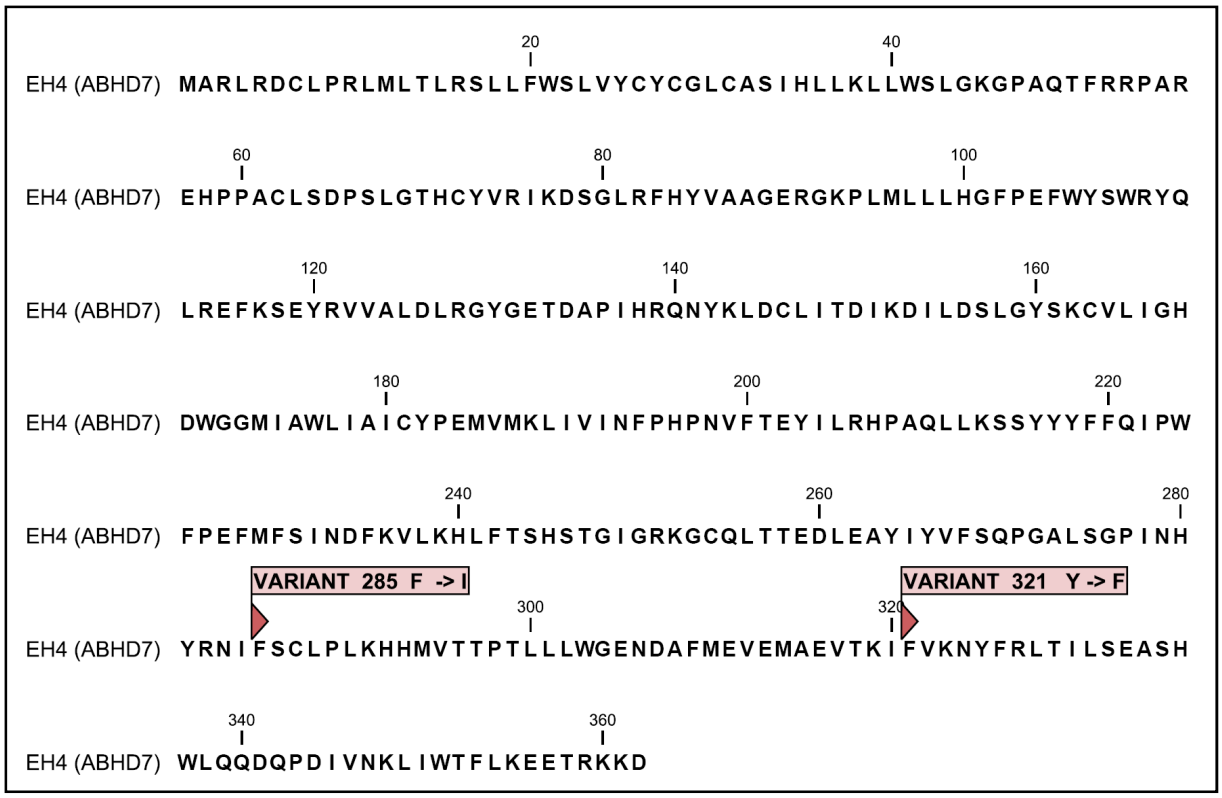

Figure 8-4: *Amino acid sequence of EH4. Indicated in red are the two observed variants (annotated as SNPs).*

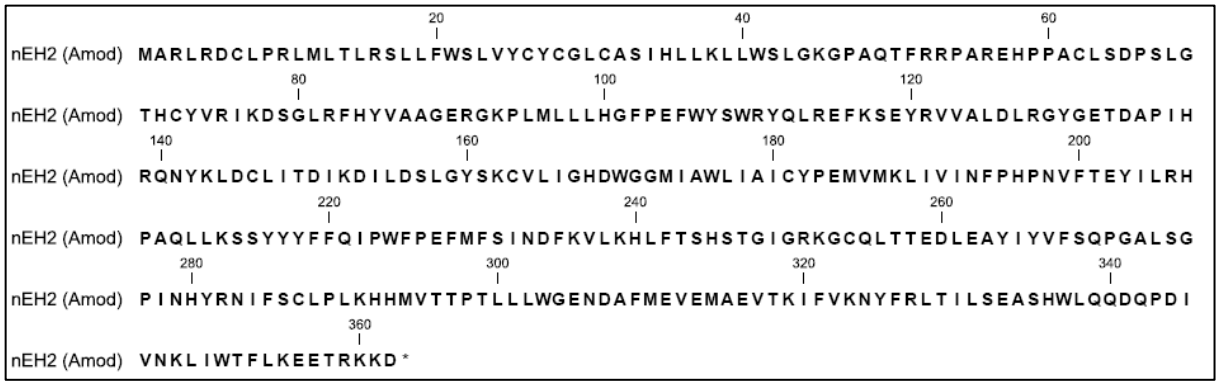

Figure 8-5: *Translation and amino acid sequence of pFastBacModnEH2 (A_{mod}) construct. The resulting protein contains all putative enzymatic active residues and the membrane anchor.*

8.3.2 His-tagged EH4 proteins

Figure 8-6: *Translation and amino acid sequence of nEH2AB_HisC (EH4AB-HisC) construct. The EH4 protein contains a C-terminal His-tag (6x) and is lacking the membrane anchor and the putative catalytically active amino acid D306 (proton donor) and H336 (proton acceptor).*

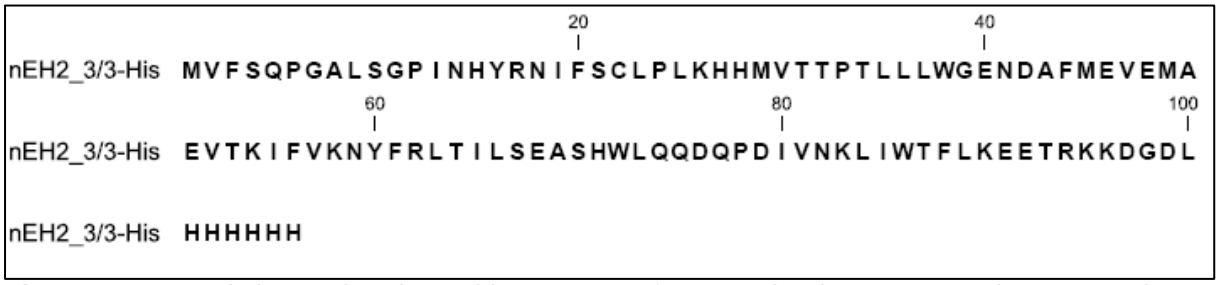

Figure 8-7: *Translation and amino acid sequence of nEH2_3/3-His construct. The truncated EH4 protein consists of the amino acids 267-362. The construct is lacking the catalytic nucleophile D169.*

Figure 8-8: *Translation and amino acid sequence of nEH2_1/3-His construct. The truncated EH4 protein consists of amino acids 1-118 and is lacking all putative catalytically active residues.*

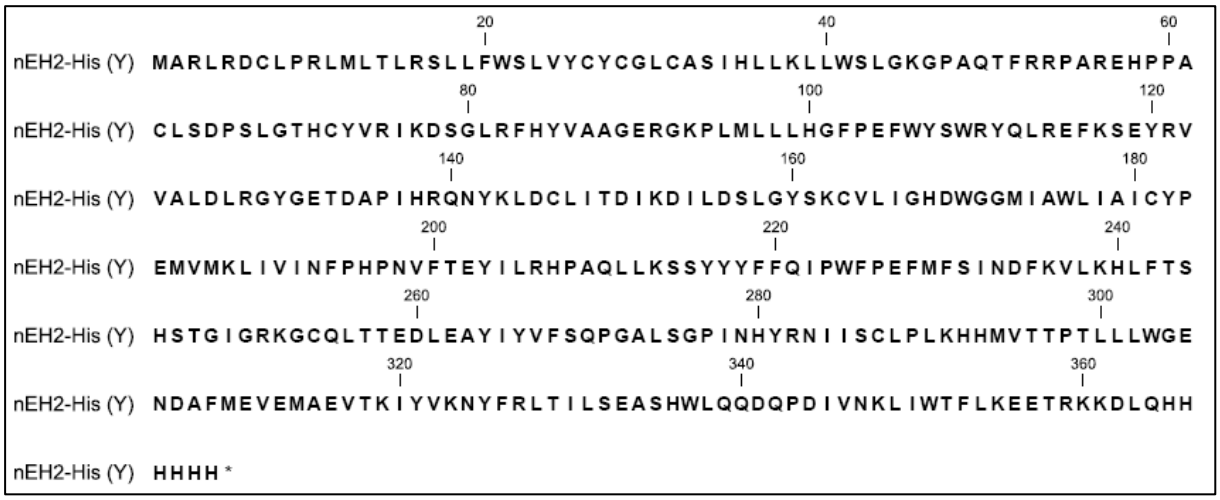

Figure 8-9: *Translation and amino acid sequence of pFastBacHis-nEH2 (Y) construct. The full length EH4 protein (all features present) is C-terminal tagged (6xHis).*

Figure 8-10: *Translation and amino acid sequence of pFastBacmod-nEH2 (B_{mod}) construct. The full length EH4 protein (all features present) is C-terminal tagged (6xHis).*

8.3.3 His tagged EH3 proteins

Figure 8-11: *Translation and amino acid sequence of pRSETb-EH3 (frameshift) construct.*

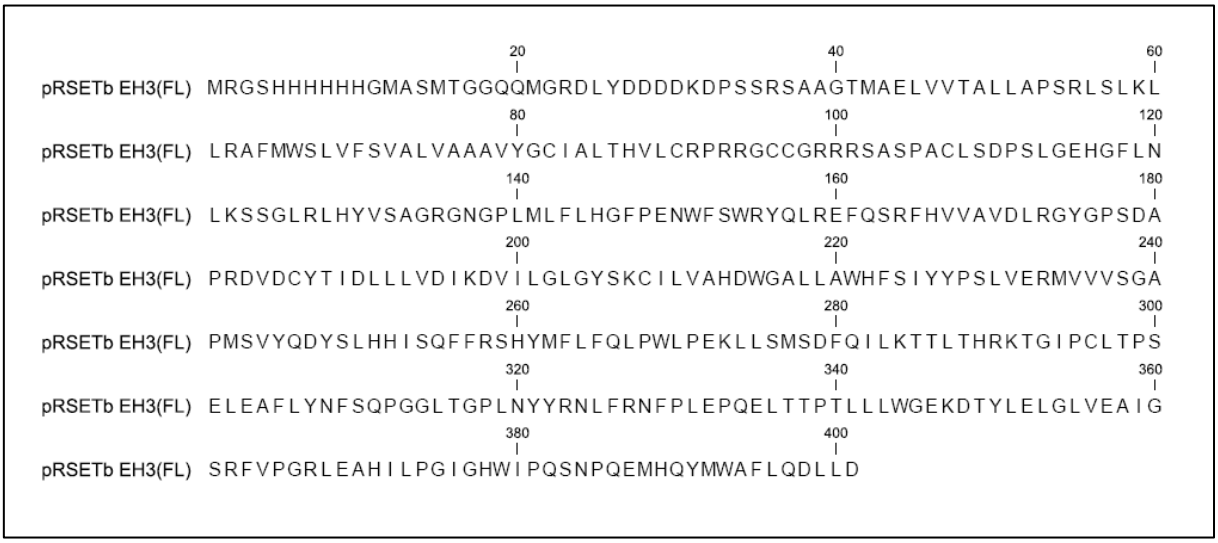

Figure 8-12: *Translation and amino acid sequence of pRSETb EH3 (FL).*

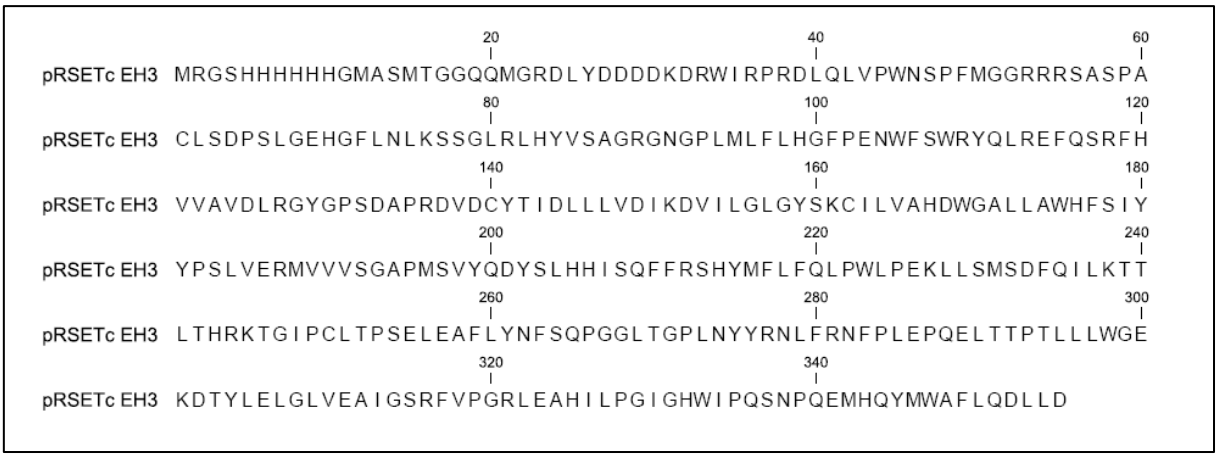

Figure 8-13: *Translation and amino acid sequence of pRSETc EH3.*

```
                                  20                  40                  60
pRSETb EH3  MRGSHHHHHHGMASMTGGQQMGRDLYDDDDKDPSSRSAAGTMGGRRRSASPACLSDPSLG
                                  80                 100                 120
pRSETb EH3  EHGFLNLKSSGLRLHYVSAGRGNGPLMLFLHGFPENWFSWRYQLREFQSRFHVVAVDLRG
                                 140                 160                 180
pRSETb EH3  YGPSDAPRDVDCYTIDLLLVDIKDVILGLGYSKCILVAHDWGALLAWHFSIYYPSLVERM
                                 200                 220                 240
pRSETb EH3  VVVSGAPMSVYQDYSLHHISQFFRSHYMFLFQLPWLPEKLLSMSDFQILKTTLTHRKTGI
                                 260                 280                 300
pRSETb EH3  PCLTPSELEAFLYNFSQPGGLTGPLNYYRNLFRNFPLEPQELTTPTLLLWGEKDTYLELG
                                 320                 340
pRSETb EH3  LVEAIGSRFVPGRLEAHILPGIGHWIPQSNPQEMHQYMWAFLQDLLD
```

Figure 8-14: *Translation and amino acid sequence of pRSETbEH3.*

8.3.4 GST tagged EH4 proteins

```
                                  20                  40                  60
pGEF-GSTnEH2  MTPILGYWKIKGLVQPTRLLLEYLEEKYEEHLYERDEGDKWRNKKFELGLEFPNLPYYID
                                  80                 100                 120
pGEF-GSTnEH2  GDVKLTQSMAIIRYIADKHNMLGGCPKERAEISMLEGAVLDIRYGVSRIAYSKDFETLKV
                                 140                 160                 180
pGEF-GSTnEH2  DFLSKLPEMLKMFEDRLCHKTYLNGDHVTHPDFMLYDALDVVLYMDPMCLDAFPKLVCFK
                                 200                 220                 240
pGEF-GSTnEH2  KRIEAIPQIDKYLKSSKYIAWPLQGWQATFGGGDHPPKSDLVPRGSAMTPACLSDPSLGT
                                 260                 280                 300
pGEF-GSTnEH2  HCYVRIKDSGLRFHYVAAGERGKPLMLLLHGFPEFWYSWRYQLREFKSEYRVVALDLRGY
                                 320                 340                 360
pGEF-GSTnEH2  GETDAPIHRQNYKLDCLITDIKDILDSLGYSKCVLIGHDWGGMIAWLIAICYPEMVMKLI
                                 380                 400                 420
pGEF-GSTnEH2  VINFPHPNVFTEYILRHPAQLLKSSYYYFFQIPWFPEFMFSINDFKVLKHLFTSHSTGIG
                                 440                 460                 480
pGEF-GSTnEH2  RKGCQLTTEDLEAYIYVFSQPGALSGPINHYRNIFSCLPLKHHMVTTPTLLLWGENDAFM
                                 500                 520
pGEF-GSTnEH2  EVEMAEVTKIFVKNYFRLTILSEASHWLQQDQPDIVNKLIWTFLRSTPSPSPLMHQLHG
```

Figure 8-15: *Translation and amino acid sequence of pGEFGSTN-nEH2AB construct. EH4 protein is N-terminally fused to GST and lacks the membrane anchor. EH4 protein starts at position 230 (**P**ACL).*

Figure 8-16: *Translation and amino acid sequence of pGEFGSTN-nEH2AB construct. EH4 protein is N-terminally fused to GST and lacks the membrane anchor. EH4 protein starts at position 230 (**P**ACL) and is lacking the catalytic residues D306 (proton donor) and H336 (proton acceptor).*

8.4 *Vector sequences (MCS)*

8.4.1 pGEF-HisC

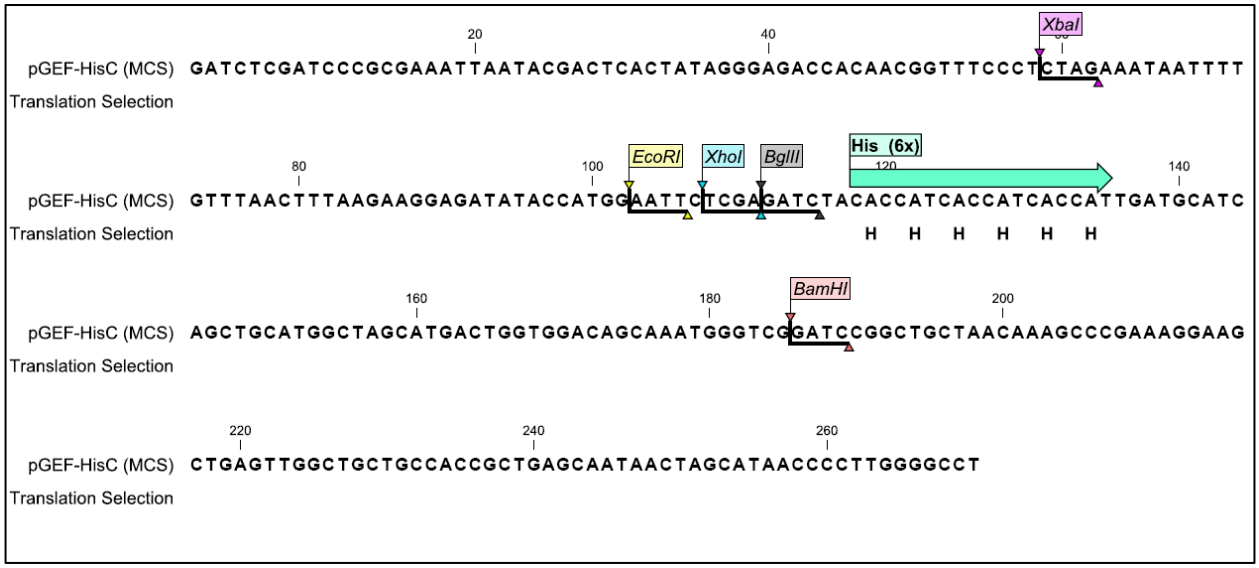

Figure 8-17: *Multiple cloning site (MCS) of pGEF-HisC.*

8.4.2 pGEF-GSTN

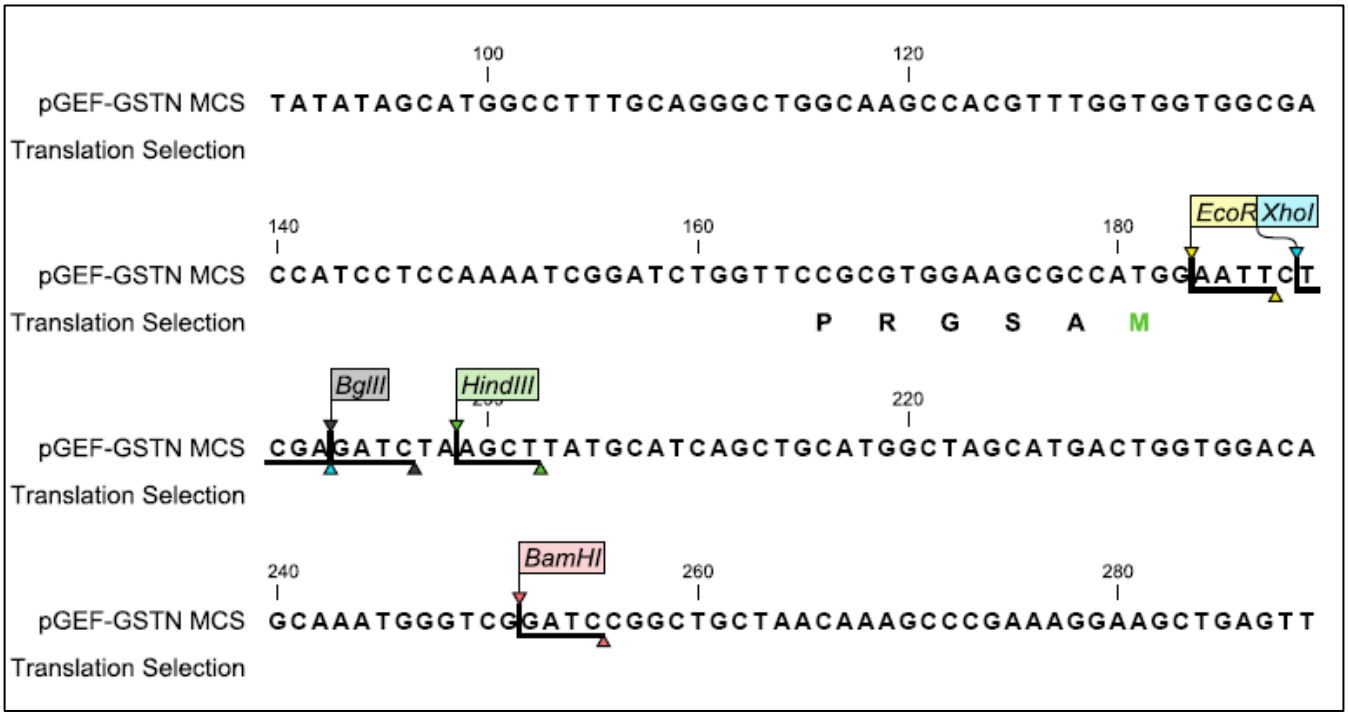

Figure 8-18: *Multiple cloning site of pGEF-GSTN. The selected translation (PRGSAM) indicates the open reading frame of GST protein.*

8.4.3 pFastBacHis

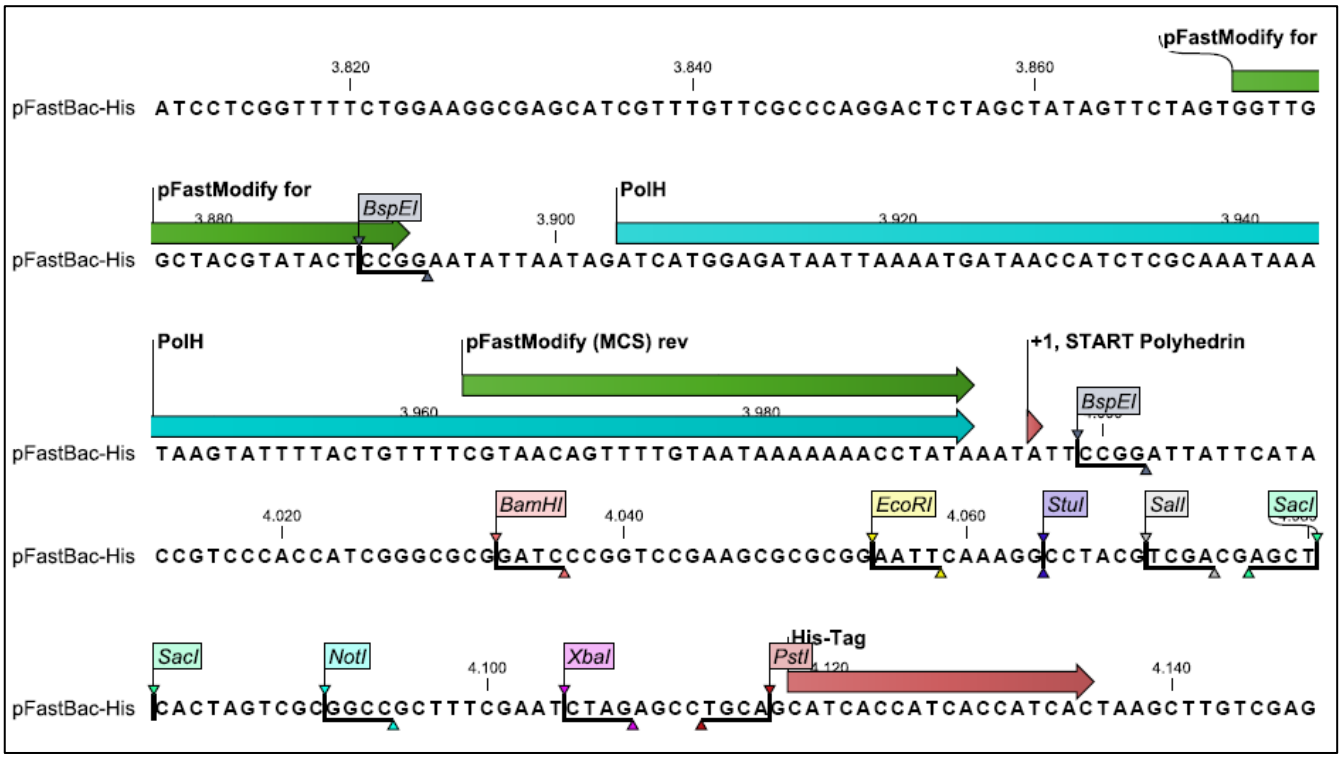

Figure 8-19: *MCS of pFastBacHisC.*

8.4.4 pFastBacHismod

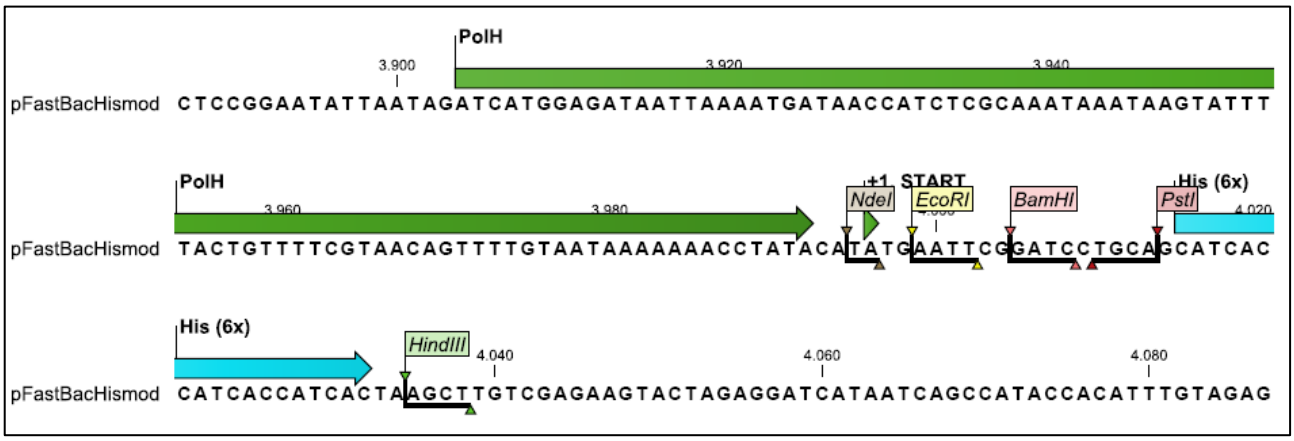

Figure 8-20: *MCS of pFastBacmod.*

8.4.5 pRSET B

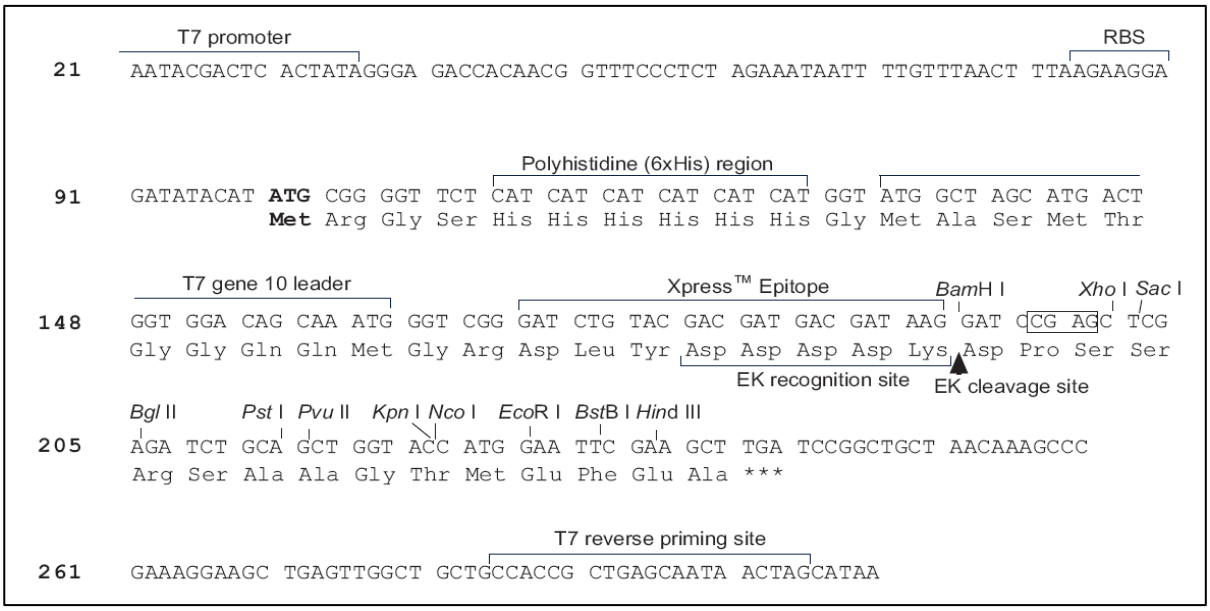

Figure 8-21*: MCS of pRSET B (source: www.invitrogen.com).*

8.4.6 pRSET C

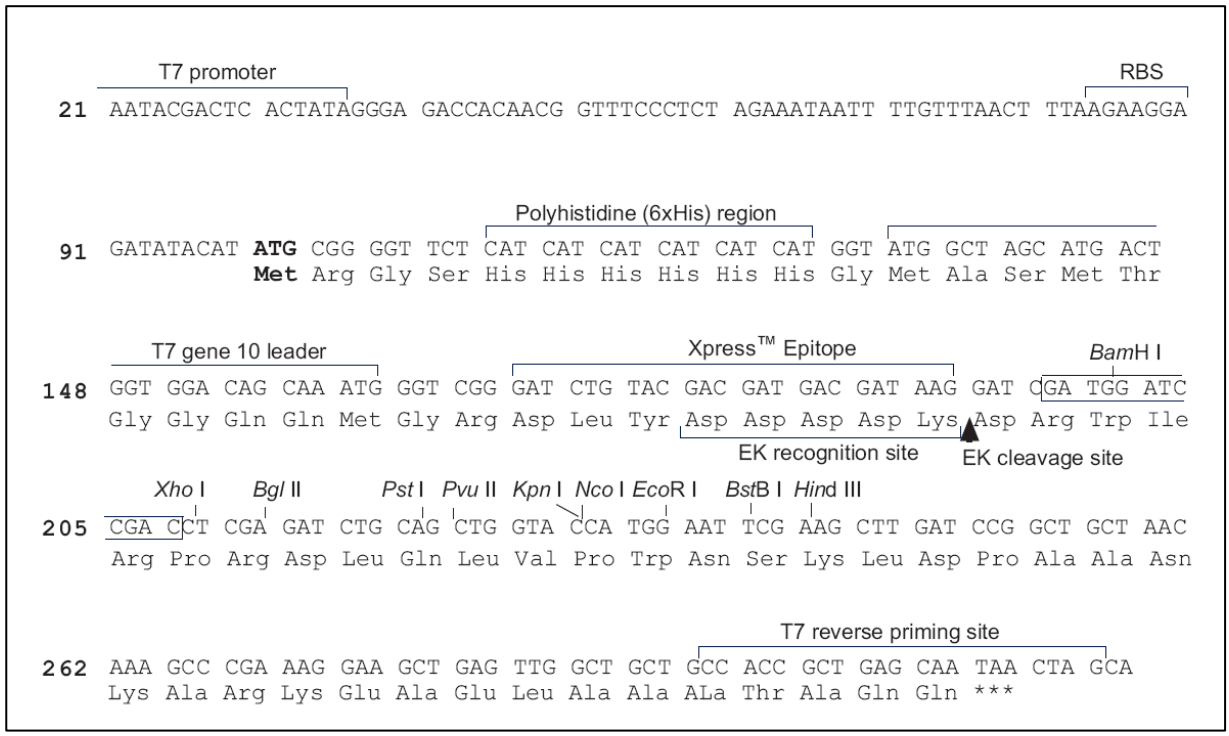

Figure 8-22: *MCS of pRSET C (source: www.invitrogen.com)*

8.5 *Vectormaps*

8.5.1 Vectors

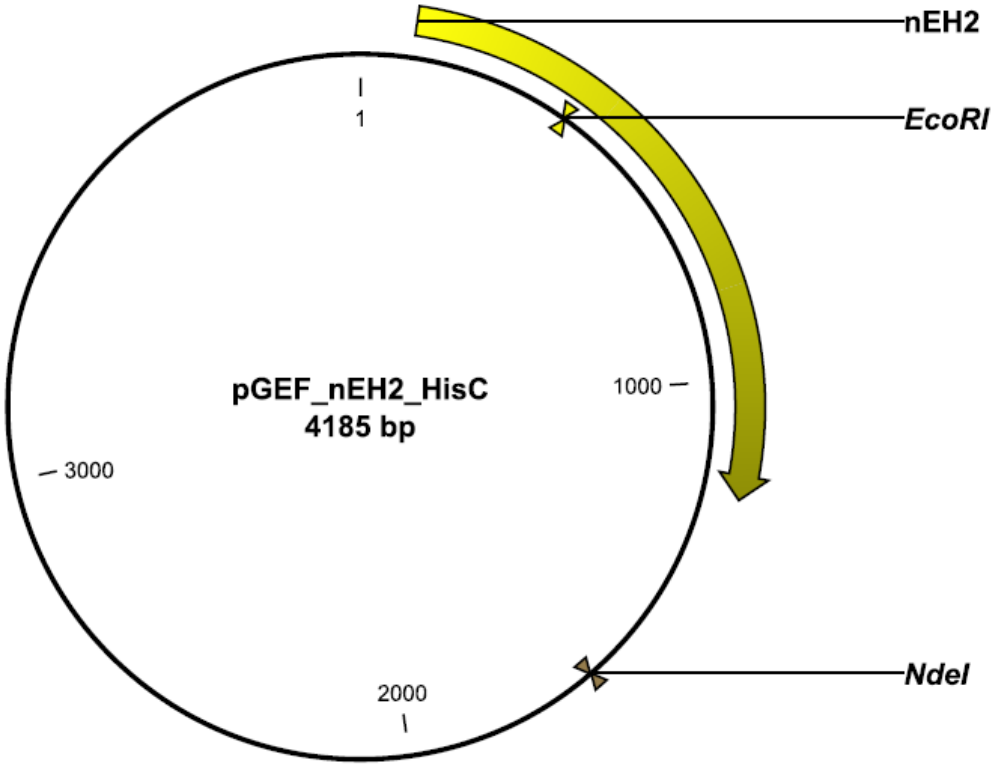

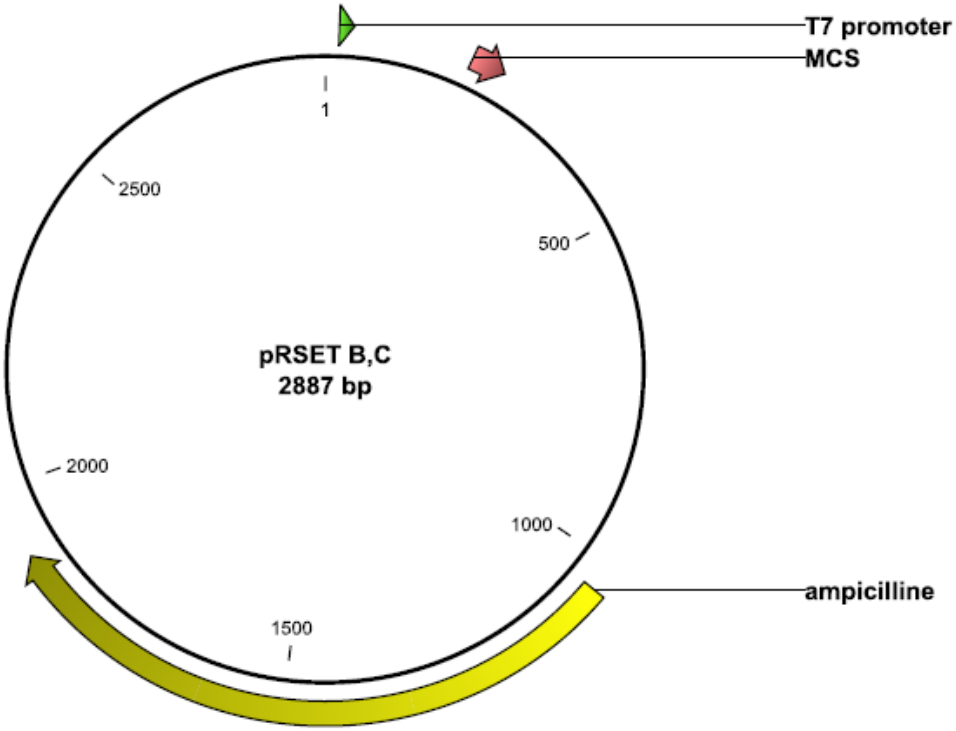

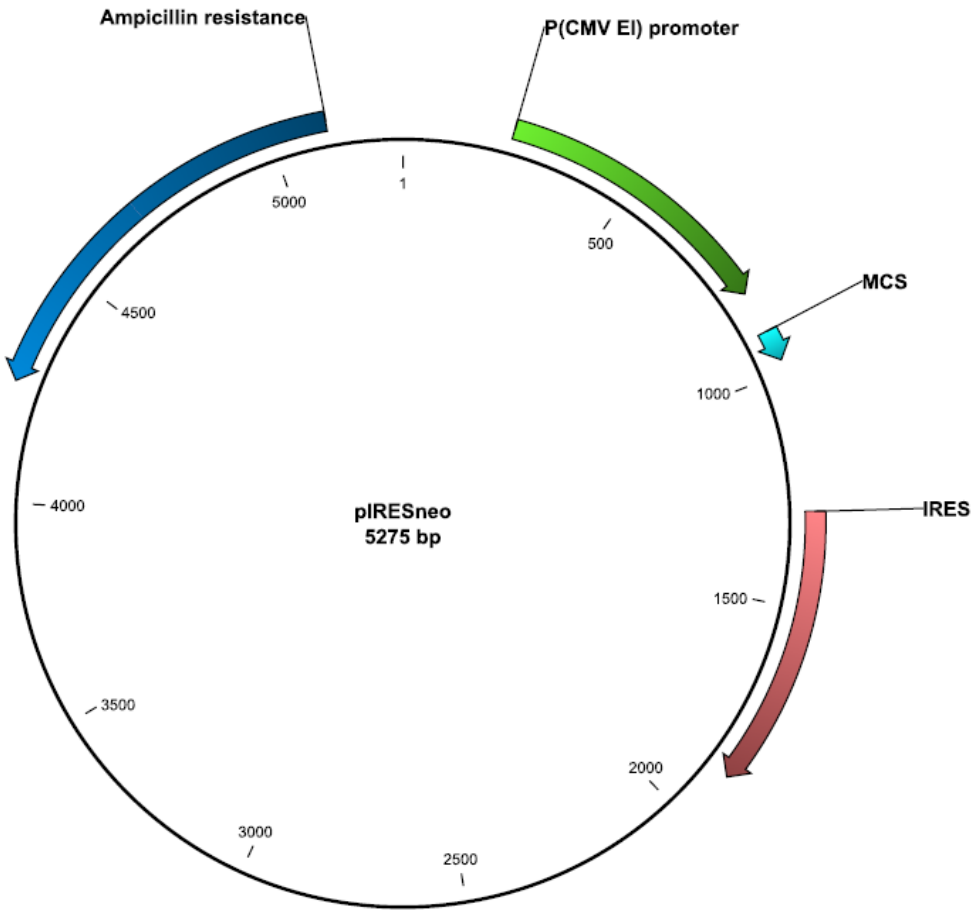
Ampicillin resistance
P(CMV EI) promoter
MCS
IRES
pIRESneo
5275 bp
1
500
1000
1500
2000
2500
3000
3500
4000
4500
5000

8.5.2 EH4-constructs

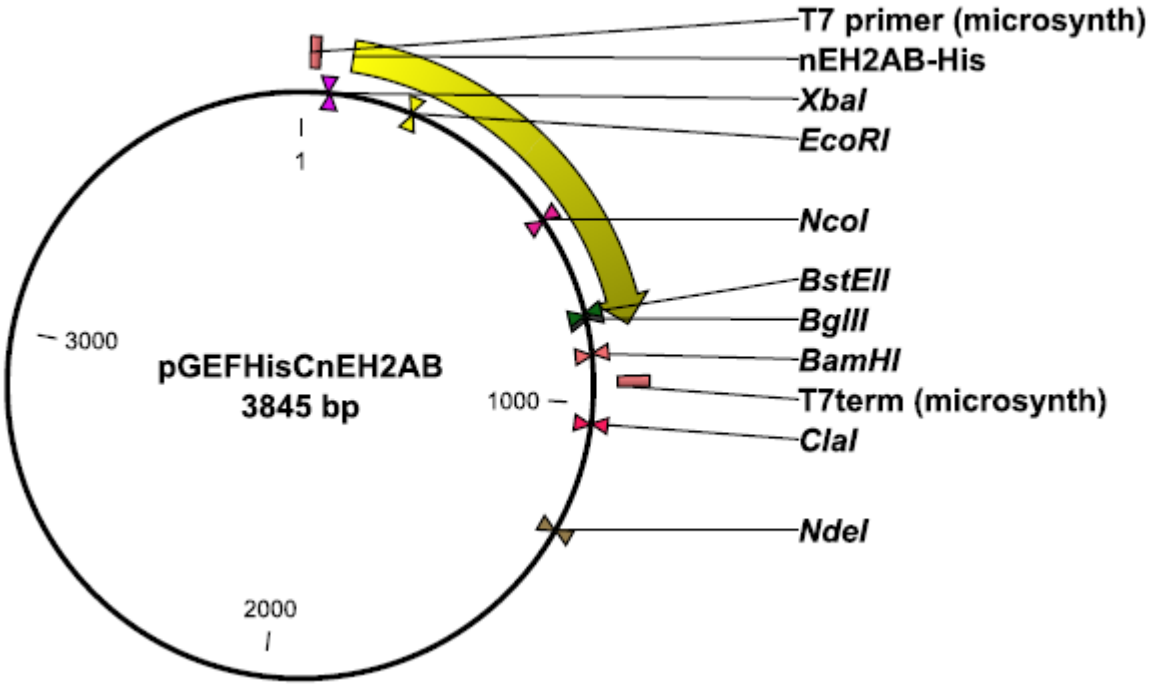

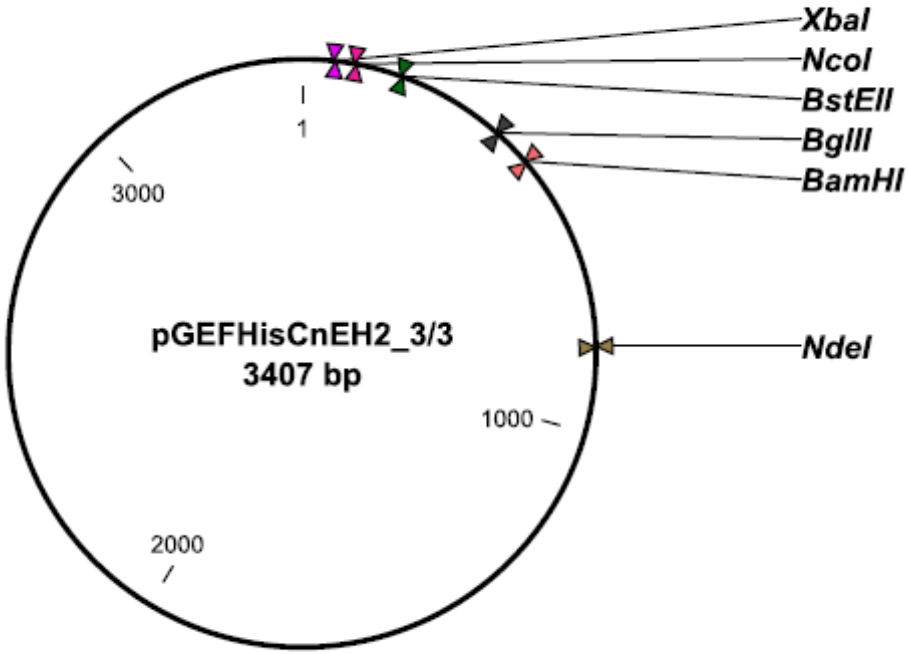

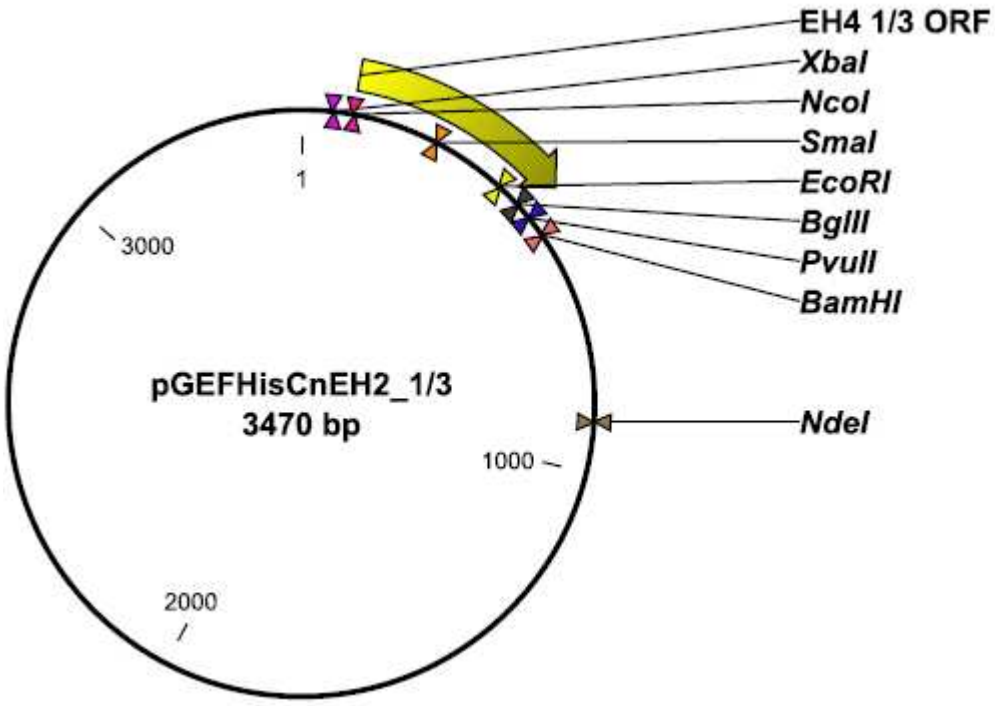
EH4 1/3 ORF
XbaI
NcoI
SmaI
EcoRI
BglII
PvuII
BamHI
NdeI
1
3000
1000
2000
pGEFHisCnEH2_1/3
3470 bp

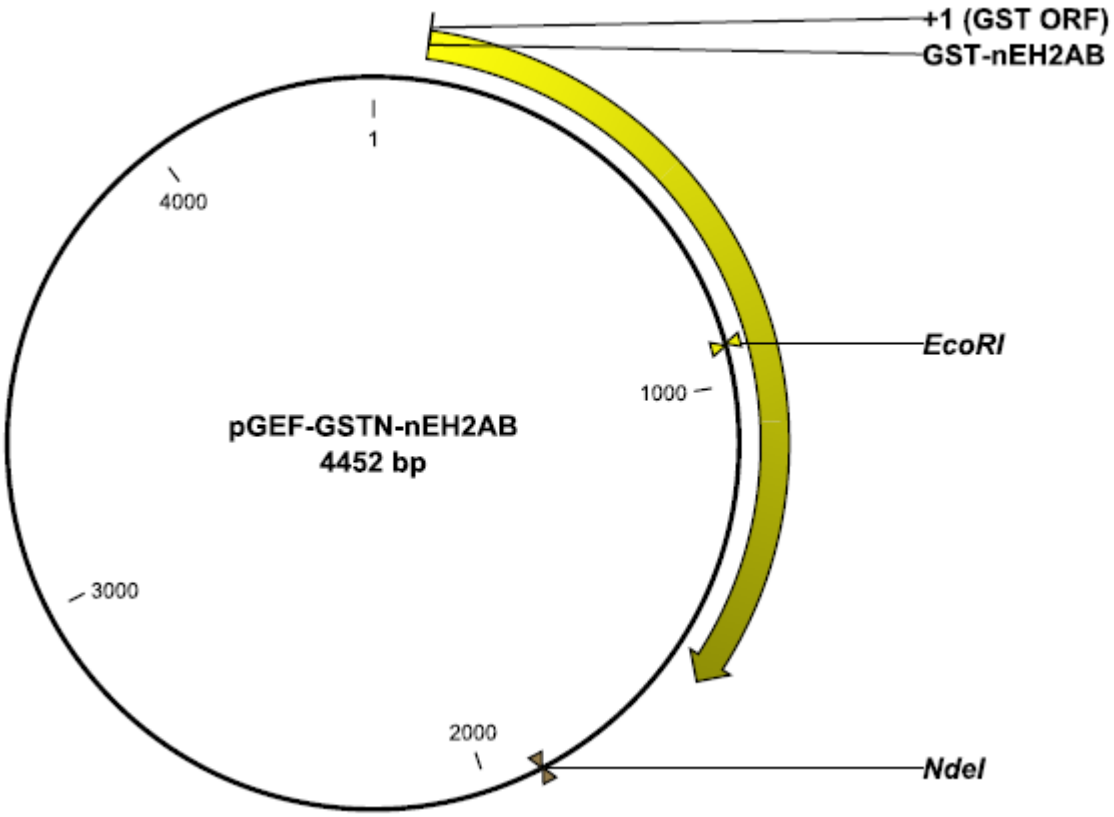
+1 (GST ORF)
GST-nEH2AB
EcoRI
NdeI
1
4000
1000
3000
2000
pGEF-GSTN-nEH2AB
4452 bp

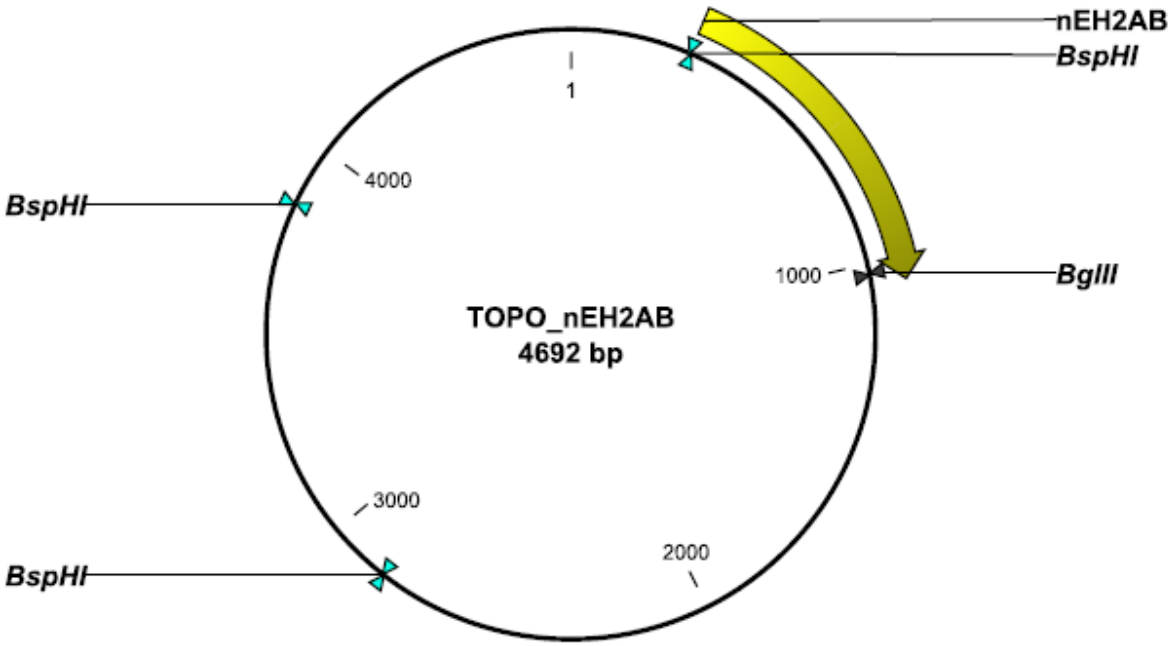
nEH2AB
BspHI
1
4000
BspHI
1000
BglII
TOPO_nEH2AB
4692 bp
3000
2000
BspHI

8.5.3 EH3-constructs

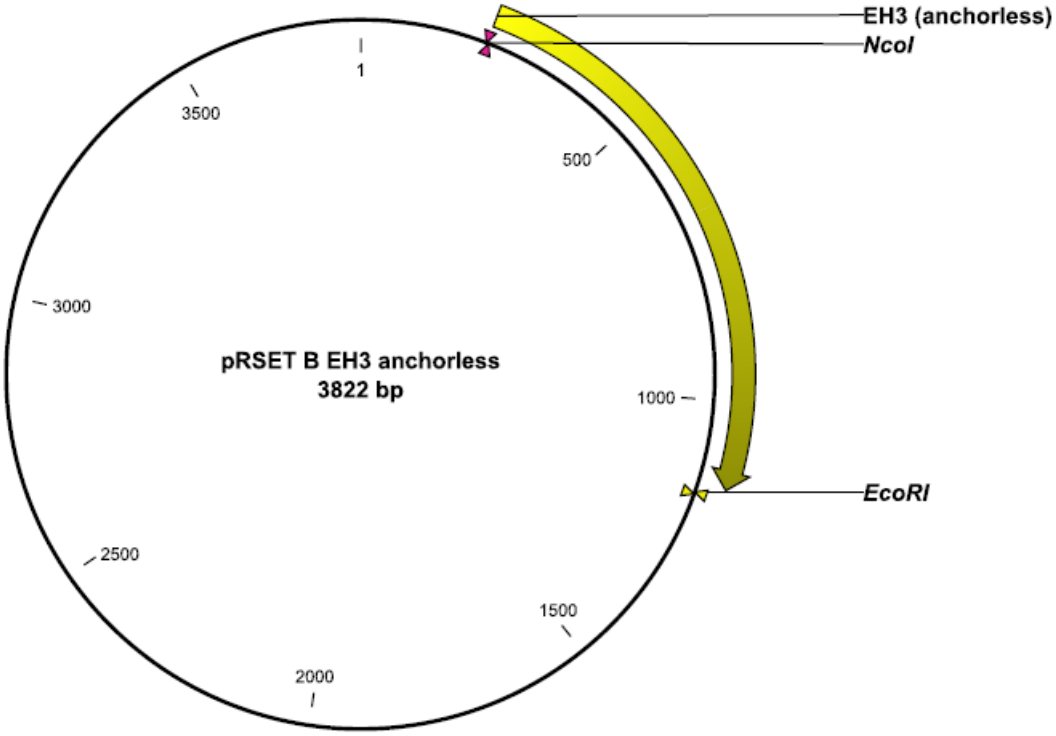

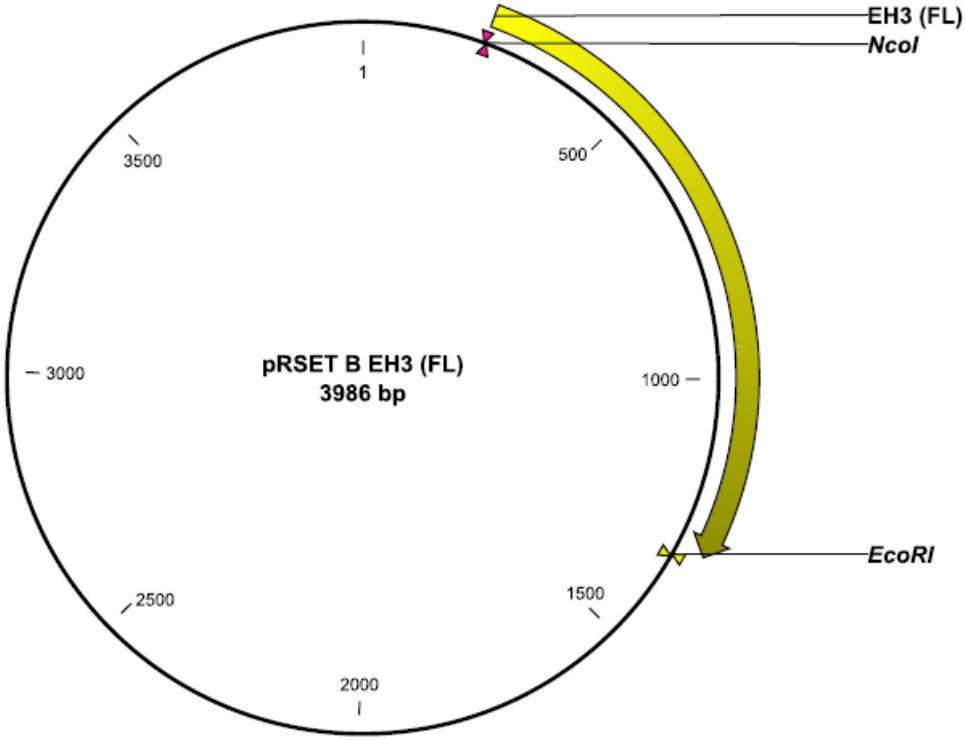

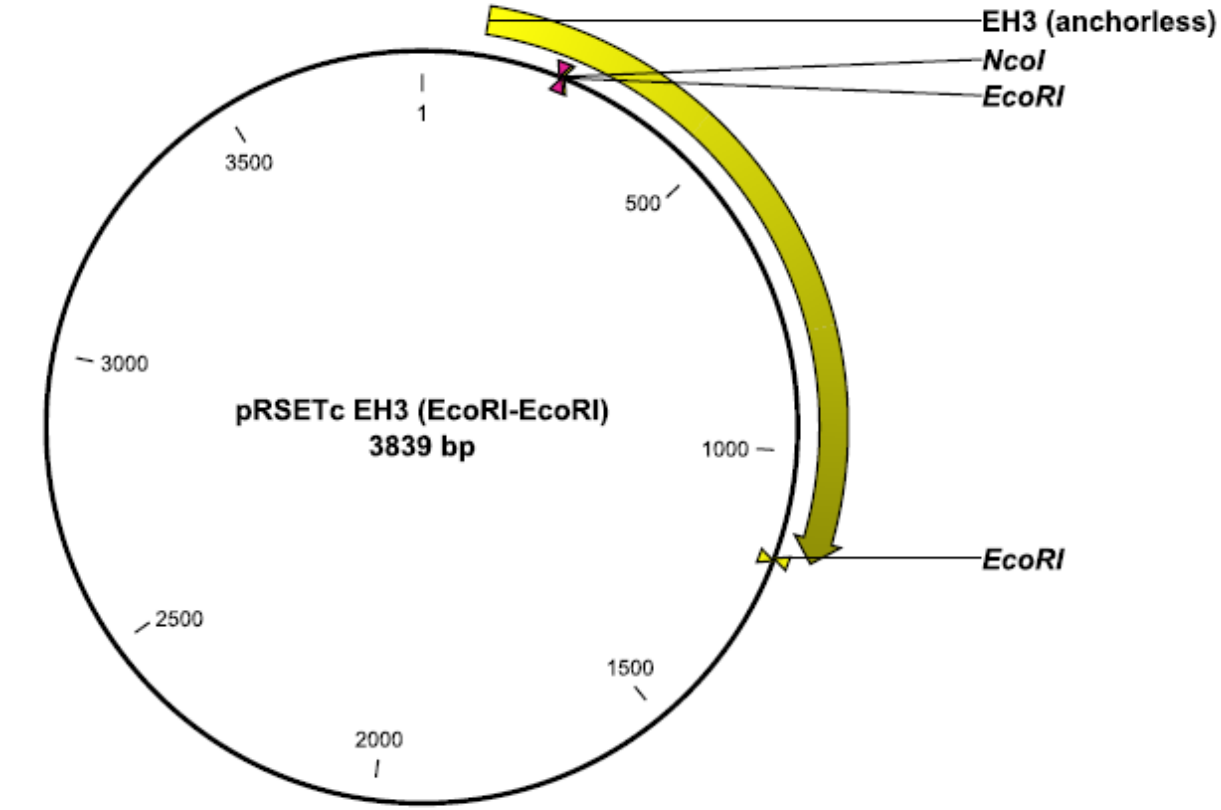
EH3 (anchorless)
NcoI
EcoRI
1
500
1000
1500
2000
2500
3000
3500
pRSETc EH3 (EcoRI-EcoRI)
3839 bp
EcoRI

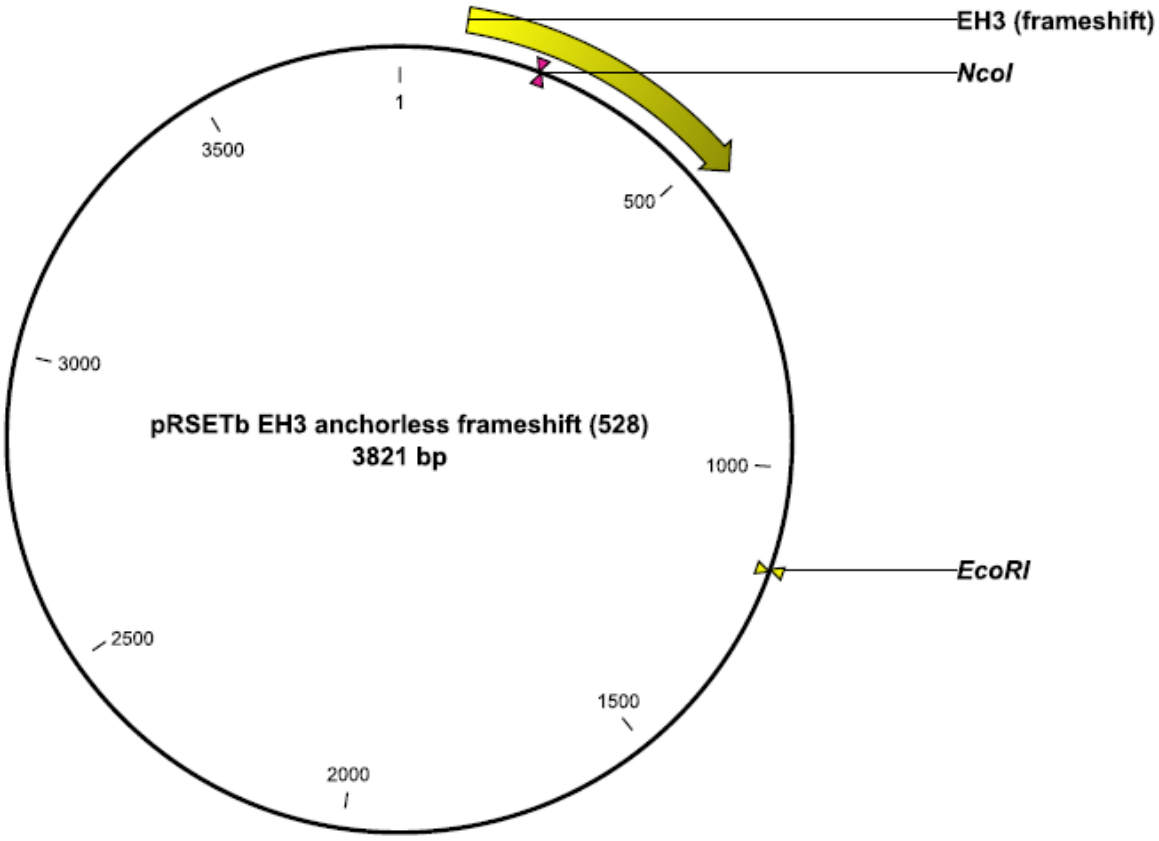
EH3 (frameshift)
NcoI
1
500
1000
1500
2000
2500
3000
3500
pRSETb EH3 anchorless frameshift (528)
3821 bp
EcoRI

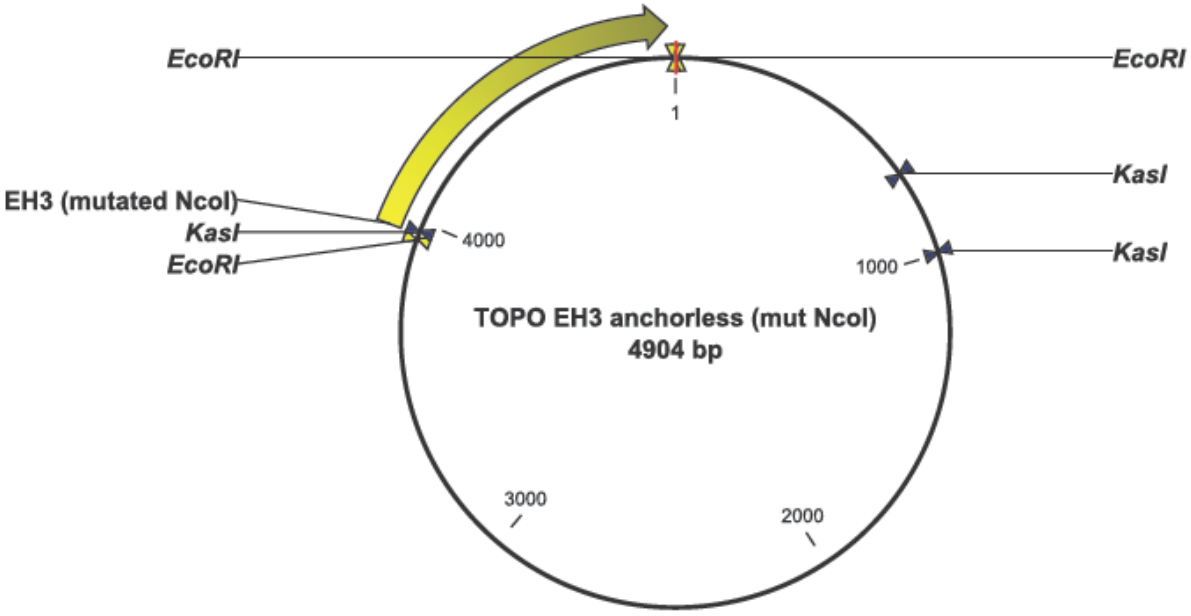
EcoRI
EcoRI
1
KasI
EH3 (mutated NcoI)
KasI
EcoRI
4000
1000
KasI
TOPO EH3 anchorless (mut NcoI)
4904 bp
3000
2000

8.6 *LC-MS/MS Data*

8.6.1 Cos-7 background activity

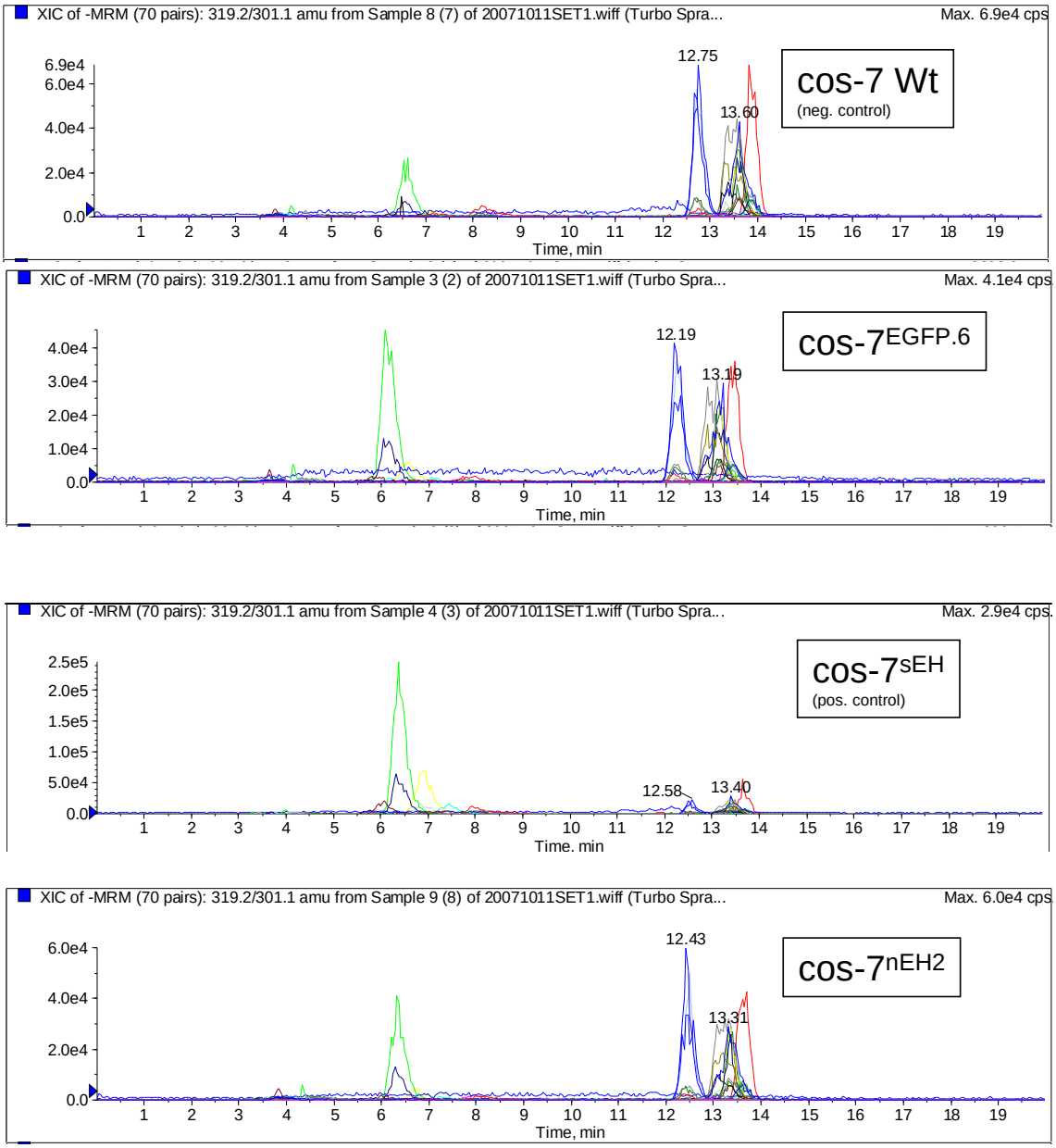

Figure 8-23: *Turnover of EET regioisomers by cos-7 and analysis by LC-MS/MS. 1x106 cells were resuspended in NH_4HCO_3 buffer. 10µl were added to 90µl substrate (3µM EET) and incubated for 15 minutes at 37℃. 100 µl ethylacetate was added to stop enzymatic reaction and to extract diols. Ethyl acetate was evaporated under a stream of nitrogen and resolved in 100µl acetonitrile before analysis by LC-MS/MS.*

8.6.2 V-79 activity assay (LC-MS/MS)

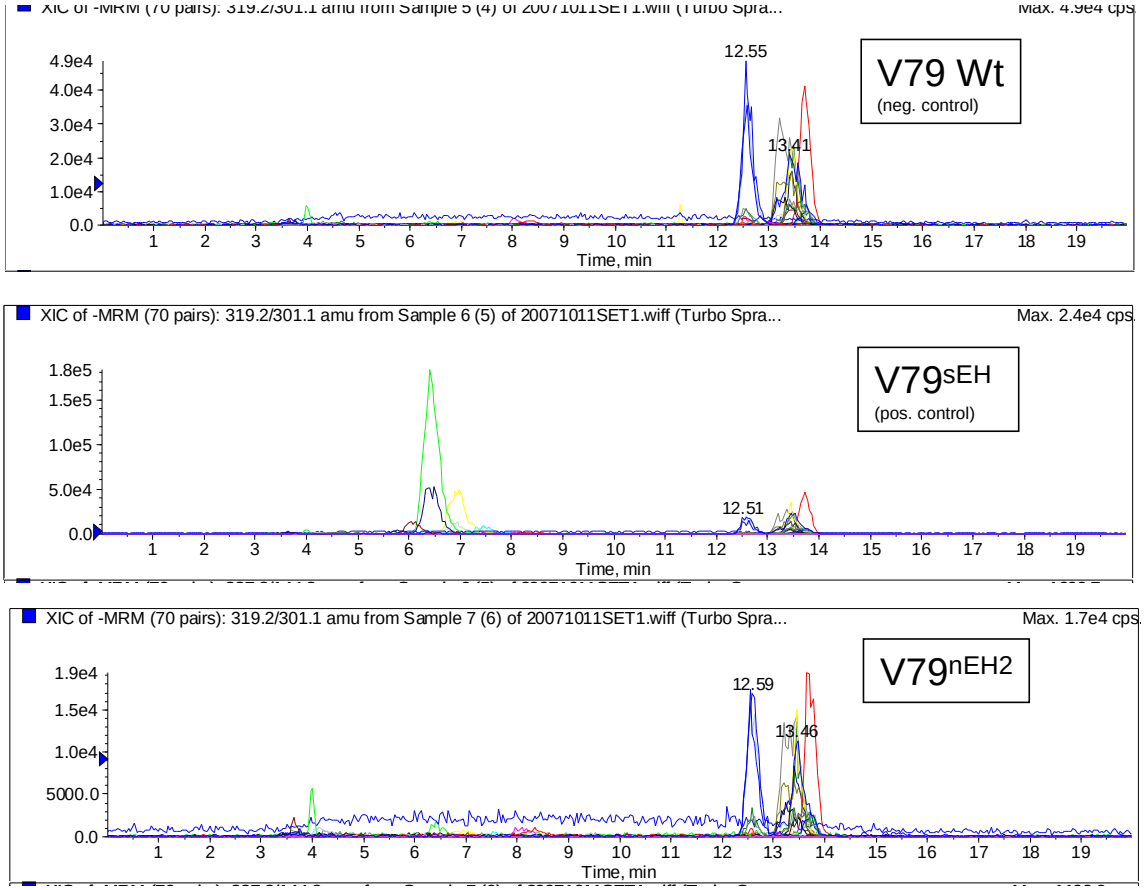

Figure 8-24: *turnover of EET regioisomers by V79 cells and analysis by LC-MS/MS. 1x106 cells were resuspended in NH4HCO3 buffer. 10µl were added to 90µl substrate (3µM EET) and incubated for 15 minutes at 37℃. 100 µl ethylacetate were added to stop enzymatic reaction and to extract diols. Ethyl acetate was evaporated under a stream of nitrogen and resolved in 100µl acetonitrile before analyzed by LC-MS/MS.*

8.6.3 EH3 turnover of 2-14(15) EET Ethanolamide

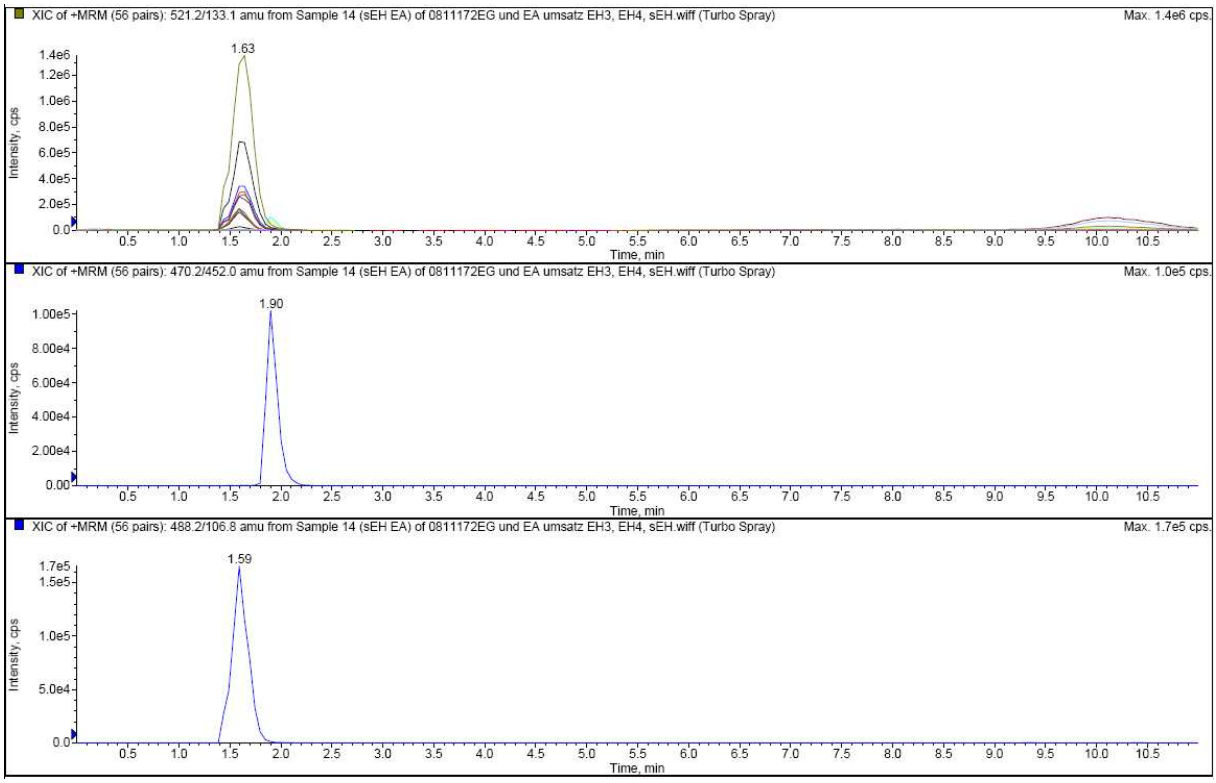

***Figure 8-25**: Turnover of 2-14(15) EET ethanol amide by sEH (see 4.9.2 for details).*

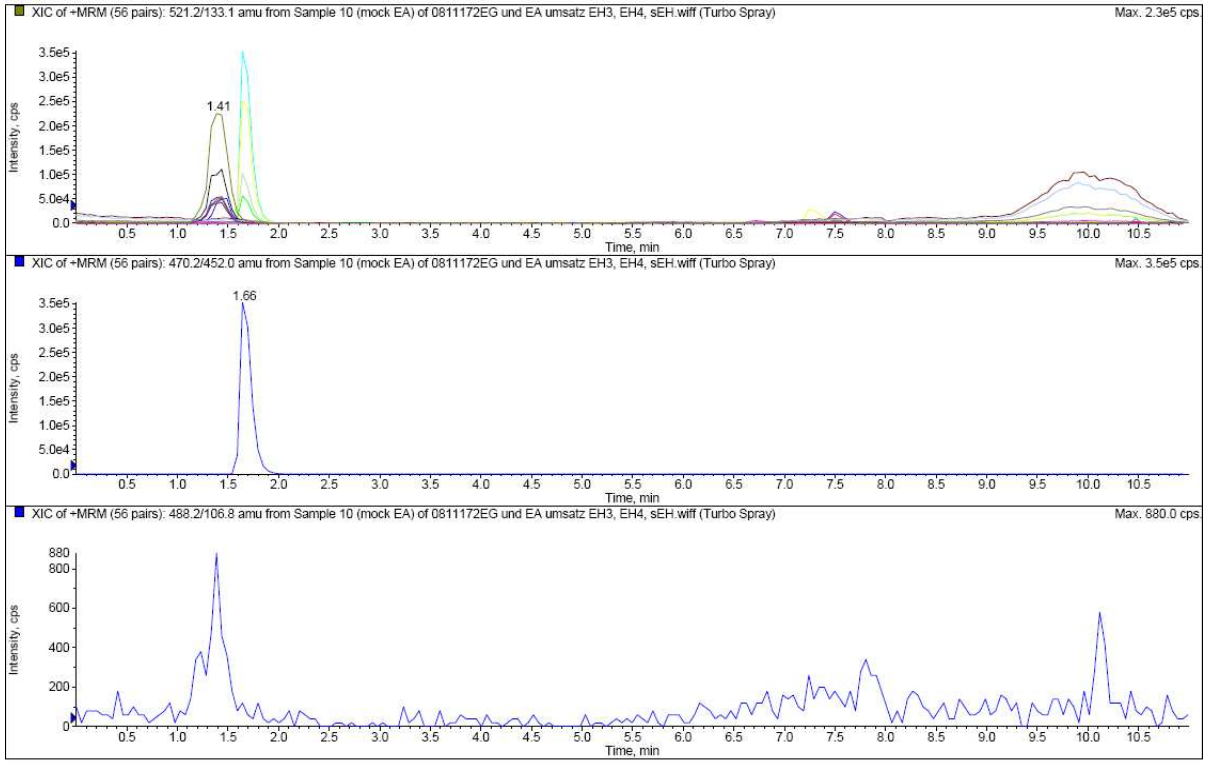

***Figure 8-26:** Turnover of 2-14(15) EET ethanol amide by mock infected Sf9 cells (see 4.9.2 for details).*

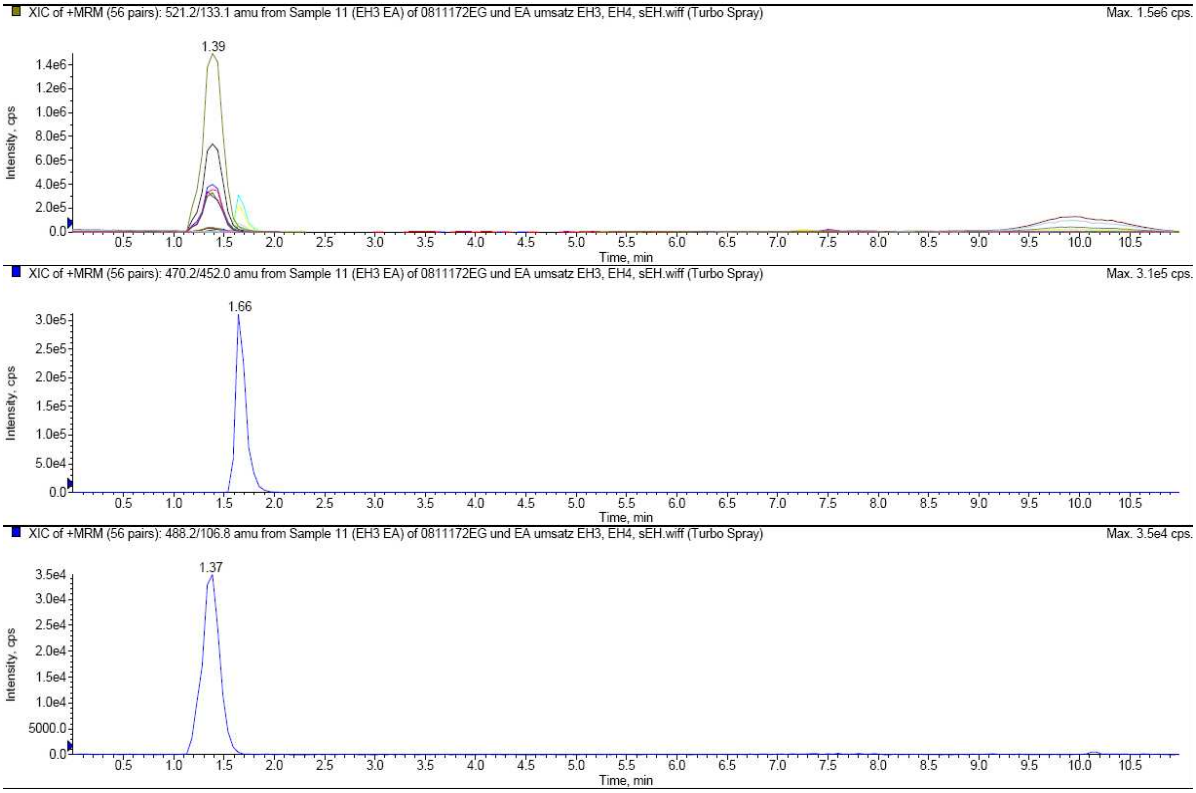

Figure 8-27: *Turnover of 2-14(15) EET ethanol amide by EH3 (see 4.9.2 for details).*

8.6.4 LC-MS/MS conditions for peptide analysis

MRM conditions for the identification of EH4 peptides on a QTrap 4000 using a MIDAS workflow integrated into the Analyst 1.4.2 acquisition method

Total transitions: 92
Dwell time: 14 ms
Total cycle time, including product ion scan: 3.22s
Monitoring criteria: Charge state: 1^+, 2^+ and 3^+, 1 missed cleavage; 400 – 2000 *m/z*.

MRM tab

Source / Gas	
Curtain gas (CUR)	25
Collision gas (CAD)	10
IonSpray Voltage (IS)	5000
Ion Source Gas1 (GS1)	40
Ion Source Gas2 (GS2)	50
Temperature (TEMP)	450

Compound	
Declustering Potential (DP)	50
Entrance Potential (EP)	10
Collision Cell Exit Potential (CXP)	15

Q1 and Q3 resolutions set to UNIT, settling time 2ms, pause between mass ranges 5.007 ms

IDA criteria tab

Select 3 of the most intense peaks
Threshold setting 200 cps
Exclude former target ions after 3 occurrences for 20 s
Mass tolerance 250 mmu
Exclude isotopes within 4 amu

EPI tab

Source / Gas	
Curtain gas (CUR)	25
Collision gas (CAD)	HIGH
IonSpray Voltage (IS)	5000
Ion Source Gas1 (GS1)	40
Ion Source Gas2 (GS2)	50
Temperature (TEMP)	450

Compound	
Declustering Potential (DP)	50
Collision Energy Spread (CES)	5
Collision Energy (CE)	60

MS		
Start (amu)	Stop (amu)	Time (s)
50	280	0.0575
275	2000	0.4313
Total Scan Time (1 scans)		0.6023 s

Advanced MS	
Scan Mode	Profile
Step Size (amu)	0.12
Q1 Resolution	Unit
Scan Rate (amu/s)	4000
Intensity Threshold (counts)	0
Settling Time (ms)	2
Pause between mass ranges (ms)	5.007
Q3 Energy Barrier (v)	8
Dynamic Fill Time	ON

Detected peptides

Sequence	**Start**	**End**	**Q1 Mass**	**Q3 Mass**	**CE**
LLWSLGK	39	45	816,5	590,3	56,4
FHYVAAGER	83	91	525,3	602,3	30,2
FHYVAAGER	83	91	1049,5	602,3	69,9
GYGETDAPI	129	139	608,3	593,3	34,2
GYGETDAPI	129	139	608,3	708,4	34,2
GYGETDAPI	129	139	1215,6	593,3	79,5
GYGETDAPI	129	139	1215,6	708,4	79,5
DILDSLGYSK	153	162	1110,6	654,3	73,4
DILDSLGYSK	153	162	1110,6	567,3	73,4
LIVINFPHPN	189	206	729,1	564,3	25
LIVINFPHPN	189	206	729,1	1154,6	25
HPAQLLK	207	213	806,5	501,3	55,8
HLFTSHSTGI	240	251	656,8	727,4	36,5
HHMVTTPTL	292	319	1077,2	1384,6	35,1
HHMVTTPTL	292	319	1077,2	1742,8	35,1
LTILSEASHW	328	348	812,4	685,4	27,4
LTILSEASHW	328	348	812,4	1297,7	27,4
LTILSEASHW	328	348	1218,1	685,4	63,5
LTILSEASHW	328	348	1218,1	1297,7	63,5

8.7 *Alignments*

Figure 8-28: *Amino acid alignment of EH4 from different species. There are different human protein sequences available of which one shows the Y321E variant (encircled in red).*

align Results

Please cite: *Pearson, W.R., Wood, T., Zhang, Z., and Miller, W. (1997) Comparision of DNA sequences with protein sequences, Genomics 46: 24-36*

```
>_                                                    159 aa vs.
>_                                                    159 aa
scoring matrix: , gap penalties: -12/-2
93.7% identity;         Global alignment score: 1031

               10        20        30        40        50        60
132118 ILRHPAQLLKSSYYYFFQIPWFPEFMFSINDFKVLKHLFTSHSTGIGRKGCQLTTEDLEA
       ::::::::..:::::::::::: :::::::::::.:::::::::::::::.::.::::::::
_      ILRHPAQMFKSSYYYFFQIPRFPEFMFSINDFKALKHLFTSHSTGIGRRGCRLTTEDFEA
               10        20        30        40        50        60

               70        80        90       100       110       120
132118 YIYVFSQPGALSGPINHYRNIFSCLPLKHHMVTTPTLLLWGENDAFMEVEMAEVTKIYVK
       :.:::::::::::::::::::::::::::::::::::::::::.::::.::::::::::::
_      YLYVFSQPGALSGPINHYRNIFSCLPLKHHMVTTPTLLLWGEKDAFMDVEMAEVTKIYVK
               70        80        90       100       110       120

              130       140       150
132118 NYFRLTILSEASHWLQQDQPDIVNKLIWTFLKEETRKKD
       ::::::::::::::::::::::::::::::::::::::::
_      NYFRLTILSEASHWLQQDQPDIVNKLIWTFLKEETRKKD
              130       140       150

Elapsed time:  0:00:00
```

Figure 8-29: *Alignment of EH4-3/3 with rabbit homologue.*

ABBREVIATIONS

aa	amino acid
ARDS	acute respiratory distress syndrome
AUDA	12-(3-adamantan-1-yl-ureido) dodecanoic acid
CDNB	1-chloro-2,4-dinitrobenzene
CDU	1-cyclohexyl-3-dodecyl-urea
ChEH	cholesterol epoxide hydrolase
DCU	N,N-dicyclohexylurea
DHA	docosahexenoic acid
DHET	dihydroxyeicosatetraenoic acid
EDHF	endothelium derived hyperpolarization factor
EDPE	epoxy docosapentaenoic acid
EET	epoxy eicosatrienoic acid
EET-EA	EET-ethanol amide
EETeE	epoxy eicosatetraenoic acid
EH	epoxide hydrolase
EH3	novel epoxide hydrolase 3
EH4	putative epoxide hydrolase 4
EPA	eicosapentaenoid acid
FP	french pressure cell press
GSH	Glutathione
GST	Glutathione -Transferase
HAD	haloalkane dehalogenase
HxA3	Hepoxilin A3
HxB3	Hepoxilin B3
LB	lysogeny broth (luria broth)
LEH	limonene epoxide hydrolase
LOX	lipoxygenase
LTA4	Leukotriene A4
MCS	multiple cloning site
mEH	microsomal epoxide hydrolase
mock	infected with Rv…
ON	over night
PUFA	polyunsaturated fatty acid
ROS	reactive oxygen species
RT	room temperature
sEH	soluble epoxide hydrolase
sEHi	sEH inhibitor(s)
STO	styrene 7,8 - oxide
WB	western blot

CURRICULUM VITAE

Surname:	Decker
First names:	Martina Marion Elisabeth
Date of birth:	June 9, 1980
Place of origin:	Nürnberg (Germany)

Education:

09. 2005 – present	PhD thesis: Institute of Pharmacology and Toxicology, University of Zurich, Zurich, Switzerland Supervision: Prof. Michael Arand Title: *Characterization of the novel human epoxide hydrolases EH3 and EH4* Funding: SNF (Swiss National Fond)
10/2001 – 07/2005	Studies in Biology: Julius Maximilians Universität Würzburg, Germany Degree: Diplom Biologin Univ. Diploma subjects: Biotechnology, Biochemistry and Pharmacology/Toxicology Diploma thesis: Institute of Pharmacology and Toxicology, University of Würzburg Supervision: PD Dr. Angela Mally Title: *Effects of Ochratoxin A on gap junctional intercellular communication (GJIC) in kidney epithelial cells (MDCK)* *Ochratoxin A alters cell adhesion and gap junction intercellular communication in MDCK cells*. Mally A, Decker M, Bekteshi M, Dekant W ; Toxicology. 2006 Jun 1;223(1-2):15-25. Epub 2006 Apr 18.
10/1999 – 10/2001	Studies in Biology: Friedrich Alexander Universität Erlangen-Nürnberg, Germany
09/1990 – 06/1999	Dietrich - Bonhoeffer Gymnasium Oberasbach, Germany Abitur

Publications:

Decker M., Arand M., Cronin A., 2009. Mammalian epoxide hydrolases in xenobiotic metabolism and signaling. Arch Toxicol 83(4): 297-318.

Decker M,. Adamska M., Di Giallonardo F., Cronin A., Falck J.R., Morisseau C., Hammock B.D., Arand M. EH3 (ABHD9) is the first member of a new family of epoxide hydrolases with a high specifity for fatty acid-derived signaling molecules. PNAS. (to be submitted)

Abstracts for posters:

Experimental Biology 2008, San Diego, April 2008

IDENTIFICATION OF A NEW POTENTIAL HUMAN EPOXIDE HYDROLASE (NEH2)
Martina Decker, Magdalena Adamska, Michael Arand.

Leopoldina Symposium of Lipid Signaling, Frankfurt, September 2008

CHARACTERIZATION OF A NOVEL HUMAN EPOXIDE HYDROLASE (EH3) CAPABLE OF CONVERTING EPOXYEICOSATRIENOIC ACIDS (EETs)
Martina Decker, Magdalena Adamska, Michael Arand.

11th International Winter Eicosanoid Conference, Baltimore, March 2009

ACTIVITY OF A NOVEL EPOXIDE HYDROLASE 3 (EH3) TOWARDS ARACHIDONIC ACID DERIVED SUBSTRATES IS AFFECTED BY AUDA - A POTENT SOLUBLE EPOXIDE HYDROLASE INHIBITOR
Martina Decker, Magdalena Adamska, Annette Cronin and Michael Arand

Presentations:

XERR 9th Annual Meeting, 2008, Zurich

CHARACTERIZATION AND INHIBITORY PROFILING OF NOVEL EPOXIDE HYDROLASE EH3

16. Toxikologisches und Pathologisches Kolloquium, 2009, Basel

EPOXIDE HYDROLASES - XENOBIOTIC METABOLIZERS OR PHYSIOLOGICAL REGULATORS?

Grants:

SST, Swiss Society of Toxicology: Travel Grant 2009